

LAGRANGIAN FILLINGS FOR LEGENDRIAN LINKS OF FINITE OR AFFINE DYNKIN TYPE

BYUNG HEE AN, YOUNGJIN BAE, AND EUNJEONG LEE

ABSTRACT. We prove that there are at least as many exact embedded Lagrangian fillings as seeds for Legendrian links of finite type ADE or affine type $\tilde{D}\tilde{E}$. We also provide as many Lagrangian fillings with rotational symmetry as seeds of type B, G_2 , \tilde{G}_2 , \tilde{B} , or \tilde{C}_2 , and with conjugation symmetry as seeds of type F_4 , C, $E_6^{(2)}$, \tilde{F}_4 , or $A_5^{(2)}$. These families are the first known Legendrian links with (infinitely many) exact Lagrangian fillings (with symmetry) that exhaust all seeds in the corresponding cluster structures beyond type AD. Furthermore, we show that the N -graph realization of (twice of) Coxeter mutation of type $\tilde{D}\tilde{E}$ corresponds to a Legendrian loop of the corresponding Legendrian links. Especially, the loop of type \tilde{D} coincides with the one considered by Casals and Ng.

CONTENTS

1. Introduction	2
1.1. Background	2
1.2. The results	2
1.3. Organization of the paper	8
Acknowledgement	9
2. Cluster algebras	9
2.1. Basics on cluster algebras	9
2.2. Cluster algebras of Dynkin type	12
2.3. Folding	14
2.4. Combinatorics of exchange graphs	18
3. Legendrians and N -graphs	25
3.1. N -graphs and Legendrian weaves	25
3.2. N -graphs on \mathbb{D}^2 and \mathbb{A}	30
3.3. One-cycles in Legendrian weaves	38
3.4. Flag moduli spaces	41
3.5. Y -seeds and Legendrian mutations	42
4. Lagrangian fillings for Legendrians links of finite or affine type	46
4.1. N -graphs of finite or affine types	46
4.2. Legendrian Coxeter mutations	54
4.3. Legendrian loops	62
4.4. Lagrangian fillings	63
5. Foldings	67
5.1. Group actions on N -graphs	68
5.2. Invariant N -graphs and Lagrangian fillings	69
Appendix A. G -invariance and G -admissibility of finite type	71
Appendix B. Supplementary pictorial proofs	74
References	78

1. INTRODUCTION

1.1. Background. Legendrian knots are central objects in the study of 3-dimensional contact manifolds. Classification of Legendrian knots is important in its own right and also plays a prominent role in classifying 4-dimensional Weinstein manifolds.

Classical Legendrian knot invariants are Thurston–Bennequin number and rotation number [31] which distinguish the pair of Legendrian knots with the same knot type. There are non-classical invariants including the Legendrian contact algebra via the method of Floer theory [21, 18], and the space of constructible sheaves using microlocal analysis [32, 43]. These non-classical invariants distinguish the Chekanov pair, a pair of Legendrian knots of type $m5_2$ having the same classical invariants.

Recently, the study of exact Lagrangian fillings for Legendrian links has been extremely plentiful. In the context of Legendrian contact algebra, an exact Lagrangian filling gives an augmentation through the functorial view point [20]. There are several level of equivalence between augmentations and the constructible sheaves for Legendrian links from counting to categorical equivalence [37]. Using these idea of augmentations and constructible sheaves, people construct infinitely many fillings for certain Legendrian links [13, 30, 15]. Here is the summarized list of methods of constructing Lagrangian fillings for Legendrian links:

- (1) Decomposable Lagrangian fillings via pinching sequences and Legendrian loops [20, 36, 14].
- (2) Alternating Legendrians and its conjugate Lagrangian fillings [42].
- (3) Legendrian weaves via N -graphs and Legendrian mutations [44, 15].
- (4) Donaldson–Thomas transformation on augmentation varieties [41, 29, 30].

Cluster algebras, introduced by Fomin and Zelevinsky [25], play a crucial role in the above constructions and applications. More precisely, the space of augmentations and the moduli of constructible sheaves of microlocal rank one adapted to Legendrian links admit structures of cluster pattern and Y -pattern, respectively [42, 41, 29]. Note that a Y -seed of cluster algebra consists of a quiver whose vertices are decorated with variables, called *coefficients*. An involutory operation at each vertex, called *mutation*, generates all seeds of the Y -pattern. The main point is to identify the mutation in the Y -pattern and an operation in the space of Lagrangian fillings. This geometric operation is deeply related to the Lagrangian surgery [39] and the wall-crossing phenomenon [4].

Indeed, a Legendrian torus link of type $(2, n)$ admits as many exact Lagrangian fillings as Catalan number up to exact Lagrangian isotopy [38, 42, 44]. Interestingly enough, the Catalan number is the number of seeds in a cluster pattern of Dynkin type A_{n-1} . There are also Legendrian links corresponding to finite Dynkin type DE, and affine Dynkin type $\tilde{D}\tilde{E}$ [30]. A conjecture by Casals [12, Conjecture 5.1] says that the number of distinct exact embedded Lagrangian fillings (up to exact Lagrangian isotopy) for Legendrian links of type ADE is exactly the same as the number of seeds of the corresponding cluster algebras.

Furthermore, it is also conjectured by Casals [12, Conjecture 5.4] that for Legendrian links of type A_{2n-1}, D_{n+1}, E_6 and D_4 , Lagrangian fillings having certain $\mathbb{Z}/2\mathbb{Z}$ or $\mathbb{Z}/3\mathbb{Z}$ -symmetry form the cluster patterns of type B_n, C_n, F_4 and G_2 , which are Dynkin diagrams obtained by *folding* as explained in [27].

1.2. The results.

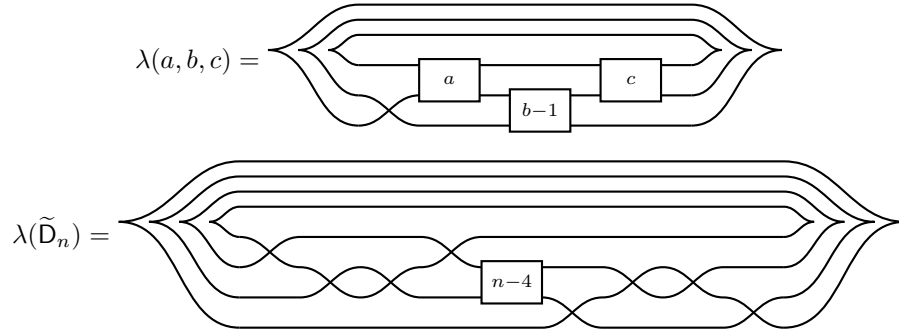
1.2.1. Lagrangian fillings for Legendrians of type ADE or $\tilde{D}\tilde{E}$. Our main result is that there are at least as many Lagrangian fillings for Legendrian links of finite type as seeds in the corresponding cluster structures. We deal with N -graphs introduced by Casals and Zaslow [15] to construct the Lagrangian fillings. An N -graph \mathcal{G} on \mathbb{D}^2 gives a Legendrian surface $\Lambda(\mathcal{G})$ in $J^1\mathbb{D}^2$ while the boundary $\partial\mathcal{G}$ on \mathbb{S}^1 induces a Legendrian link $\lambda(\partial\mathcal{G})$. Then projection of $\Lambda(\mathcal{G})$ along the Reeb direction becomes a Lagrangian filling of $\lambda(\partial\mathcal{G})$.

As mentioned above, we interpret an N -graph as a Y -seed in the corresponding Y -pattern. A one-cycle in the Legendrian surface $\Lambda(\mathcal{G})$ corresponds to a vertex of the quiver, and a signed intersection between one-cycles gives an arrow between corresponding vertices. From constructible

sheaves adapted to $\Lambda(\mathcal{G})$, one can assign a monodromy to each one-cycle which becomes the coefficient at each vertex.

There is an operation so called a *Legendrian mutation* μ_γ on an N -graph \mathcal{G} along one-cycle $[\gamma] \in H_1(\Lambda(\mathcal{G}))$ which is the counterpart of the mutation on the Y -pattern, see Proposition 3.42. The delicate and challenging part is that we do not know whether Legendrian mutations are always possible or not. Simply put, this is because the mutation in cluster side is algebraic, whereas the Legendrian mutation is rather geometric.

The main idea of our construction is to consider N -graphs $\mathcal{G}(a, b, c)$ and $\mathcal{G}(\tilde{D}_n)$ bounding Legendrian links $\lambda(a, b, c)$ and $\lambda(\tilde{D}_n)$, respectively.



Note that the above Legendrians $\lambda(a, b, c)$ and $\lambda(\tilde{D}_n)$ can be obtained by (-1) -closure of the following braids, respectively,

$$\beta(a, b, c) = \sigma_2 \sigma_1^{a+1} \sigma_2 \sigma_1^{b+1} \sigma_2 \sigma_1^{c+1}, \quad \beta(\tilde{D}_n) = (\sigma_2 \sigma_1^3 \sigma_2 \sigma_1^3 \sigma_2 \sigma_1^k \sigma_3) \cdot (\sigma_2 \sigma_1^3 \sigma_2 \sigma_1^3 \sigma_2 \sigma_1^\ell \sigma_3),$$

where $k = \lfloor \frac{n-3}{2} \rfloor$ and $\ell = \lfloor \frac{n-4}{2} \rfloor$, see Section 4. Those braids provide boundary data of the following N -graphs which represent exact Lagrangian fillings of corresponding Legendrian links:

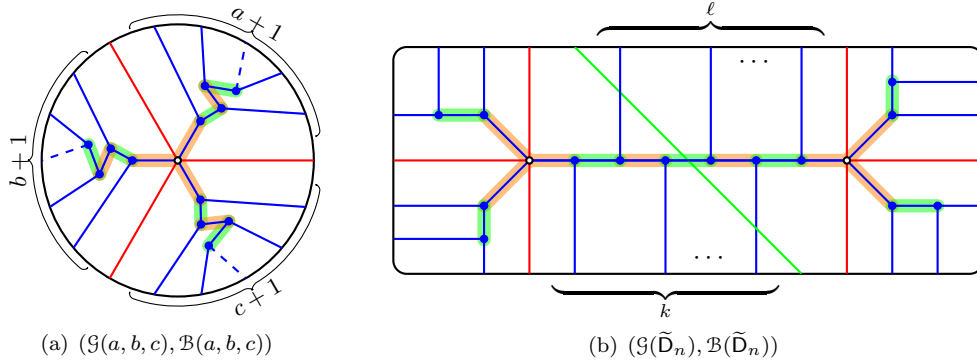


FIGURE 1. Pairs of N -graphs and tuples of cycles

Here, the **orange**- and **green**-shaded edges indicate a tuple of one-cycles \mathcal{B} in the corresponding Legendrian surface. See §3.3 for the detail.

The Legendrians $\lambda(a, b, c), \lambda(\tilde{D}_n)$ are the rainbow closure of *positive braids*. By the work of Shen–Weng [41], it is direct to check that the corresponding cluster structure of Legendrian $\lambda(Z)$ is indeed of type Z for $Z \in \{A, D, E, \tilde{D}, \tilde{E}\}$. More precisely, the coordinate ring of the moduli space $\mathcal{M}_1(\lambda(Z))$ of microlocal rank one sheaves in $\text{Sh}_{\lambda(Z)}^\bullet(\mathbb{R}^2)$ admits the aforementioned Y -pattern structure. By the way, the (candidate) Legendrians of type \tilde{A} are not the rainbow closure of positive braids, in general. Indeed, Casals–Ng [14] considered a Legendrian link of type $\tilde{A}_{1,1}$ which is not the rainbow closure of a positive braid. So we can not directly apply the subsequent argument to Legendrians of type \tilde{A} .

To prove the realizability of each Y -seed in the corresponding Y -pattern, we use an induction argument on the rank of the type Z . More precisely, for each Y -pattern, we consider the *exchange graph*, whose vertices are the Y -seeds and whose edges connect the vertices related by a single mutation. It has been known that the exchange graph of a Y -pattern is determined by the Dynkin type Z of the Y -pattern when Z is finite or affine (cf. Propositions 2.24 and 2.25). Because of this, we denote by $\text{Ex}(\Phi(Z))$ the exchange graph of a Y -pattern of type Z . Here, $\Phi(Z)$ is the root system of type Z . Note that when Z is of finite type, the exchange graph $\text{Ex}(\Phi(Z))$ becomes the one-skeleton of a polytope, called the (*generalized*) *associahedron* (see Figures 2 and 12).

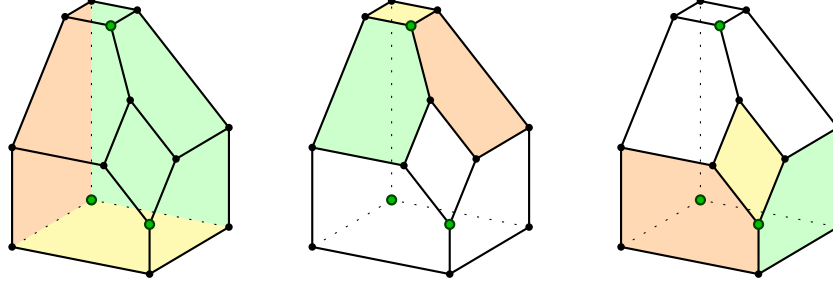


FIGURE 2. The type A_3 associahedron

A (fixed) sequence of mutations corresponding to a chosen Coxeter element provides an action on the exchange graph. We call this specific sequence of mutations a *Coxeter mutation* μ_Q . The orbit of the initial seed is called *bipartite belt*. The green dots in Figure 2 present the elements of the bipartite belt. We notice that the facets meeting at the initial seed correspond to the exchange graphs $\text{Ex}(\Phi(Z \setminus \{i\}))$. In Figure 2, there are two pentagons and one square intersecting a green dot. Indeed, a pentagon is the type A_2 generalized associahedron; a square is the type $A_1 \times A_1$ generalized associahedron. Moreover, by applying the Coxeter mutation on these facets iteratively, one can obtain all facets in the associahedron. Even though we do not have a polytope model for the exchange graph of affine type, similar properties hold, that is, one can reach any Y -seed in the exchange graph from the initial seed by taking Coxeter mutations and then applying a certain sequence of mutations omitting at least one vertex.

The following good properties of the above pairs $(\mathcal{G}(a, b, c), \mathcal{B}(a, b, c))$ and $(\mathcal{G}(\tilde{D}_n), \mathcal{B}(\tilde{D}_n))$ play a crucial role in interpreting the Coxeter mutation μ_Q in terms of N -graphs:

- (1) The geometric and algebraic intersection numbers between chosen one-cycles coincide.
- (2) The corresponding quivers $\mathcal{Q}(a, b, c)$, $\mathcal{Q}(\tilde{D}_n)$ are bipartite, see §3.5 for the details.

The property (2) naturally splits \mathcal{B} into two subsets \mathcal{B}_+ and \mathcal{B}_- . In Figure 1, they consist of orange- and green-shaded edges, respectively. Then the property (1) enables us to perform the *Legendrian Coxeter mutation*, which is the N -graph realization of the Coxeter mutation defined by the sequence of Legendrian mutations:

$$\mu_{\mathcal{G}} = \prod_{\gamma \in \mathcal{B}_+} \mu_{\gamma} \cdot \prod_{\gamma \in \mathcal{B}_-} \mu_{\gamma}.$$

Then the resulting N -graphs $\mu_{\mathcal{G}}(\mathcal{G}(a, b, c), \mathcal{B}(a, b, c))$ and $\mu_{\mathcal{G}}(\mathcal{G}(\tilde{D}_n), \mathcal{B}(\tilde{D}_n))$ become the N -graphs shown in Figure 3 up to a sequence of Move (II) in Figure 18.

Removing the gray-shaded annulus region, $(\mathcal{G}(\tilde{D}_n), \mathcal{B}(\tilde{D}_n))$ and $\mu_{\mathcal{G}}(\mathcal{G}(\tilde{D}_n), \mathcal{B}(\tilde{D}_n))$ are identical, and the only difference between $(\mathcal{G}(a, b, c), \mathcal{B}(a, b, c))$ and $\mu_{\mathcal{G}}(\mathcal{G}(a, b, c), \mathcal{B}(a, b, c))$ is the reverse of the color. Note that the intersection pattern between one-cycles and the Legendrian mutability are preserved under the action of the Legendrian Coxeter mutation $\mu_{\mathcal{G}}$. By the induction argument on the rank of root system, we conclude that there is no (geometric) obstruction to realize each seed via the N -graph.

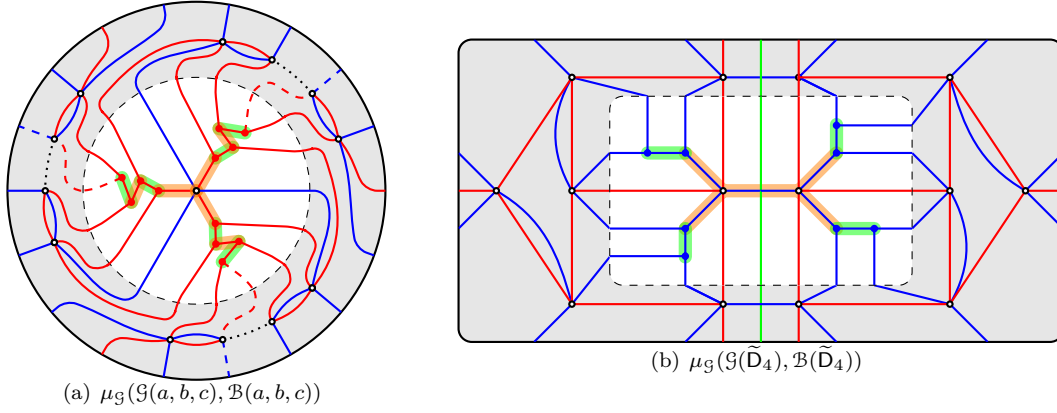


FIGURE 3. After applying Legendrian Coxeter mutation on the initial pair

Note that the N -graphs $\mathcal{G}(a, b, c)$ and $\mathcal{G}(\tilde{D}_n)$ cover Lagrangian fillings of Legendrian links of type $Z \in \{A, D, E, \tilde{D}, \tilde{E}\}$, see Table 8. In particular, $\mathcal{G}(a, b, c)$ is of type ADE or $\tilde{D}\tilde{E}$ if and only if $\frac{1}{a} + \frac{1}{b} + \frac{1}{c} > 1$ or $\frac{1}{a} + \frac{1}{b} + \frac{1}{c} = 1$, respectively.

This guarantees that there are at least as many Lagrangian fillings as seeds for $\lambda(Z)$ for $Z \in \{A, D, E, \tilde{D}, \tilde{E}\}$.

Theorem 1.1 (Theorem 4.31). *Let λ be a Legendrian knot or link of type ADE or type $\tilde{D}\tilde{E}$. Then it admits as many exact embedded Lagrangian fillings as the number of seeds in the seed pattern of the same type. See Table 4 for the number of seeds of finite type.*

There are several ways of constructing exact embedded Lagrangian fillings as mentioned above. Especially in D_4 case, there are 34 distinct Lagrangian fillings constructed by the method of the alternating Legendrians [6, 42], while the above N -graphs give seeds many 50 Lagrangian fillings. Most recently, for Legendrian links of type D_n , Hughes [33] makes use of 3-graphs together with 1-cycles to show that every sequence of quiver mutations can be realized by Legendrian weave mutations. Compared with our strategy using structural results of the cluster pattern, he studies 3-graph moves arise from quivers of type D_n in a more direct and concrete way. As a corollary, he also obtained at least as many Lagrangian fillings as seeds in the cluster algebra of type D_n .

There are many results showing the existence of (infinitely many) distinct Lagrangian fillings for Legendrian links, see [20, 38, 44, 42, 13, 15, 30, 14]. To the best of authors' knowledge, Theorem 1.1 is the first results of (infinitely many) Lagrangian fillings of Legendrian links which exhaust all seeds in the corresponding cluster pattern beyond type AD.

The gray-shaded annular N -graphs in the above figure can be seen as exact Lagrangian cobordisms. In particular, the annular N -graph in $\mu_{\mathcal{G}}(\mathcal{G}(\tilde{D}_4), \mathcal{B}(\tilde{D}_4))$ corresponds to the cobordism from the Legendrian $\lambda(\tilde{D}_4)$ onto itself which defines the *Legendrian loop* $\vartheta(\tilde{D}_4)$. See Figure 44 in general. Note that this coincides with the Legendrian loop described in [14, Figure 2] up to Reidemeister moves. For type \tilde{E} , the twice of Legendrian Coxeter mutation on the pair $(\mathcal{G}(a, b, c), \mathcal{B}(a, b, c))$ gives the Legendrian loop $\vartheta(\tilde{E})$ of $\lambda(\tilde{E})$ as shown in Figure 43. The Legendrian loop $\vartheta(\tilde{E})$ can be interpreted as the move of the half twist Δ_3 along the three-strand braid band, whereas the Legendrian loop $\vartheta(\tilde{D}_n)$ is essentially the move of the half twist Δ_2 along the two-strand braid band as depicted in Figure 44.

Theorem 1.2 (Theorem 4.30). *The Legendrian Coxeter mutation $\mu_{\mathcal{G}}$ on $(\mathcal{G}(\tilde{D}), \mathcal{B}(\tilde{D}))$ and twice of Legendrian mutation $\mu_{\mathcal{G}}^2$ on $(\mathcal{G}(\tilde{E}), \mathcal{B}(\tilde{E}))$ induce Legendrian loops $\vartheta(\tilde{D})$ and $\vartheta(\tilde{E})$ in Figures 43 and 44, respectively. In particular, the order of the Legendrian loops are infinite as elements of the fundamental group of the space of Legendrians isotopic to $\lambda(\tilde{D})$ and $\lambda(\tilde{E})$, respectively.*

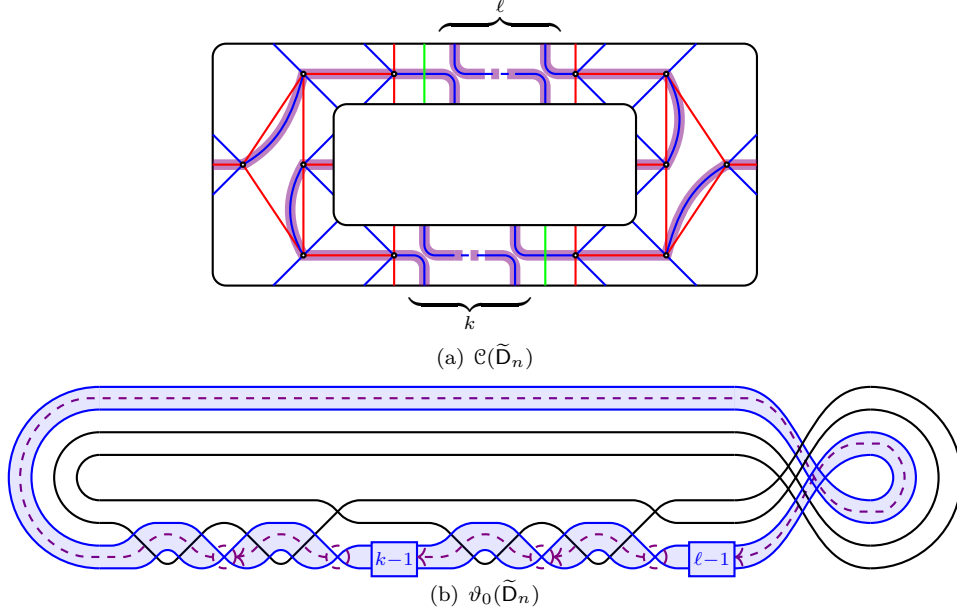


FIGURE 4. Legendrian Coxeter padding $\mathcal{C}(\tilde{D}_n)$ and the corresponding Legendrian loop $\vartheta_0(\tilde{D}_n)$

Note that the above idea of Coxeter mutation also works for $(\mathcal{G}(a, b, c), \mathcal{B}(a, b, c))$ with $\frac{1}{a} + \frac{1}{b} + \frac{1}{c} < 1$. Indeed the operation $\mu_{\mathcal{Q}}$ is of infinite order and so is $\mu_{\mathcal{G}}$, hence Legendrian weaves

$$\Lambda(\mu_{\mathcal{G}}^r(\mathcal{G}(a, b, c), \mathcal{B}(a, b, c)))$$

produce infinitely many distinct Lagrangian fillings. The quiver $\mathcal{Q}(a, b, c)$ is also bipartite and one can perform the Legendrian Coxeter mutation $\mu_{\mathcal{G}}$ on the N -graph $\mathcal{G}(a, b, c)$ by stacking the gray-shaded annulus like as before. Therefore, there is no obstruction to realize seeds obtained by mutations $\mu_{\mathcal{G}}^r$ via the N -graphs. Since the order of the Legendrian Coxeter mutation is infinite (see Lemma 2.32), we obtain infinitely many N -graphs and hence infinitely many exact embedded Lagrangian fillings for the Legendrian link $\lambda(a, b, c)$ with $\frac{1}{a} + \frac{1}{b} + \frac{1}{c} < 1$.

Theorem 1.3 (Theorem 4.23). *For each $a, b, c \geq 1$, the Legendrian knot or link $\lambda(a, b, c)$ has infinitely many distinct Lagrangian fillings if*

$$\frac{1}{a} + \frac{1}{b} + \frac{1}{c} < 1.$$

Gao–Shen–Weng [30] already proved the existence of infinitely many Lagrangian fillings for much general type of positive braid Legendrian links. Their main idea is to use the aperiodicity of *Donaldson–Thomas transformation* (DT) on cluster varieties. An interesting observation is that the corresponding action of DT on the bipartite quivers in the Y -pattern becomes the Coxeter mutation. Accordingly, Theorem 1.3 can be interpreted as an N -graph analogue of the aperiodicity of DT.

1.2.2. Lagrangian fillings for Legendrians of type BCFG or standard affine type with symmetry. Now we move to cluster structure of type BCFG and standard affine types with certain symmetry. They are obtained by the folding procedure from type ADE or $\tilde{D}\tilde{E}$, see Table 10.

In order to interpret those symmetries into Legendrians links and surfaces, we need to introduce corresponding actions on symplectic- and contact manifolds. Consider two actions on $\mathbb{S}^3 \times \mathbb{R}_u$,

the rotation R_{θ_0} and conjugation η as follows:

$$\begin{aligned} R_{\theta_0}(z_1, z_2, u) &= (z_1 \cos \theta_0 - z_2 \sin \theta_0, z_1 \sin \theta_0 + z_2 \cos \theta_0, u); \\ \eta(z_1, z_2, u) &= (\bar{z}_1, \bar{z}_2, u). \end{aligned}$$

Here \mathbb{S}^3 is the unit sphere in \mathbb{C}^2 with coordinates $z_1 = r_1 e^{i\theta_1}, z_2 = r_2 e^{i\theta_2}$ with $r_1^2 + r_2^2 = 1$. Note that η is an anti-symplectic involution which naturally gives $\mathbb{Z}/2\mathbb{Z}$ -action on the symplectic manifold. Under certain coordinate changes, the restrictions of R_{θ_0} and η on $J^1\mathbb{S}^1$ become

$$\begin{aligned} R_{\theta_0}|_{J^1\mathbb{S}^1}(\theta, p_\theta, z) &= (\theta + \theta_0, p_\theta, z); \\ \eta|_{J^1\mathbb{S}^1}(\theta, p_\theta, z) &= (\theta, -p_\theta, -z). \end{aligned}$$

In turn, the rotation R_{θ_0} acts on the N -graph $\mathcal{G}(\mathbb{Z})$ by rotating the disk \mathbb{D}^2 , and η acts by flipping the z -coordinate.

Any Y -pattern of non-simply-laced finite or affine type can be obtained by folding a Y -pattern of type ADE or $\tilde{\text{ADE}}$. In other words, those Y -pattern of non-simply-laced type can be seen as sub-patterns of ADE- or $\tilde{\text{ADE}}$ -types consisting of Y -seeds with certain symmetries of finite group G action. We call such Y -seeds or N -graphs G -admissible, and the mutation in the folded cluster structure is a sequence of mutations respecting the G -orbits. We say that a Y -seed (or an N -graph) is *globally foldable* if it is G -admissible and its arbitrary mutations along G -orbits are again G -admissible.

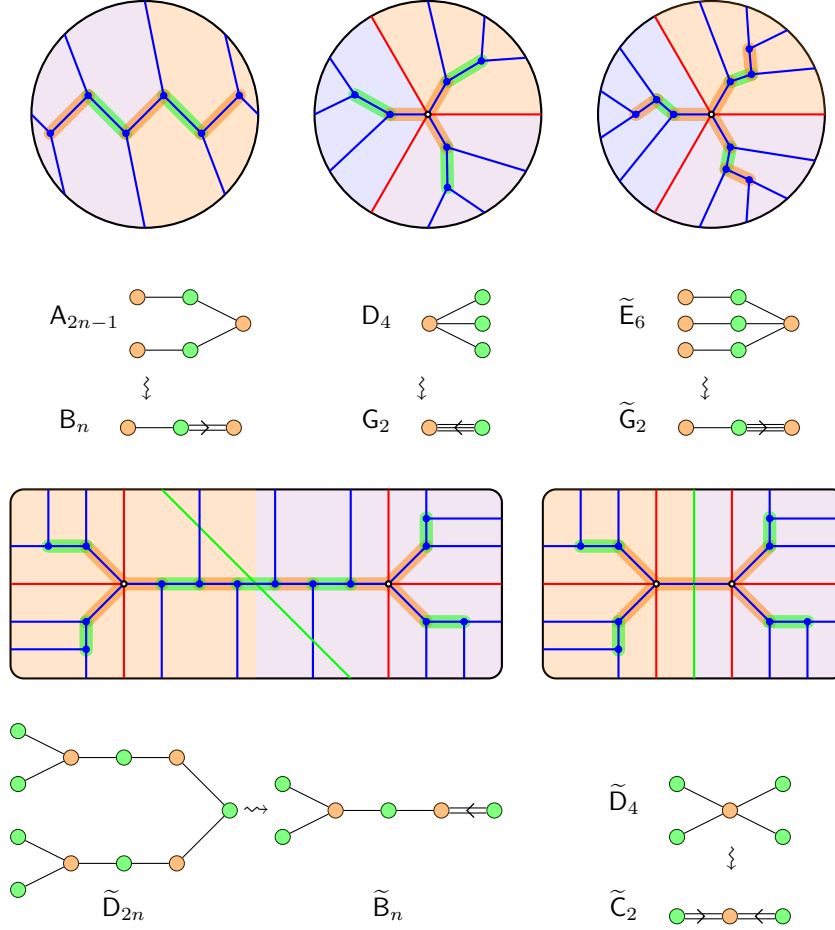
Figure 5 illustrates the N -graphs with rotational symmetry and the corresponding Y -patterns of folding. Indeed, they are $\mathcal{G}(1, n, n)$, $\mathcal{G}(2, 2, 2)$, $\mathcal{G}(3, 3, 3)$, $\mathcal{G}(\tilde{\text{D}}_{2n})$, $\mathcal{G}(\tilde{\text{D}}_4)$ which admits $\mathbb{Z}/2\mathbb{Z}$ -, $\mathbb{Z}/3\mathbb{Z}$ -, $\mathbb{Z}/3\mathbb{Z}$ -, $\mathbb{Z}/2\mathbb{Z}$ -, $\mathbb{Z}/2\mathbb{Z}$ -action, respectively.

In order to present conjugation invariant N -graphs, we need to adopt a degenerate version of N -graphs which allows overlapping edges and cycles as in Figure 6. They are equivalent to $\mathcal{G}(\tilde{\text{D}}_{n+1})$, $\mathcal{G}(\tilde{\text{D}}_4)$, $\mathcal{G}(2, 3, 3)$, $\mathcal{G}(3, 3, 3)$, and $\mathcal{G}(2, 4, 4)$ up to ∂ -Legendrian isotopy see Definition 3.17, respectively.

Theorem 1.4 (Theorem 5.8). *The following holds:*

- (1) The Legendrian $\lambda(\text{A}_{2n-1})$ has $\binom{2n}{n}$ Lagrangian fillings which are invariant under the π -rotation and admit the Y -pattern of type B_n .
- (2) The Legendrian $\lambda(\text{D}_4)$ has 8 Lagrangian fillings which are invariant under the $2\pi/3$ -rotation and admit the Y -pattern of type G_2 .
- (3) The Legendrian $\lambda(\tilde{\text{E}}_6)$ has Lagrangian fillings which are invariant under the $2\pi/3$ -rotation and admit the Y -pattern of type $\tilde{\text{G}}_2$.
- (4) The Legendrian $\lambda(\tilde{\text{D}}_{2n})$ with $n \geq 3$ has Lagrangian fillings which are invariant under the π -rotation and admit the Y -pattern of type $\tilde{\text{B}}_n$.
- (5) The Legendrian $\lambda(\tilde{\text{D}}_4)$ has Lagrangian fillings which are invariant under the π -rotation and admit the Y -pattern of type $\tilde{\text{C}}_2$.
- (6) The Legendrian $\tilde{\lambda}(\text{E}_6)$ has 105 Lagrangian fillings which are invariant under the antisymplectic involution and admit the Y -pattern of type F_4 .
- (7) The Legendrian $\tilde{\lambda}(\text{D}_{n+1})$ has $\binom{2n}{n}$ Lagrangian fillings which are invariant under the anti-symplectic involution and admit the Y -pattern of type C_n .
- (8) The Legendrian $\tilde{\lambda}(\tilde{\text{E}}_6)$ has Lagrangian fillings which are invariant under the antisymplectic involution and admit the Y -pattern of type $\text{E}_6^{(2)}$.
- (9) The Legendrian $\tilde{\lambda}(\tilde{\text{E}}_7)$ has Lagrangian fillings which are invariant under the antisymplectic involution and admit the Y -pattern of type $\tilde{\text{F}}_4$.
- (10) The Legendrian $\tilde{\lambda}(\tilde{\text{D}}_4)$ has Lagrangian fillings which are invariant under the antisymplectic involution and admit the Y -pattern of type $\text{A}_5^{(2)}$.

The study of Lagrangian fillings with symmetry, again to the best of authors' knowledge, is started from [12]. We clarify the actions on the symplectic and contact manifold, together with the induced actions on Lagrangian fillings and Legendrian links. The items (1),(2),(6),(7) in

FIGURE 5. Examples of N -graphs with rotational symmetry

Theorem 1.4 answer that the conjecture [12, Conjecture 5.4] is true, and furthermore we extend our results to certain non-simply-laced affine types.

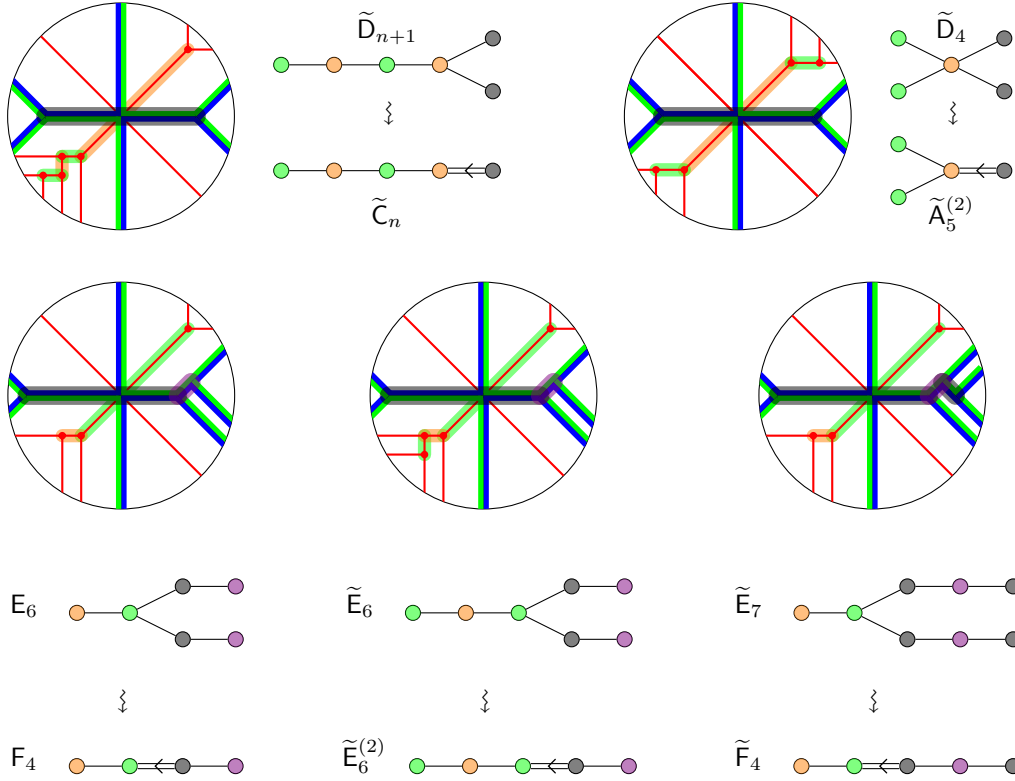
1.3. Organization of the paper. The rest of the paper is divided into six sections including appendices. We review, in Section 2, some basics on finite and affine cluster algebra. Especially we focus on structural results about the combinatorics of exchange graphs using Coxeter mutations.

In Section 3, we recall how N -graphs and their moves encode Legendrian surfaces and the Legendrian isotopies. We also introduce degenerate N -graphs which will be used to construct Lagrangian fillings having conjugation symmetry. After that we review the assignment of Y -seeds in the cluster structure from N -graphs together with certain flag moduli. We also discuss the Legendrian mutation on (degenerate) N -graphs.

In Section 4, we investigate Legendrian links and N -graphs of type ADE or \tilde{DE} . We discuss N -graph realization of the Coxeter mutation and prove Theorem 1.2 on the relationship between Coxeter mutations and Legendrian loops. By combining the structural results in the seed pattern of cluster algebra and N -graph realization of the Coxeter mutation, we construct as many Lagrangian fillings as seeds for Legendrian links of type ADE or \tilde{DE} , and hence prove Theorem 1.1.

In Section 5, we discuss rotation and conjugation actions on N -graphs and invariant N -graphs. We also prove Theorem 1.4.

In Appendix A, we argue that G -invariance of type ADE implies G -admissibility. Finally, in Appendix B, we collect several equivalences between different presentation of N -graphs.

FIGURE 6. Examples of N -graphs with conjugation symmetry

If some readers are familiar with the notion of cluster algebra and N -graph, then one may skip Section 2 and Section 3, respectively, and start from Section 4.

Acknowledgement. B. An and Y. Bae were supported by the National Research Foundation of Korea (NRF) grant funded by the Korea government (MSIT) (No. 2020R1A2C1A0100320). E. Lee was supported by the Institute for Basic Science (IBS-R003-D1).

2. CLUSTER ALGEBRAS

Cluster algebras, introduced by Fomin and Zelevinsky [25], are commutative algebras with specific generators, called *cluster variables*, defined recursively. In this section, we recall basic notions in the theory of cluster algebras. For more details, we refer the reader to [25, 26, 28].

Throughout this section, we fix $m, n \in \mathbb{Z}_{>0}$ such that $n \leq m$, and we let \mathbb{F} be the rational function field with m independent variables over \mathbb{C} .

2.1. Basics on cluster algebras.

Definition 2.1 (cf. [25, 26, 28]). A seed and Y -seed are defined as follows.

- (1) A *seed* $(\mathbf{x}, \tilde{\mathcal{B}})$ is a pair of
 - a tuple $\mathbf{x} = (x_1, \dots, x_m)$ of algebraically independent generators of \mathbb{F} , that is, $\mathbb{F} = \mathbb{C}(x_1, \dots, x_m)$;
 - an $m \times n$ integer matrix $\tilde{\mathcal{B}} = (b_{i,j})_{i,j}$ such that the *principal part* $\mathcal{B} := (b_{i,j})_{1 \leq i,j \leq n}$ is skew-symmetrizable, that is, there exist positive integers d_1, \dots, d_n such that

$$\text{diag}(d_1, \dots, d_n) \cdot \mathcal{B}$$

is a skew-symmetric matrix.

- We refer to \mathbf{x} as the *cluster* of a seed $(\mathbf{x}, \tilde{\mathcal{B}})$, to elements x_1, \dots, x_m as *cluster variables*, and to $\tilde{\mathcal{B}}$ as the *exchange matrix*. Moreover, we call x_1, \dots, x_n *unfrozen* (or, *mutable*) variables and x_{n+1}, \dots, x_m *frozen* variables.
- (2) A *Y-seed* $(\mathbf{y}, \mathcal{B})$ is a pair of an n -tuple $\mathbf{y} = (y_1, \dots, y_n)$ of elements in \mathbb{F} and an $n \times n$ skew-symmetrizable matrix \mathcal{B} . We call \mathbf{y} the *coefficient tuple* of a *Y-seed* $(\mathbf{y}, \mathcal{B})$ and call y_1, \dots, y_n *coefficients*.

We say that two seeds $(\mathbf{x}, \tilde{\mathcal{B}})$ and $(\mathbf{x}', \tilde{\mathcal{B}}')$ are *equivalent*, denoted by $(\mathbf{x}, \tilde{\mathcal{B}}) \sim (\mathbf{x}', \tilde{\mathcal{B}}')$ if there exists a permutation σ on $[m]$ such that $\sigma|_{[n]} = [n]$,

$$x'_i = x_{\sigma(i)} \quad \text{and} \quad b'_{i,j} = b_{\sigma(i), \sigma(j)} \quad \text{for } 1 \leq i \leq m, 1 \leq j \leq n,$$

where $\mathbf{x} = (x_1, \dots, x_m)$, $\mathbf{x}' = (x'_1, \dots, x'_m)$, $\tilde{\mathcal{B}} = (b_{i,j})$, and $\tilde{\mathcal{B}}' = (b'_{i,j})$. Similarly, two *Y-seeds* $(\mathbf{y}, \mathcal{B})$ and $(\mathbf{y}', \mathcal{B}')$ are *equivalent* and denoted by $(\mathbf{y}, \mathcal{B}) \sim (\mathbf{y}', \mathcal{B}')$ if there exists a permutation σ on $[n]$ such that

$$y'_i = y_{\sigma(i)} \quad \text{and} \quad b'_{i,j} = b_{\sigma(i), \sigma(j)} \quad \text{for } 1 \leq i, j \leq n.$$

To define cluster algebras, we introduce mutations on exchange matrices, and quivers, and seeds as follows.

- (1) (Mutation on exchange matrices) For an exchange matrix $\tilde{\mathcal{B}}$ and $1 \leq k \leq n$, the mutation $\mu_k(\tilde{\mathcal{B}}) = (\tilde{b}'_{i,j})$ is defined as follows.

$$b'_{i,j} = \begin{cases} -b_{i,j} & \text{if } i = k \text{ or } j = k, \\ b_{i,j} + \frac{|b_{i,k}|b_{k,j} + b_{i,k}|b_{k,j}|}{2} & \text{otherwise.} \end{cases}$$

We say that $\tilde{\mathcal{B}}' = (\tilde{b}'_{i,j})$ is the *mutation of $\tilde{\mathcal{B}}$ at k* .

- (2) (Mutation on quivers) We call a finite directed multigraph \mathcal{Q} a *quiver* if it does not have oriented cycles of length at most 2. The adjacency matrix $\tilde{\mathcal{B}}(\mathcal{Q})$ of a quiver is always skew-symmetric. Moreover, $\mu_k(\tilde{\mathcal{B}}(\mathcal{Q}))$ is again the adjacency matrix of a quiver \mathcal{Q}' . We define $\mu_k(\mathcal{Q})$ to be the quiver satisfying

$$\tilde{\mathcal{B}}(\mu_k(\mathcal{Q})) = \mu_k(\tilde{\mathcal{B}}(\mathcal{Q})),$$

and say that $\mu_k(\mathcal{Q})$ is the *mutation of \mathcal{Q} at k* .

- (3) (Mutation on seeds) For a seed $(\mathbf{x}, \tilde{\mathcal{B}})$ and an integer $1 \leq k \leq n$, the *mutation* $\mu_k(\mathbf{x}, \tilde{\mathcal{B}}) = (\mathbf{x}', \mu_k(\tilde{\mathcal{B}}))$ is defined as follows:

$$x'_i = \begin{cases} x_i & \text{if } i \neq k, \\ x_k^{-1} \left(\prod_{b_{j,k} > 0} x_j^{b_{j,k}} + \prod_{b_{j,k} < 0} x_j^{-b_{j,k}} \right) & \text{otherwise.} \end{cases}$$

- (4) (Mutation on *Y-seeds*) The *Y-seed mutation* (or, *cluster \mathcal{X} -mutation*, *\mathcal{X} -cluster mutation*) on a *Y-seed* $(\mathbf{y}, \mathcal{B})$ at $k \in [n]$ is a *Y-seed* $(\mathbf{y}' = (y'_1, \dots, y'_n), \mathcal{B}' = \mu_k(\mathcal{B}))$, where for each $1 \leq i \leq n$,

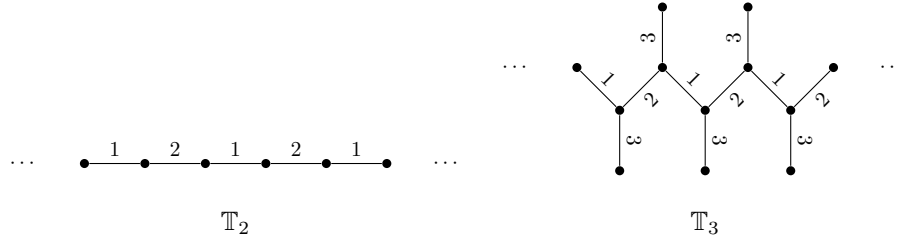
$$y'_i = \begin{cases} y_i y_k^{\max\{b_{i,k}, 0\}} (1 + y_k)^{-b_{i,k}} & \text{if } i \neq k, \\ y_k^{-1} & \text{otherwise.} \end{cases}$$

Example 2.2. Let $n = m = 2$. Suppose that an initial seed is given by

$$(\mathbf{x}_{t_0}, \tilde{\mathcal{B}}_{t_0}) = \left((x_1, x_2), \begin{pmatrix} 0 & 1 \\ -3 & 0 \end{pmatrix} \right).$$

Considering mutations $\mu_1(\mathbf{x}_{t_0}, \tilde{\mathcal{B}}_{t_0})$ and $\mu_2\mu_1(\mathbf{x}_{t_0}, \tilde{\mathcal{B}}_{t_0})$, we obtain the following.

$$\begin{aligned} \mu_1(\mathbf{x}_{t_0}, \tilde{\mathcal{B}}_{t_0}) &= \left(\left(\frac{1+x_2^3}{x_1}, x_2 \right), \begin{pmatrix} 0 & -1 \\ 3 & 0 \end{pmatrix} \right), \\ \mu_2\mu_1(\mathbf{x}_{t_0}, \tilde{\mathcal{B}}_{t_0}) &= \left(\left(\frac{1+x_2^3}{x_1}, \frac{1+x_1+x_2^3}{x_1 x_2} \right), \begin{pmatrix} 0 & 1 \\ -3 & 0 \end{pmatrix} \right). \end{aligned}$$

FIGURE 7. The n -regular trees for $n = 2$ and $n = 3$.

Remark 2.3. Let k be a vertex in a quiver \mathcal{Q} on $[m]$. The mutation $\mu_k(\mathcal{Q})$ can also be described via a sequence of three steps:

- (1) For each directed two-arrow path $i \rightarrow k \rightarrow j$, add a new arrow $i \rightarrow j$.
- (2) Reverse the direction of all arrows incident to the vertex k .
- (3) Repeatedly remove directed 2-cycles until unable to do so.

Remark 2.4. Let $\tilde{\mathcal{B}} = (b_{i,j})$ be an exchange matrix of size $m \times n$. For $k, \ell \in [n]$, if $b_{k,\ell} = b_{\ell,k} = 0$, then the mutations at k and ℓ commute with each other: $\mu_\ell(\mu_k(\tilde{\mathcal{B}})) = \mu_k(\mu_\ell(\tilde{\mathcal{B}}))$. Similarly, for a quiver \mathcal{Q} on $[m]$, if there does not exist an arrow connecting mutable vertices k and ℓ , then we have $\mu_\ell(\mu_k(\mathcal{Q})) = \mu_k(\mu_\ell(\mathcal{Q}))$.

We say a quiver \mathcal{Q}' is *mutation equivalent* to another quiver \mathcal{Q} if there exists a sequence of mutations $\mu_{j_1}, \dots, \mu_{j_\ell}$ which connects \mathcal{Q}' and \mathcal{Q} , that is,

$$\mathcal{Q}' = (\mu_{j_\ell} \cdots \mu_{j_1})(\mathcal{Q}).$$

Similarly, we say an exchange matrix $\tilde{\mathcal{B}}'$ is *mutation equivalent* to another matrix $\tilde{\mathcal{B}}$ if $\tilde{\mathcal{B}}'$ is obtained by applying a sequence of mutations to $\tilde{\mathcal{B}}$.

An immediate check shows that $\mu_k(\mathbf{x}, \tilde{\mathcal{B}})$ is again a seed $\mu_k(\mathbf{y}, \mathcal{B})$ is a Y -seed, and a mutation is an involution, that is, its square is the identity. Also, note that the mutation on seeds does not change frozen variables x_{n+1}, \dots, x_m . Let \mathbb{T}_n denote the n -regular tree whose edges are labeled by $1, \dots, n$. Except for $n = 1$, there are infinitely many vertices on the tree \mathbb{T}_n . For example, we present regular trees \mathbb{T}_2 and \mathbb{T}_3 in Figure 7. A *cluster pattern* (or *seed pattern*) is an assignment

$$\mathbb{T}_n \rightarrow \{\text{seeds in } \mathbb{F}\}, \quad t \mapsto (\mathbf{x}_t, \tilde{\mathcal{B}}_t)$$

such that if $t \xrightarrow{k} t'$ in \mathbb{T}_n , then $\mu_k(\mathbf{x}_t, \tilde{\mathcal{B}}_t) = (\mathbf{x}_{t'}, \tilde{\mathcal{B}}_{t'})$. Let $\{(\mathbf{x}_t, \tilde{\mathcal{B}}_t)\}_{t \in \mathbb{T}_n}$ be a cluster pattern with $\mathbf{x}_t = (x_{1;t}, \dots, x_{m;t})$. Since the mutation does not change frozen variables, we may let $x_{n+1} = x_{n+1;t}, \dots, x_m = x_{m;t}$.

Definition 2.5 (cf. [26]). Let $\{(\mathbf{x}_t, \tilde{\mathcal{B}}_t)\}_{t \in \mathbb{T}_n}$ be a cluster pattern with $\mathbf{x}_t = (x_{1;t}, \dots, x_{m;t})$. The *cluster algebra* $\mathcal{A}(\{(\mathbf{x}_t, \tilde{\mathcal{B}}_t)\}_{t \in \mathbb{T}_n})$ is defined to be the $\mathbb{C}[x_{n+1}, \dots, x_m]$ -subalgebra of \mathbb{F} generated by all the cluster variables $\bigcup_{t \in \mathbb{T}_n} \{x_{1;t}, \dots, x_{n;t}\}$.

If we fix a vertex $t_0 \in \mathbb{T}_n$, then a cluster pattern $\{(\mathbf{x}_t, \tilde{\mathcal{B}}_t)\}_{t \in \mathbb{T}_n}$ is constructed from the seed $(\mathbf{x}_{t_0}, \tilde{\mathcal{B}}_{t_0})$. In this case, we call $(\mathbf{x}_{t_0}, \tilde{\mathcal{B}}_{t_0})$ an *initial seed*. Because of this reason, we simply denote by $\mathcal{A}(\mathbf{x}_{t_0}, \tilde{\mathcal{B}}_{t_0})$ the cluster algebra given by the cluster pattern constructed from the initial seed $(\mathbf{x}_{t_0}, \tilde{\mathcal{B}}_{t_0})$.

Example 2.6. Let $n = m = 2$. Suppose that an initial seed is given by

$$(\mathbf{x}_{t_0}, \tilde{\mathcal{B}}_{t_0}) = \left((x_1, x_2), \begin{pmatrix} 0 & 1 \\ -1 & 0 \end{pmatrix} \right).$$

We present the cluster pattern obtained by the initial seed $(\mathbf{x}_{t_0}, \tilde{\mathcal{B}}_{t_0})$.

$$\begin{array}{ccc}
\left((x_2, x_1), \begin{pmatrix} 0 & -1 \\ 1 & 0 \end{pmatrix} \right) & \sim & (\mathbf{x}_{t_0}, \tilde{\mathcal{B}}_{t_0}) = \left((x_1, x_2), \begin{pmatrix} 0 & 1 \\ -1 & 0 \end{pmatrix} \right) \\
\updownarrow \mu_1 & & \updownarrow \mu_1 \\
\left(\left(\frac{1+x_1}{x_2}, x_1 \right), \begin{pmatrix} 0 & 1 \\ -1 & 0 \end{pmatrix} \right) & & \left(\left(\frac{1+x_2}{x_1}, x_2 \right), \begin{pmatrix} 0 & -1 \\ 1 & 0 \end{pmatrix} \right) \\
\updownarrow \mu_2 & & \updownarrow \mu_2 \\
\left(\left(\frac{1+x_1}{x_2}, \frac{1+x_1+x_2}{x_1 x_2} \right), \begin{pmatrix} 0 & -1 \\ 1 & 0 \end{pmatrix} \right) & \xleftrightarrow{\mu_1} & \left(\left(\frac{1+x_2}{x_1}, \frac{1+x_1+x_2}{x_1 x_2} \right), \begin{pmatrix} 0 & 1 \\ -1 & 0 \end{pmatrix} \right)
\end{array}$$

Accordingly, we have

$$\mathcal{A}(\Sigma_{t_0}) = \mathcal{A}(\{\Sigma_t\}_{t \in \mathbb{T}_n}) = \mathbb{C} \left[x_1, x_2, \frac{1+x_2}{x_1}, \frac{1+x_1+x_2}{x_1 x_2}, \frac{1+x_1}{x_2} \right].$$

We notice that there are only five seeds in this case. Indeed, it becomes a cluster pattern of type \mathbf{A}_2 (see Example 2.13).

Remark 2.7. One can obtain a Y -pattern from a given cluster pattern as follows. Let $\{(\mathbf{x}_t, \tilde{\mathcal{B}}_t)\}_{t \in \mathbb{T}_n}$ be a cluster pattern with $\mathbf{x}_t = (x_{1;t}, \dots, x_{m;t})$. For $t \in \mathbb{T}_n$ and $i \in [n]$, we defined an assignment $(\mathbf{x}_t, \tilde{\mathcal{B}}_t) \xrightarrow{\Theta} (\hat{\mathbf{y}}_t, \mathcal{B})$, where $\hat{\mathbf{y}}_t = (\hat{y}_{1;t}, \dots, \hat{y}_{n;t})$ is defined by

$$\hat{y}_{i;t} = \prod_{j \in [m]} x_{j;t}^{b_{i,j}^{(t)}}$$

Here, $\tilde{\mathcal{B}}_t = (b_{i,j}^{(t)})$ and \mathcal{B}_t is the principal part of $\tilde{\mathcal{B}}_t$. Then the assignment $t \mapsto (\hat{\mathbf{y}}_t, \mathcal{B})$ provides a Y -pattern and commutes with the mutation maps, indeed, we obtain $\mu_k(\Theta(\mathbf{x}, \tilde{\mathcal{B}})) = \Theta(\mu_k(\mathbf{x}, \tilde{\mathcal{B}}))$. We notice that if the exchange matrix $\tilde{\mathcal{B}}_t$ has full rank, then the variables $\hat{y}_{1;t}, \dots, \hat{y}_{n;t}$ are algebraically independent. Note that the mutation preserves the rank of the exchange matrix as proved in [5, Lemma 3.2].

2.2. Cluster algebras of Dynkin type. The number of cluster variables in Example 2.6 is finite even though the number of vertices in the graph \mathbb{T}_2 is infinite. We call such cluster algebras of *finite type*. More precisely, we recall the following definition.

Definition 2.8 ([26]). A cluster algebra is said to be of *finite type* if it has finitely many cluster variables.

It has been realized that classifying finite type cluster algebras is related to studying exchange matrices. The *Cartan counterpart* $C(\mathcal{B}) = (c_{i,j})$ of the principal part \mathcal{B} of an exchange matrix $\tilde{\mathcal{B}}$ is defined by

$$c_{i,j} = \begin{cases} 2 & \text{if } i = j, \\ -|b_{i,j}| & \text{otherwise.} \end{cases}$$

Since \mathcal{B} is skew-symmetrizable, its Cartan counterpart $C(\mathcal{B})$ is symmetrizable.

We say that a quiver \mathcal{Q} is *acyclic* if it does not have directed cycles. Similarly, for a skew-symmetrizable matrix $\mathcal{B} = (b_{i,j})$, we say that it is *acyclic* if there are no sequences j_1, j_2, \dots, j_ℓ with $\ell \geq 3$ such that

$$b_{j_1, j_2}, b_{j_2, j_3}, \dots, b_{j_{\ell-1}, j_\ell}, b_{j_\ell, j_1} > 0.$$

We say a seed $\Sigma = (\mathbf{x}, \tilde{\mathcal{B}})$ is *acyclic* if so is its principal part \mathcal{B} .

Definition 2.9. For a finite or affine Dynkin type Z , we define a quiver \mathcal{Q} , a matrix $\tilde{\mathcal{B}}$, a cluster pattern $\{(\mathbf{x}_t, \tilde{\mathcal{B}}_t)\}_{t \in \mathbb{T}_n}$, a Y -pattern $\{(\mathbf{y}_t, \mathcal{B}_t)\}_{t \in \mathbb{T}_n}$, or a cluster algebra $\mathcal{A}(\mathbf{x}_{t_0}, \tilde{\mathcal{B}}_{t_0})$ of *type* Z as follows.

- (1) A quiver is of *type* Z if it is mutation equivalent to an *acyclic* quiver whose underlying graph is isomorphic to the Dynkin diagram of type Z .

- (2) A skew-symmetrizable matrix \mathcal{B} is of type Z if it is mutation equivalent to an acyclic skew-symmetrizable matrix whose Cartan counterpart $C(\mathcal{B})$ is isomorphic to the Cartan matrix of type Z .
- (3) A cluster pattern $\{(\mathbf{x}_t, \tilde{\mathcal{B}}_t)\}_{t \in \mathbb{T}_n}$ or a Y -pattern $\{(\mathbf{y}_t, \mathcal{B}_t)\}_{t \in \mathbb{T}_n}$ is of type Z if for some $t \in \mathbb{T}_n$, the Cartan counterpart $C(\mathcal{B}_t)$ is of type Z .
- (4) A cluster algebra $\mathcal{A}(\mathbf{x}_{t_0}, \tilde{\mathcal{B}}_{t_0})$ is of type Z if its cluster pattern is of type Z .

Here, we say that two matrices C_1 and C_2 are *isomorphic* if they are conjugate to each other via a permutation matrix, that is, $C_2 = P^{-1}C_1P$ for some permutation matrix P . One may wonder whether there exist exchange matrices in the same seed pattern having different Dynkin type. However, it is proved in [10, Corollary 4] that if two acyclic skew-symmetrizable matrices are mutation equivalent, then there exists a sequence of mutations from one to other such that intermediate skew-symmetrizable matrices are all acyclic. Indeed, if two acyclic skew-symmetrizable matrices are mutation equivalent, then their Cartan counterparts are isomorphic.

Proposition 2.10 (cf. [10, Corollary 4]). *Let \mathcal{B} and \mathcal{B}' be acyclic skew-symmetrizable matrices. Then the following are equivalent:*

- (1) *the Cartan matrices $C(\mathcal{B})$ and $C(\mathcal{B}')$ are isomorphic;*
- (2) *\mathcal{B} and \mathcal{B}' are mutation equivalent.*

Accordingly, a quiver, a matrix, a cluster pattern, or a cluster algebra of type Z is well-defined. The following theorem presents a classification of cluster algebras of finite type.

Theorem 2.11 ([26]). *Let $\{(\mathbf{x}_t, \tilde{\mathcal{B}}_t)\}_{t \in \mathbb{T}_n}$ be a cluster pattern with an initial seed $(\mathbf{x}_{t_0}, \tilde{\mathcal{B}}_{t_0})$. Let $\mathcal{A}(\mathbf{x}_{t_0}, \tilde{\mathcal{B}}_{t_0})$ be the corresponding cluster algebra. Then, the cluster algebra $\mathcal{A}(\mathbf{x}_{t_0}, \tilde{\mathcal{B}}_{t_0})$ is of finite type if and only if $\mathcal{A}(\mathbf{x}_{t_0}, \tilde{\mathcal{B}}_{t_0})$ is of finite Dynkin type.*

We provide a list of all of the irreducible finite type root systems and their Dynkin diagram in Table 1. In Tables 2 and 3, we present lists of standard affine root systems and twisted affine root systems, respectively. They are the same as presented in Tables Aff 1, Aff 2, and Aff 3 of [35, Chapter 4], and we denote by $\tilde{Z} = Z^{(1)}$. We notice that the number of vertices of the standard affine Dynkin diagram of type \tilde{Z}_{n-1} is n while we do not specify the vertex numbering.

We note that all Dynkin diagram of finite or affine type but \tilde{A}_{n-1} do not have (undirected) cycles. Accordingly, we may omit the acyclicity condition in Definition 2.9 except \tilde{A}_{n-1} -type. On the other hand, if a quiver is a directed n -cycle, then the corresponding Cartan counterpart is of type \tilde{A}_{n-1} while it is mutation equivalent to a quiver of type D_n (see Type IV in [45]).

The mutation equivalence classes of acyclic quivers of type \tilde{A}_{n-1} are described in [23, Lemma 6.8]. Let \mathcal{Q} and \mathcal{Q}' are two n -cycles for $n \geq 3$. Suppose that in \mathcal{Q} , there are p edges of one direction and $q = n - p$ edges of the opposite direction. Also, in \mathcal{Q}' , there are p' edges of one direction and $q' = n - p'$ edges of the opposite direction. Then two quivers \mathcal{Q} and \mathcal{Q}' are mutation equivalent if and only if the unordered pairs $\{p, q\}$ and $\{p', q'\}$ coincide. We say that a quiver \mathcal{Q} is of type $\tilde{A}_{p,q}$ if it has p edges of one direction and q edges of the opposite direction. We depict some examples for quivers of type $\tilde{A}_{p,q}$ in Figure 8.

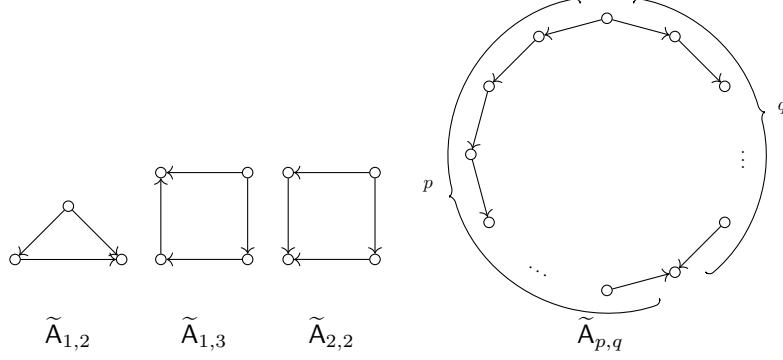
In what follows, we fix an ordering on the simple roots as in Table 1; our conventions agree with that in the standard textbook of Humphreys [34].

For a Dynkin type Z , we say that Z is *simply-laced* if its Dynkin diagram has only single edges, otherwise, Z is *non-simply-laced*. Recall that the Cartan matrix associated to a Dynkin diagram Z can be read directly from the diagram Z as follows:

$\circ \text{---} \circ$ $i \qquad j$	$\circ \text{--}\!\!\!\rightarrow \!\!\!\circ$ $i \qquad j$	$\circ \text{--}\!\!\!\Rightarrow \!\!\!\circ$ $i \qquad j$	$\circ \text{--}\!\!\!\Leftarrow \!\!\!\circ$ $i \qquad j$	$\circ \text{--}\!\!\!\Leftarrow \!\!\!\circ$ $i \qquad j$
$c_{i,j} = -1$	$c_{i,j} = -2$	$c_{i,j} = -3$	$c_{i,j} = -4$	$c_{i,j} = -2$
$c_{j,i} = -1$	$c_{j,i} = -1$	$c_{j,i} = -1$	$c_{j,i} = -1$	$c_{j,i} = -2$

For example, the Cartan matrix $(c_{i,j})$ of the diagram $\circ \text{--}\!\!\!\Leftarrow \!\!\!\circ$ of type G_2 is

$$\begin{pmatrix} 2 & -1 \\ -3 & 2 \end{pmatrix}. \quad (2.1)$$

FIGURE 8. Quivers of type $\tilde{A}_{p,q}$.

Φ	Dynkin diagram
A_n ($n \geq 1$)	$\circ - \circ - \circ \cdots \circ - \circ$
B_n ($n \geq 2$)	$\circ - \circ \cdots \circ \rightleftarrows \circ$
C_n ($n \geq 3$)	$\circ - \circ \cdots \circ \rightleftarrows \circ$
D_n ($n \geq 4$)	$\circ - \circ \cdots \circ \begin{matrix} \nearrow \circ \\ \searrow \circ \end{matrix}$
E_6	$\begin{matrix} & \circ & \\ & & \\ \circ - \circ - \circ & - \circ & - \circ - \circ \\ & & \\ & \circ & \end{matrix}$
E_7	$\begin{matrix} & \circ & \\ & & \\ \circ - \circ - \circ & - \circ & - \circ - \circ - \circ \\ & & \\ & \circ & \end{matrix}$
E_8	$\begin{matrix} & \circ & \\ & & \\ \circ - \circ - \circ & - \circ & - \circ - \circ - \circ - \circ \\ & & \\ & \circ & \end{matrix}$
F_4	$\circ \rightleftarrows \circ \rightleftarrows \circ - \circ$
G_2	$\circ \rightleftarrows \circ$

TABLE 1. Dynkin diagrams of finite type

Therefore, for each non-simply-laced Dynkin diagram Z , any exchange matrix \mathcal{B} of type Z is *not* skew-symmetric but skew-symmetrizable. Hence it never comes from any quiver.

Assumption 2.12. Throughout this paper, we assume that for any cluster algebra, the principal part \mathcal{B}_{t_0} of the initial exchange matrix is acyclic of *finite or affine Dynkin* type unless mentioned otherwise.

In Table 4, we provide enumeration on the number of cluster variables and clusters in each cluster algebra of finite (irreducible) type (cf. [24, Figure 5.17]).

Example 2.13. Continuing Example 2.6, the Cartan counterpart of the principal part \mathcal{B}_{t_0} is given by

$$C(\mathcal{B}_{t_0}) = \begin{pmatrix} 2 & -1 \\ -1 & 2 \end{pmatrix},$$

which is the Cartan matrix of type A_2 . Accordingly, by Theorem 2.11, the cluster algebra $\mathcal{A}(\mathbf{x}_{t_0}, \tilde{\mathcal{B}}_{t_0})$ is of finite type. Indeed, there are only five seeds in the seed pattern.

2.3. Folding. Under certain conditions, one can *fold* cluster patterns to produce new ones. This procedure is used to study cluster algebras of non-simply-laced type from those of simply-laced

Φ	Dynkin diagram
\tilde{A}_1	
$\tilde{A}_{n-1} (n \geq 3)$	
$\tilde{B}_{n-1} (n \geq 4)$	
$\tilde{C}_{n-1} (n \geq 3)$	
$\tilde{D}_{n-1} (n \geq 5)$	
\tilde{E}_6	
\tilde{E}_7	
\tilde{E}_8	
\tilde{F}_4	
\tilde{G}_2	

TABLE 2. Dynkin diagrams of standard affine root systems

Φ	Dynkin diagram
$A_2^{(2)}$	
$A_{2(n-1)}^{(2)} (n \geq 3)$	
$A_{2(n-1)-1}^{(2)} (n \geq 4)$	
$D_n^{(2)} (n \geq 3)$	
$E_6^{(2)}$	
$D_4^{(3)}$	

TABLE 3. Dynkin diagrams of twisted affine root systems

type (see Figure 9 and Table 5). In this section, we recall *folding* of cluster algebras from [24]. We also refer the reader to [19].

Let \mathcal{Q} be a quiver on $[m]$. Let G be a finite group acting on the set $[m]$. The notation $i \sim i'$ will mean that i and i' lie in the same G -orbit. To study folding of cluster algebras, we prepare some terminologies.

Φ	A_n	B_n	C_n	D_n	E_6	E_7	E_8	F_4	G_2
#seeds	$\frac{1}{n+2} \binom{2n+2}{n+1}$	$\binom{2n}{n}$	$\binom{2n}{n}$	$\frac{3n-2}{n} \binom{2n-2}{n-1}$	833	4160	25080	105	8
#clvar	$\frac{n(n+3)}{2}$	$n(n+1)$	$n(n+1)$	n^2	42	70	128	28	8

TABLE 4. Enumeration of seeds and cluster variables

We denote by $\tilde{B} = \tilde{B}(\mathcal{Q})$ the submatrix $(b_{i,j})_{1 \leq i \leq m, 1 \leq j \leq n}$ of the adjacency matrix $(b_{i,j})_{1 \leq i,j \leq m}$ of the quiver \mathcal{Q} . Also, we denote by $B = B(\mathcal{Q})$ the principal part of $\tilde{B}(\mathcal{Q})$. For each $g \in G$, let $\mathcal{Q}' = g \cdot \mathcal{Q}$ be the quiver such that $\tilde{B}(\mathcal{Q}') = (b'_{i,j})$ is given by

$$b'_{i,j} = b_{g(i),g(j)}.$$

Definition 2.14 (cf. [24, §4.4] and [19, §3]). Let \mathcal{Q} be a quiver on $[m]$ and G a finite group acting on the set $[m]$.

- (1) A quiver \mathcal{Q} is *G-invariant* if $g \cdot \mathcal{Q} = \mathcal{Q}$ for any $g \in G$.
- (2) A *G-invariant* quiver \mathcal{Q} is *G-admissible* if
 - (a) for any $i \sim i'$, index i is mutable if and only if so is i' ;
 - (b) for mutable indices $i \sim i'$, we have $b_{i,i'} = 0$;
 - (c) for any $i \sim i'$, and any mutable j , we have $b_{i,j}b_{i',j} \geq 0$.
- (3) For a *G-admissible* quiver \mathcal{Q} , we call a *G-orbit mutable* (respectively, *frozen*) if it consists of mutable (respectively, frozen) vertices.

For a *G-admissible* quiver \mathcal{Q} , we define the matrix $\tilde{B}^G = \tilde{B}(\mathcal{Q})^G = (b_{I,J}^G)$ whose rows (respectively, columns) are labeled by the *G-orbits* (respectively, mutable *G-orbits*) by

$$b_{I,J}^G = \sum_{i \in I} b_{i,j}$$

where j is an arbitrary index in J . We then say \tilde{B}^G is obtained from \tilde{B} (or from the quiver \mathcal{Q}) by *folding* with respect to the given *G-action*.

Remark 2.15. We note that the *G-admissibility* and the folding can also be defined for exchange matrices.

Example 2.16. Let \mathcal{Q} be a quiver of type D_4 given as follows.

$$\begin{array}{c}
 \begin{array}{c} \text{green } 2 \\ \text{orange } 1 \rightarrow \text{green } 3 \\ \text{orange } 1 \rightarrow \text{green } 4 \end{array} \quad \rightsquigarrow \quad \tilde{B}(\mathcal{Q}) = \begin{pmatrix} 0 & -1 & -1 & -1 \\ 1 & 0 & 0 & 0 \\ 1 & 0 & 0 & 0 \\ 1 & 0 & 0 & 0 \end{pmatrix}
 \end{array}$$

The finite group $G = \mathbb{Z}/3\mathbb{Z}$ acts on $[4]$ by sending $2 \mapsto 3 \mapsto 4 \mapsto 2$ and $1 \mapsto 1$. Here, we decorate vertices of the quiver \mathcal{Q} with green and orange colors for presenting sources and sinks, respectively. One may check that the quiver \mathcal{Q} is *G-admissible*. By setting $I_1 = \{1\}$ and $I_2 = \{2, 3, 4\}$, we obtain

$$\begin{aligned}
 b_{I_1, I_2}^G &= \sum_{i \in I_1} b_{i,2} = b_{1,2} = -1, \\
 b_{I_2, I_1}^G &= \sum_{i \in I_2} b_{i,1} = b_{2,1} + b_{3,1} + b_{4,1} = 3.
 \end{aligned}$$

Accordingly, we obtain the matrix $\tilde{B}^G = \begin{pmatrix} 0 & -1 \\ 3 & 0 \end{pmatrix}$ whose Cartan counterpart is the Cartan matrix of type G_2 (cf. (2.1)).

For a G -admissible quiver \mathcal{Q} and a mutable G -orbit I , we consider a composition of mutations given by

$$\mu_I = \prod_{i \in I} \mu_i$$

which is well-defined because of the definition of admissible quivers (cf. Remark 2.4). If $\mu_I(\mathcal{Q})$ is again G -admissible, then we have that

$$(\mu_I(\tilde{\mathcal{B}}))^G = \mu_I(\tilde{\mathcal{B}}^G).$$

We notice that the quiver $\mu_I(\mathcal{Q})$ is *not* G -admissible in general. Therefore, we present the following definition.

Definition 2.17. Let G be a group acting on the vertex set of a quiver \mathcal{Q} . We say that \mathcal{Q} is *globally foldable* with respect to G if \mathcal{Q} is G -admissible and moreover for any sequence of mutable G -orbits I_1, \dots, I_ℓ , the quiver $(\mu_{I_\ell} \dots \mu_{I_1})(\mathcal{Q})$ is G -admissible.

For a globally foldable quiver, we can fold all the seeds in the corresponding seed pattern. Let \mathbb{F}^G be the field of rational functions in $\#([m]/G)$ independent variables. Let $\psi: \mathbb{F} \rightarrow \mathbb{F}^G$ be a surjective homomorphism. A seed $(\mathbf{x}, \tilde{\mathcal{B}})$ or a Y -seed $(\mathbf{y}, \mathcal{B})$ is called (G, ψ) -invariant or *admissible* if

- \mathcal{Q} is a G -invariant or admissible quiver, respectively;
- for any $i \sim i'$, we have $\psi(x_i) = \psi(x_{i'})$ or $\psi(y_i) = \psi(y_{i'})$.

In this situation, we define new “folded” seed $(\mathbf{x}, \tilde{\mathcal{B}})^G = (\mathbf{x}^G, \tilde{\mathcal{B}}^G)$ and Y -seed $(\mathbf{y}, \mathcal{B})^G = (\mathbf{y}^G, \mathcal{B}^G)$ in \mathbb{F}^G whose exchange matrix is given as before and cluster variables $\mathbf{x}^G = (x_I)$ and $\mathbf{y}^G = (y_I)$ are indexed by the G -orbits and given by $x_I = \psi(x_i)$ and $y_I = \psi(y_i)$.

We notice that for a (G, ψ) -admissible seed $(\mathbf{x}, \tilde{\mathcal{B}})$ or a (G, ψ) -admissible Y -seed $(\mathbf{y}, \mathcal{B})$, the folding process is equivariant under the orbit-wise mutation, that is, for any mutable G -orbit I , we have

$$(\mu_I(\mathbf{x}, \tilde{\mathcal{B}}))^G = \mu_I((\mathbf{x}, \tilde{\mathcal{B}})^G) \quad \text{and} \quad (\mu_I(\mathbf{y}, \mathcal{B}))^G = \mu_I((\mathbf{y}, \mathcal{B})^G).$$

Proposition 2.18 (cf. [24, Corollary 4.4.11]). *Let \mathcal{Q} be a quiver which is globally foldable with respect to a group G acting on the set of its vertices. Let $(\mathbf{x}, \tilde{\mathcal{B}})$ and $(\mathbf{y}, \mathcal{B})$ be a seed and a Y -seed in the field \mathbb{F} of rational functions freely generated by $\mathbf{x} = (x_1, \dots, x_m)$. Then we have the following.*

- (1) *Define $\psi: \mathbb{F} \rightarrow \mathbb{F}^G$ so that $(\mathbf{x}, \tilde{\mathcal{B}})$ is a (G, ψ) -admissible seed. Then, for any mutable G -orbits I_1, \dots, I_ℓ , the seed $(\mu_{I_\ell} \dots \mu_{I_1})(\mathbf{x}, \tilde{\mathcal{B}})$ is (G, ψ) -admissible, and moreover the folded seeds $((\mu_{I_\ell} \dots \mu_{I_1})(\mathbf{x}, \tilde{\mathcal{B}}))^G$ form a seed pattern in \mathbb{F}^G with the initial seed $(\mathbf{x}, \tilde{\mathcal{B}})^G = (\mathbf{x}^G, \tilde{\mathcal{B}}^G)$.*
- (2) *Define $\psi: \mathbb{F} \rightarrow \mathbb{F}^G$ so that $(\mathbf{y}, \mathcal{B})$ is a (G, ψ) -admissible seed. Then, for any mutable G -orbits I_1, \dots, I_ℓ , the Y -seed $(\mu_{I_\ell} \dots \mu_{I_1})(\mathbf{y}, \mathcal{B})$ is (G, ψ) -admissible, and moreover the folded Y -seeds $((\mu_{I_\ell} \dots \mu_{I_1})(\mathbf{y}, \mathcal{B}))^G$ form a Y -pattern in \mathbb{F}^G with the initial seed $(\mathbf{y}, \mathcal{B})^G = (\mathbf{y}^G, \mathcal{B}^G)$.*

Example 2.19. The quiver in Example 2.16 is globally foldable, and moreover the corresponding seed pattern is of type G_2 . In fact, seed patterns of type BCFG are obtained by folding quivers of type ADE; seed patterns of type $\tilde{B}\tilde{C}\tilde{F}\tilde{G}$ are obtained by folding quivers of type $\tilde{D}\tilde{E}$ (cf. [22]). In Figures 9 and 10, we present the corresponding quivers of type ADE and type \tilde{E} . We decorate vertices of quivers with green and orange colors for presenting source and sink, respectively. As one may see, we have to put arrows on the Dynkin diagram alternately. The alternating colorings on quivers of type ADE provide that on quivers of type BCFG as displayed in the right column of Figure 9. Foldings between simply-laced and non-simply-laced finite and affine Dynkin diagrams are given in Table 5.

For a quiver of type ADE, one can prove that the G -invariance is equivalent to the G -admissible as follows:

Theorem 2.20. *Let \mathcal{Q} be a quiver of type ADE, which is invariant under the G -action given by Figure 9. Then the \mathcal{Q} is G -admissible.*

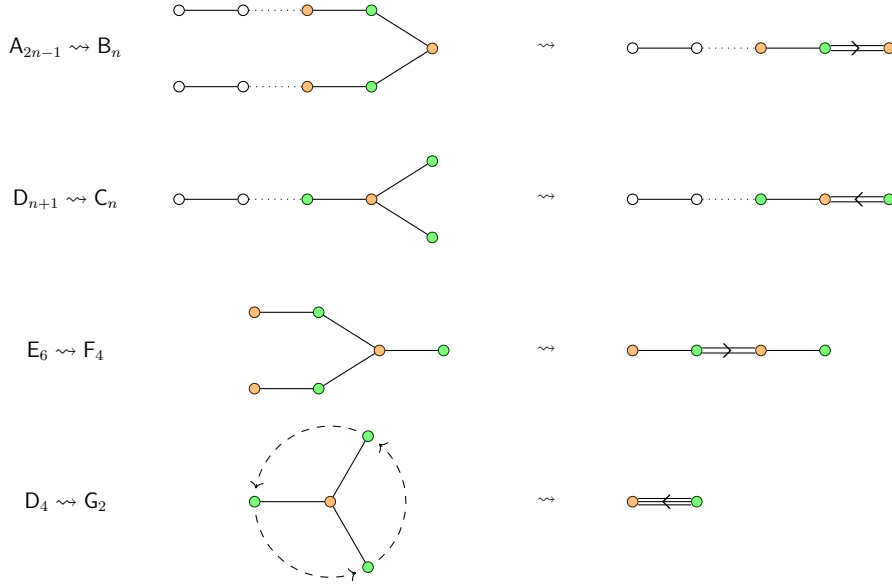


FIGURE 9. Foldings in Dynkin diagrams of finite type (for seed patterns)

Z	A_{2n-1}	D_{n+1}	E_6	D_4
G	$\mathbb{Z}/2\mathbb{Z}$	$\mathbb{Z}/2\mathbb{Z}$	$\mathbb{Z}/2\mathbb{Z}$	$\mathbb{Z}/3\mathbb{Z}$
Z^G	B_n	C_n	F_4	G_2

Z	$\tilde{A}_{2,2}$	$\tilde{A}_{n,n}$	\tilde{D}_4	\tilde{D}_n	\tilde{D}_{2n}	\tilde{E}_6	\tilde{E}_7
G	$\mathbb{Z}/2\mathbb{Z}$	$\mathbb{Z}/2\mathbb{Z}$	$(\mathbb{Z}/2\mathbb{Z})^2$	$\mathbb{Z}/3\mathbb{Z}$	$\mathbb{Z}/2\mathbb{Z}$	$\mathbb{Z}/2\mathbb{Z}$	$\mathbb{Z}/2\mathbb{Z}$
Z^G	\tilde{A}_1	$D_{n+1}^{(2)}$	$A_2^{(2)}$	$D_4^{(3)}$	\tilde{C}_{n-2}	$A_{2(n-1)-1}^{(2)}$	\tilde{B}_n

TABLE 5. Foldings appearing in finite and affine Dynkin diagrams

The proof of Theorem 2.20 is given in Appendix A.

As we saw in Definition 2.14, if a seed $\Sigma = (\mathbf{x}, Q)$ is (G, ψ) -admissible, then Σ is (G, ψ) -invariant. The converse holds when we consider the foldings presented in Table 5, and moreover they form the folded cluster pattern.

Theorem 2.21 ([2]). *Let (Z, G, Z^G) be a triple given by a column of Table 5. Let $\Sigma_{t_0} = (\mathbf{x}_{t_0}, Q_{t_0})$ be a seed in the field \mathbb{F} . Suppose that Q_{t_0} is of type Z . Define $\psi: \mathbb{F} \rightarrow \mathbb{F}^G$ so that Σ_{t_0} is a (G, ψ) -admissible seed. Then, for any seed $\Sigma = (\mathbf{x}, Q)$ in the cluster pattern, if the quiver Q is G -invariant, then it is G -admissible. Moreover, any (G, ψ) -invariant seed $\Sigma = (\mathbf{x}, Q)$ can be reached with a sequence of orbit mutations from the initial seed. Indeed, the set of such seeds forms the cluster pattern of the ‘folded’ cluster algebra $\mathcal{A}(\Sigma_{t_0}^G)$ of type Z^G .*

2.4. Combinatorics of exchange graphs. The *exchange graph* of a cluster pattern or a Y -pattern is the n -regular (finite or infinite) connected graph whose vertices are the seeds of the cluster pattern and whose edges connect the seeds related by a single mutation. In this section, we recall the combinatorics of exchange graphs which will be used later. For more details, we refer the reader to [26, 27, 28].

Definition 2.22 (Exchange graphs). Exchange graphs for seed patterns or Y -patterns are defined as follows.

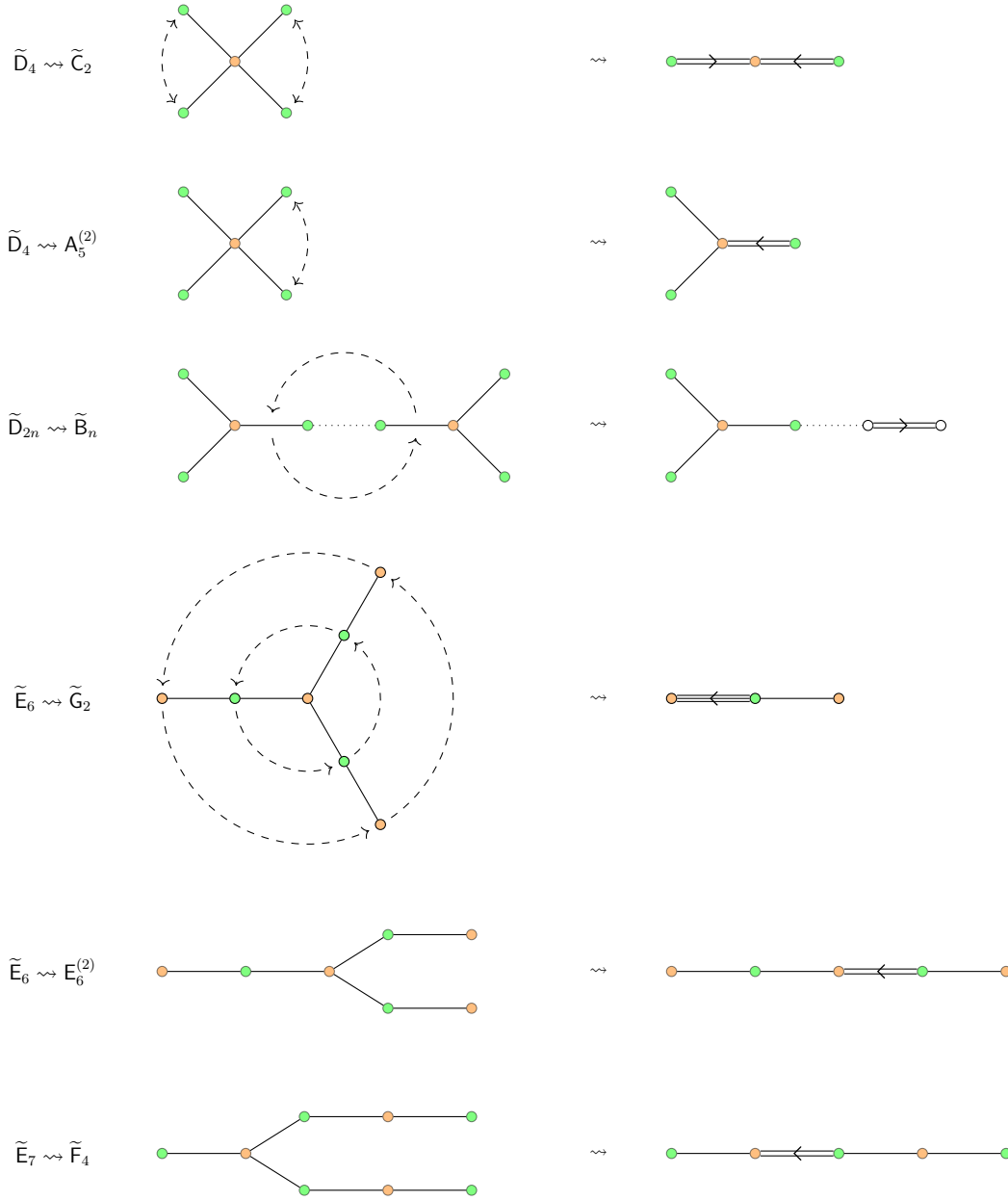


FIGURE 10. Foldings in Dynkin diagrams of affine type (for seed patterns)

- (1) The *exchange graph* $\text{Ex}(\{(\mathbf{x}_t, \tilde{\mathcal{B}}_t)\}_{t \in \mathbb{T}_n})$ of the cluster pattern $\{(\mathbf{x}_t, \tilde{\mathcal{B}}_t)\}_{t \in \mathbb{T}_n}$ is a quotient of the tree \mathbb{T}_n modulo the equivalence relation on vertices defined by setting $t \sim t'$ if and only if $(\mathbf{x}_t, \tilde{\mathcal{B}}_t) \sim (\mathbf{x}_{t'}, \tilde{\mathcal{B}}_{t'})$.
- (2) The *exchange graph* $\text{Ex}(\{(\mathbf{y}_t, \mathcal{B}_t)\}_{t \in \mathbb{T}_n})$ of the Y -pattern $\{(\mathbf{y}_t, \mathcal{B}_t)\}_{t \in \mathbb{T}_n}$ is a quotient of the tree \mathbb{T}_n modulo the equivalence relation on vertices defined by setting $t \sim t'$ if and only if $(\mathbf{y}_t, \mathcal{B}_t) \sim (\mathbf{y}_{t'}, \mathcal{B}_{t'})$.

For example, the exchange graph in Example 2.6 is a cycle graph with 5 vertices. As we already have seen in Theorem 2.11, cluster algebras of finite type are classified by Cartan matrices of finite type. Moreover, for a cluster algebra of finite or affine type, the exchange graph depends only on the exchange matrix (see Theorem 2.24). To explain this observation, we need some terminologies.

For $\Sigma_{t_0} = (\mathbf{x}_{t_0}, \tilde{\mathcal{B}}_{t_0})$, the cluster algebra $\mathcal{A}(\Sigma_{t_0})$ is said to have *principal coefficients* if the exchange matrix $\tilde{\mathcal{B}}_{t_0}$ is a $(2n \times n)$ -matrix of the form $\begin{pmatrix} \mathcal{B}_{t_0} \\ \mathcal{I}_n \end{pmatrix}$, and have *trivial coefficients* if $\tilde{\mathcal{B}}_{t_0} = \mathcal{B}_{t_0}$. Here, \mathcal{I}_n is the identity matrix of size $n \times n$. We recall the following result on the combinatorics of exchange graphs.

Theorem 2.23 ([28, Theorem 4.6]). *The exchange graph of an arbitrary cluster pattern $\{(\mathbf{x}_t, \tilde{\mathcal{B}}_t)\}_{t \in \mathbb{T}_n}$ is covered by the exchange graph of the cluster pattern $\{(\mathbf{x}_t, \tilde{\mathcal{B}}'_t)\}_{t \in \mathbb{T}_n}$ having principal coefficients and the set of principal part of exchange matrices are the same.*

One of the direct consequence is that the exchange graph of the cluster pattern $\{(\mathbf{x}_t, \tilde{\mathcal{B}}_t)\}_{t \in \mathbb{T}_n}$ having trivial coefficients is covered by the exchange graph of the cluster pattern whose initial exchange matrix has the principal part $\tilde{\mathcal{B}}_{t_0}$. Therefore, for a fixed principal part of the exchange matrix, the cluster pattern having principal coefficients has the largest exchange graph while that having trivial coefficients has the smallest one (see [28, Section 4]).

However, it is unknown whether the largest exchange graph is strictly larger than the smallest one or not. Indeed, it is conjectured in [28, Conjecture 4.3] that the exchange graph of a cluster pattern is determined by the initial principal part \mathcal{B}_{t_0} only. The conjecture is confirmed for finite cases [26] or exchange matrices coming from quivers [16]. We furthermore extend this result to cluster algebras whose initial exchange matrices are of affine type.

Theorem 2.24 (cf. [26, Theorem 1.13] and [16, Theorem 4.6]). *Let $\Sigma_{t_0} = (\mathbf{x}_{t_0}, \tilde{\mathcal{B}}_{t_0})$ be an initial seed. If the principal part \mathcal{B}_{t_0} of $\tilde{\mathcal{B}}_{t_0}$ is of finite or affine type, then the exchange graph of the cluster pattern $\{(\mathbf{x}_t, \tilde{\mathcal{B}}_t)\}_{t \in \mathbb{T}_n}$ only depends on \mathcal{B}_{t_0} .*

Proof. We first notice that the statement holds if the principal part \mathcal{B}_{t_0} is of finite type [26, Theorem 1.13] or exchange matrices are obtained from quivers [16, Theorem 4.6]. It is enough to consider the case when the principal part is of *non-simply-laced affine type*. Let (Z, G, Z^G) be a column in Table 5. Let $\mathcal{Q}(Z)$ be the quiver of type Z and $\mathcal{B}(Z) = \mathcal{B}(\mathcal{Q}(Z))$ be the adjacency matrix of $\mathcal{Q}(Z)$, which is a square matrix of size n . Let $\tilde{\mathcal{B}}(Z) = \begin{pmatrix} \mathcal{B}(Z) \\ \mathcal{I}_n \end{pmatrix}$ be the $(2n \times n)$ matrix having principal coefficients whose principal part is $\mathcal{B}(Z)$. On the other hand, we consider a quiver $\overline{\mathcal{Q}}(X)$ by adding $n^G := \#([n]/G)$ frozen vertices and arrows. Here, each frozen vertex is indexed by a G -orbit and we draw an arrow from the frozen vertex to each mutable vertex in the corresponding G -orbit. For algebraic independent elements $\mathbf{x} = (x_1, \dots, x_n)$, $\overline{\mathbf{x}} = (x_1, \dots, x_n, x_{n+1}, \dots, x_{n+n^G})$, and $\tilde{\mathbf{x}} = (x_1, \dots, x_n, x_{n+1}, \dots, x_{2n})$ in \mathbb{F} , we obtain seeds

$$\tilde{\Sigma}_{t_0} = (\tilde{\mathbf{x}}, \tilde{\mathcal{B}}(Z)), \quad \overline{\Sigma}_{t_0} = (\overline{\mathbf{x}}, \mathcal{B}(\overline{\mathcal{Q}}(Z))), \quad \text{and} \quad \Sigma_{t_0} = \mathcal{A}(\mathbf{x}, \mathcal{B}(Z)).$$

Since the exchange matrices come from quivers, the exchange graphs given by seeds $\tilde{\Sigma}_{t_0}, \overline{\Sigma}_{t_0}, \Sigma_{t_0}$ are isomorphic. Indeed, we have

$$\{\tilde{\Sigma}_t\}_{t \in \mathbb{T}_n} / \sim = \{\overline{\Sigma}_t\}_{t \in \mathbb{T}_n} / \sim = \{\Sigma_t\}_{t \in \mathbb{T}_n} / \sim \quad (2.2)$$

Extending the action of G on \mathcal{Q} of type Z to $\overline{\mathcal{Q}}(Z)$ such that G acts trivially on frozen vertices, the quiver $\overline{\mathcal{Q}}(Z)$ becomes a globally foldable quiver with respect to G (see [24, Lemma 5.5.3]). Moreover, via $\psi: \mathbb{F} \rightarrow \mathbb{F}^G$, the folded seed $\overline{\Sigma}_{t_0}^G = (\overline{\mathbf{x}}, \overline{\mathcal{Q}}(Z))^G$ produces the principal coefficient cluster algebra of type Z^G . This produces the following diagram.

$$\begin{array}{ccccc} \{\tilde{\Sigma}_t\}_{t \in \mathbb{T}_n} / \sim & \xrightarrow{=} & \{\overline{\Sigma}_t\}_{t \in \mathbb{T}_n} / \sim & \xrightarrow{=} & \{\Sigma_t\}_{t \in \mathbb{T}_n} / \sim \\ & & \uparrow & & \uparrow \\ & & \{(G, \psi)\text{-admissible seeds } \overline{\Sigma}_t\} / \sim & \xrightarrow{\succ} & \{(G, \psi)\text{-admissible seeds } \Sigma_t\} / \sim \\ & & \parallel & & \parallel \\ & & \{\overline{\Sigma}_t^G\}_{t \in \mathbb{T}_n} / \sim & \xrightarrow{\succ} & \{\Sigma_t^G\}_{t \in \mathbb{T}_n} / \sim \end{array}$$

The equalities on the top row are obtained by (2.2). The surjectivity in the bottom row is induced by the maximality of the exchange graph of a cluster algebra having principal coefficients in Theorem 2.23. Moreover, the equalities connecting the second and third rows are given by Theorem 2.21. This proves the theorem. \square

We recall from [11] the relation between the cluster pattern and Y -pattern having the *same* initial exchange matrix.

Proposition 2.25 ([11, Theorem 2.5]). *Let $(\mathbf{y}_{t_0}, \mathcal{B}_{t_0})$ be a Y -seed and let $\{(\mathbf{y}_t, \mathcal{B}_t)\}_{t \in \mathbb{T}_n}$ be the Y -pattern. Let $(\mathbf{x}_{t_0}, \tilde{\mathcal{B}}_{t_0})$ be a cluster seed such that the principal part of the exchange matrix $\tilde{\mathcal{B}}_{t_0}$ is \mathcal{B}_{t_0} and let $\{(\mathbf{x}_t, \tilde{\mathcal{B}}_t)\}_{t \in \mathbb{T}_n}$ be the cluster pattern. Suppose that the initial variables $y_{1;t_0}, \dots, y_{n;t_0}$ are algebraically independent. Then, we have*

$$\text{Ex}(\{(\mathbf{x}_t, \tilde{\mathcal{B}}_t)\}_{t \in \mathbb{T}_n}) = \text{Ex}(\{(\mathbf{y}_t, \mathcal{B}_t)\}_{t \in \mathbb{T}_n}).$$

Because of Assumption 2.12, Theorem 2.24, and Proposition 2.25, when the initial variables $y_{1;t_0}, \dots, y_{n;t_0}$ are algebraically independent, all the following exchange graphs are the same.

$$\text{Ex}(\{(\mathbf{x}_t, \tilde{\mathcal{B}}_t)\}_{t \in \mathbb{T}_n}) = \text{Ex}(\{(\mathbf{x}_t, \mathcal{B}_t)\}_{t \in \mathbb{T}_n}) = \text{Ex}(\{(\mathbf{y}_t, \mathcal{B}_t)\}_{t \in \mathbb{T}_n}).$$

We simply denote the above exchange graphs with the associated root system Φ by

$$\text{Ex}(\Phi) = \text{Ex}(\{(\mathbf{x}_t, \tilde{\mathcal{B}}_t)\}_{t \in \mathbb{T}_n}) = \text{Ex}(\{(\mathbf{x}_t, \mathcal{B}_t)\}_{t \in \mathbb{T}_n}) = \text{Ex}(\{(\mathbf{y}_t, \mathcal{B}_t)\}_{t \in \mathbb{T}_n}). \quad (2.3)$$

Since the exchange graph of a cluster pattern of finite type and that of a Y -pattern having the same type are the same, we will mainly treat exchange graphs of cluster patterns of finite or affine type from now on.

Let Φ be the root system defined by the Cartan counterpart of \mathcal{B} . It is proved in [26] and [40] that there is a bijective correspondence between a subset $\Phi_{\geq -1} \subset \Phi$, called *almost positive roots*, and the set of cluster variables.

$$\Phi_{\geq -1} \xleftrightarrow{1:1} \{\text{cluster variables in } \mathcal{A} \text{ of type } Z\} \quad (2.4)$$

More precisely, one may associate the set $-\Pi$ of negative simple roots with the set of cluster variables $x_{1;t_0}, \dots, x_{n;t_0}$ in the initial seed $(\mathbf{x}_{t_0}, \tilde{\mathcal{B}}_{t_0})$; a positive root $\sum_{i=1}^n d_i \alpha_i$ is associated to a (non-initial) cluster variable of the form

$$\frac{f(\mathbf{x}_{t_0})}{x_{1;t_0}^{d_1} \cdots x_{n;t_0}^{d_n}}, \quad f(\mathbf{x}_{t_0}) \in \mathbb{C}[x_{1;t_0}, \dots, x_{m;t_0}].$$

Accordingly, each vertex of the exchange graph $\text{Ex}(\Phi)$ corresponds to an n -subset of $\Phi_{\geq -1}$. We notice that when Φ is of finite type, the set $\Phi_{\geq -1}$ is given by $\Phi_{\geq -1} := \Phi^+ \cup -\Pi$. Here, Φ^+ is the set of positive roots and $\Pi = \{\alpha_1, \dots, \alpha_n\}$ is the set of simple roots.

To study the combinatorics of exchange graphs, we prepare some terminologies. Let Φ be a rank n root system. For every subset $J \subset [n]$, let $\Phi(J)$ denote the root subsystem of Φ spanned by the set of simple roots $\{\alpha_i \mid i \in J\}$. Indeed, the Dynkin diagram of $\Phi(J)$ is the full subdiagram on the vertices in J . Note that $\Phi(J)$ may not be irreducible even if Φ is.

A *Coxeter element* is the product of all simple reflections. The order h of a Coxeter element in W is called the *Coxeter number* of Φ . We present the known formula of Coxeter numbers h in Table 6 (see [7, Appendix]).

The Dynkin diagrams of finite or affine root systems do not have cycles except of type \tilde{A}_{n-1} for $n \geq 3$. We consider *bipartite coloring* on Dynkin diagrams except of type \tilde{A} , that is, we have a function $\varepsilon: [n] \rightarrow \{+, -\}$, called a *coloring*, such that any two vertices i and j connected by an edge have different colors. Since we are considering tree-shaped diagrams, they admit

Φ	A_n	B_n	C_n	D_n	E_6	E_7	E_8	F_4	G_2
h	$n+1$	$2n$	$2n$	$2n-2$	12	18	30	12	6

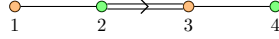
TABLE 6. Coxeter numbers

bipartite colorings. We notice that a bipartite coloring on a Dynkin diagram decides a *bipartite* skew-symmetrizable matrix $\mathcal{B} = (b_{i,j})$ of the same type by setting

$$b_{i,j} > 0 \iff \varepsilon(i) = + \text{ and } \varepsilon(j) = -. \quad (2.5)$$

Here, a skew-symmetrizable matrix is called *bipartite* if there exists a coloring ε satisfying (2.5). Moreover, for a simply-laced Dynkin diagram, a bipartite coloring defines a *bipartite quiver*, that is, each vertex of the quiver is either source or sink. More precisely, we let i be a source if $\varepsilon(i) = +$; otherwise, a sink.

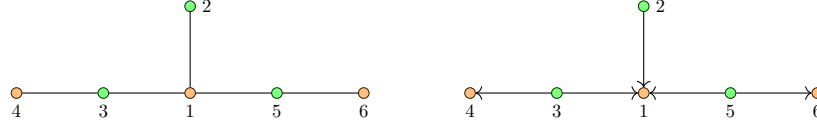
Example 2.26. Consider the coloring on the Dynkin diagram of F_4 .



Here, green nodes have color $+$; orange nodes have color $-$. This coloring gives a skew-symmetrizable matrix \mathcal{B} whose Cartan counterpart $C(\mathcal{B})$ is of type F_4 .

$$\mathcal{B} = \begin{pmatrix} 0 & -1 & 0 & 0 \\ 1 & 0 & 2 & 0 \\ 0 & -1 & 0 & -1 \\ 0 & 0 & 1 & 0 \end{pmatrix}, \quad C(\mathcal{B}) = \begin{pmatrix} 2 & -1 & 0 & 0 \\ -1 & 2 & -2 & 0 \\ 0 & -1 & 2 & -1 \\ 0 & 0 & -1 & 2 \end{pmatrix}.$$

The coloring on the Dynkin diagram of E_6 as shown on the left provides the bipartite quiver like the one on the right.



Let I_+ and I_- be two parts of the set of vertices of the Dynkin diagram given by a bipartite coloring; they are determined uniquely up to renaming. Consider the composition $\mu_{\mathcal{Q}} = \mu_+ \mu_-$ of a sequence of mutations where

$$\mu_{\varepsilon} = \prod_{i \in I_{\varepsilon}} \mu_i \quad \text{for } \varepsilon \in \{+, -\},$$

which is well-defined (cf. Remark 2.4). We call $\mu_{\mathcal{Q}}$ a *Coxeter mutation*. Because of the definition, for a bipartite skew-symmetrizable matrix \mathcal{B} or a bipartite quiver \mathcal{Q} , we obtain

$$\mu_{\mathcal{Q}}(\mathcal{B}) = \mathcal{B}, \quad \mu_{\mathcal{Q}}(\mathcal{Q}) = \mathcal{Q}.$$

The initial seed $\Sigma_{t_0} = \Sigma_0 = (\mathbf{x}_0, \tilde{\mathcal{B}}_0)$ is included in the *bipartite belt* consisting of the seeds $\Sigma_r = (\mathbf{x}_r, \tilde{\mathcal{B}}_0)$ for $r \in \mathbb{Z}$ defined by

$$\Sigma_r = (\mathbf{x}_r, \tilde{\mathcal{B}}_0) = \begin{cases} \mu_{\mathcal{Q}}^r(\Sigma_0) & \text{if } r > 0, \\ (\mu_- \mu_+)^{-r}(\Sigma_0) & \text{if } r < 0. \end{cases}$$

We write

$$\mathbf{x}_r = (x_{1;r}, \dots, x_{n;r}) \quad \text{for } r \in \mathbb{Z}.$$

It is known from [27] and [40] that both μ_+ and μ_- act on the set $\Phi_{\geq -1}$ of almost positive roots and on the set $V(\text{Ex}(\Phi))$ of vertices via the bijective correspondence (2.4). We summarize the properties of the action of Coxeter mutation as follows.

Proposition 2.27 (cf. [27, Propositions 2.5, 3.5, and 3.6] for finite type; [40, Propositions 5.4 and 5.14] for affine type). *Let Φ be a finite or affine root system of type \mathbb{Z} . Let $\{(\mathbf{x}_t, \tilde{\mathcal{B}}_t)\}_{t \in \mathbb{T}}$ be a cluster pattern of type \mathbb{Z} and $\text{Ex}(\Phi)$ its exchange graph. Then the following holds.*

- (1) *For $\ell \in [n]$ and $r \in \mathbb{Z}$, we denote by $\text{Ex}(\Phi, x_{\ell;r})$ the induced subgraph of $\text{Ex}(\Phi)$ consisting of seeds having the cluster variable $x_{\ell;r}$. Then, we have*

$$\text{Ex}(\Phi, x_{\ell;r}) \cong \text{Ex}(\Phi([n] \setminus \{\ell\})).$$

- (2) *Both μ_+ and μ_- act on the exchange graph $\text{Ex}(\Phi)$.*

(3) For any seed $(\mathbf{x}, \tilde{\mathcal{B}}) \in \text{Ex}(\Phi)$, there exists $r \in \mathbb{Z}$ such that

$$|\{x_{1;r}, \dots, x_{n;r}\} \cap \{x_1, \dots, x_n\}| \geq 2.$$

Furthermore, if Φ is of finite type having even Coxeter number $h = 2e$, then $r \in \{0, 1, \dots, e\}$.

As a direct consequence of Proposition 2.27, we have the following lemma which will be used later.

Lemma 2.28. *Let $(\mathbf{y}_{t_0}, \mathcal{B}_{t_0})$ be a Y -seed such that the Cartan counterpart $C(\mathcal{B}_{t_0})$ is of finite or affine type. For a Y -seed $(\mathbf{y}, \mathcal{B})$ in the seed pattern, there exist $r \in \mathbb{Z}$, $\ell \in [n]$, and $j_1, \dots, j_L \in [n] \setminus \{\ell\}$ such that a sequence $\mu_{j_1}, \dots, \mu_{j_L}$ of mutations connecting $\mu_{\mathcal{Q}}^r(\mathbf{y}_{t_0}, \mathcal{B}_{t_0})$ and $(\mathbf{y}, \mathcal{B})$, that is,*

$$(\mathbf{y}, \mathcal{B}) = (\mu_{j_L} \cdots \mu_{j_1})(\mu_{\mathcal{Q}}^r(\mathbf{y}_{t_0}, \mathcal{B}_{t_0})).$$

Furthermore, if Φ is of finite type and has even Coxeter number $h = 2e$, then $r \in \{0, 1, \dots, e\}$.

Proof. Since the exchange graph $\text{Ex}(\{(\mathbf{y}_t, \mathcal{B}_t)\}_{t \in \mathbb{T}_n})$ is the graph $\text{Ex}(\Phi)$ by Proposition 2.25, it is enough to prove the claim in terms of seeds. Let $(\mathbf{x}, \tilde{\mathcal{B}}) \in \text{Ex}(\Phi)$ be a seed. By Proposition 2.27(3), there exist $\ell \in [n]$ and $r \in \mathbb{Z}$ such that $x_{\ell;r} \in \{x_1, \dots, x_n\}$. Accordingly, both seeds $\mu_{\mathcal{Q}}^r(\mathbf{x}_{t_0}, \tilde{\mathcal{B}}_{t_0})$ and $(\mathbf{x}, \tilde{\mathcal{B}})$ are contained in the induced subgraph $\text{Ex}(\Phi, x_{\ell;r})$. Since the subgraph $\text{Ex}(\Phi, x_{\ell;r})$ itself is the exchange graph of the root subsystem $\Phi([n] \setminus \{\ell\})$ by Proposition 2.25(1), it is connected. Accordingly, two seeds $\mu_{\mathcal{Q}}^r(\mathbf{x}_{t_0}, \tilde{\mathcal{B}}_{t_0})$ and $(\mathbf{x}, \tilde{\mathcal{B}})$ are connected without applying mutations at the vertex ℓ , that is, there exists a sequence $j_1, \dots, j_L \in [n] \setminus \{\ell\}$ such that $(\mathbf{x}, \tilde{\mathcal{B}}) = (\mu_{j_L} \cdots \mu_{j_1})(\mu_{\mathcal{Q}}^r(\mathbf{x}_{t_0}, \tilde{\mathcal{B}}_{t_0}))$ as desired. \square

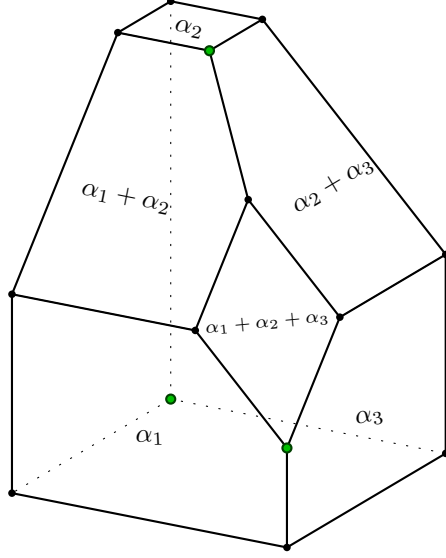
For a finite root system Φ , the exchange graph $\text{Ex}(\Phi)$ becomes the one-skeleton of an n -dimensional polytope $P(\Phi)$, called the *generalized associahedron*. Moreover, there is a bijective correspondence between the set $\mathcal{F}(P(\Phi))$ of codimension-one faces, called *facets*, of $P(\Phi)$ and the set of almost positive roots $\Phi_{\geq -1}$. We denote by F_{β} the facet of the polytope $P(\Phi)$ corresponding to a root $\beta \in \Phi_{\geq -1}$. We demonstrate Proposition 2.27 for root systems of type A_3 and D_4 .

Example 2.29. Consider the root system Φ of type A_3 . In this case, the Coxeter number is 4, which is even (cf. Table 6). In Table 7, we present how $\mu_{\mathcal{Q}}$ acts on the set of almost positive roots. Here, we use the convention that $I_+ = \{1, 3\}$ and $I_- = \{2\}$. The generalized associahedron of type A_3 is presented in Figure 11. We label each codimension-one face the corresponding almost positive root. The back-side facets are associated with the set of negative simple roots. As one may see that the face posets of $\mu_{\mathcal{Q}}^r(F_{-\alpha_i})$ are the same as that of the generalized associahedron $P(\Phi([n] \setminus \{i\}))$. Indeed, the facets $\mu_{\mathcal{Q}}^r(F_{-\alpha_1})$ and $\mu_{\mathcal{Q}}^r(F_{-\alpha_3})$ are pentagons, and the facets $\mu_{\mathcal{Q}}^r(F_{-\alpha_2})$ are squares. For $(\mathbf{x}, \tilde{\mathcal{B}}) = F_{-\alpha_1} \cap F_{-\alpha_2} \cap F_{-\alpha_3}$, we decorate the vertices $\{\mu_{\mathcal{Q}}^r(\mathbf{x}, \tilde{\mathcal{B}}) \mid r = 0, 1, 2\}$ with green. As one can see, the orbits of $F_{-\alpha_1}, F_{-\alpha_2}, F_{-\alpha_3}$ exhaust all vertices as claimed in Proposition 2.27(3).

Example 2.30. We consider the generalized associahedron of type D_4 and present four facets corresponding to the negative simple roots in Figure 12. The facet corresponding to $-\alpha_2$ is combinatorially equivalent to $P(\Phi(\{1\})) \times P(\Phi(\{3\})) \times P(\Phi(\{4\}))$, which is a 3-cube presented in the boundary. The intersection of these four facets is a vertex sits in the bottom colored in green. The Coxeter mutation $\mu_{\mathcal{Q}}$ acts on the face poset of the permutohedron, especially, four green vertices are in the same orbit.

r	$\mu_{\mathcal{Q}}^r(-\alpha_1)$	$\mu_{\mathcal{Q}}^r(-\alpha_2)$	$\mu_{\mathcal{Q}}^r(-\alpha_3)$
0	$-\alpha_1$	$-\alpha_2$	$-\alpha_3$
1	$\alpha_1 + \alpha_2$	α_2	$\alpha_2 + \alpha_3$
2	α_3	$\alpha_1 + \alpha_2 + \alpha_3$	α_1

TABLE 7. Computation $\mu_{\mathcal{Q}}^r(-\alpha_i)$ for type A_3

FIGURE 11. The type A_3 generalized associahedron

Remark 2.31. As saw in Example 2.19, bipartite coloring on quivers of type ADE induce that on quivers of type BCFG. Accordingly, if a seed pattern of simply-laced type Z gives a seed pattern of type Z^G via the folding procedure, then the Coxeter mutation of type Z^G is the same as that of type Z . More precisely, for a globally foldable Y -seed $(\mathbf{y}, \mathcal{B})$ with respect to G of type Z and its Coxeter mutation μ_Q^Z , we have

$$\mu_Q^{Z^G}((\mathbf{y}, \mathcal{B})^G) = (\mu_Q^Z(\mathbf{y}, \mathcal{B}))^G.$$

Here, $\mu_Q^{Z^G}$ is the Coxeter mutation on the seed pattern determined by $(\mathbf{y}, \mathcal{B})^G$.

Moreover, Coxeter numbers of Z and Z^G are the same. Indeed,

$$h(A_{2n-1}) = h(B_n) = 2n,$$

$$h(D_{n+1}) = h(C_n) = 2n,$$

$$h(E_6) = h(F_4) = 12,$$

$$h(D_4) = h(G_2) = 6.$$

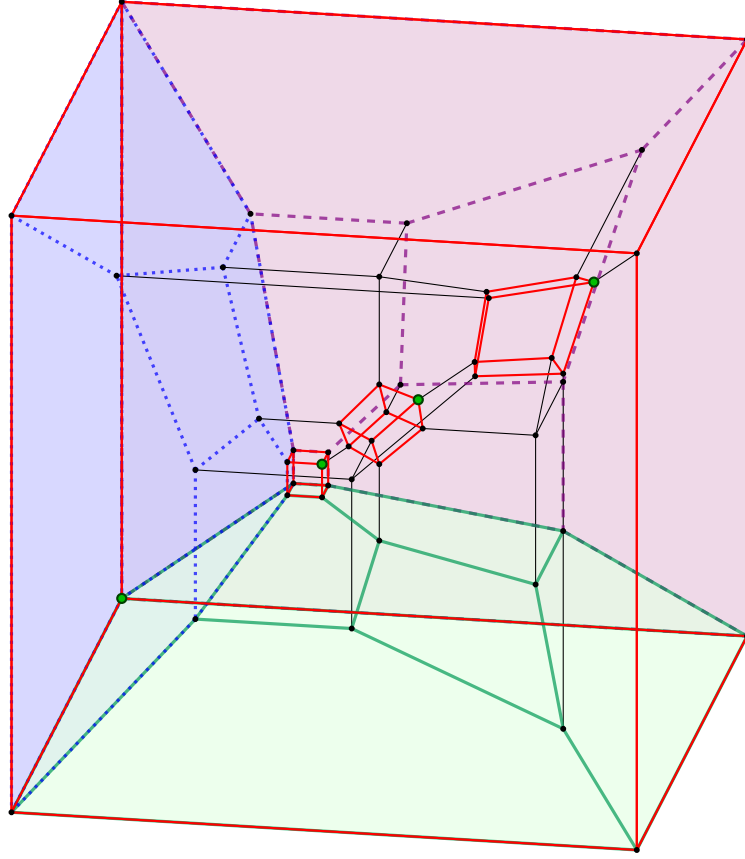
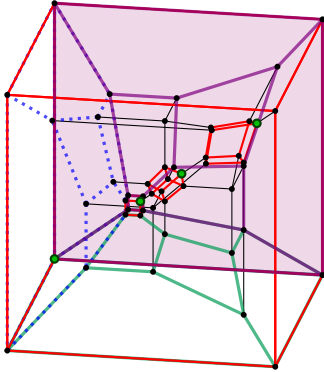
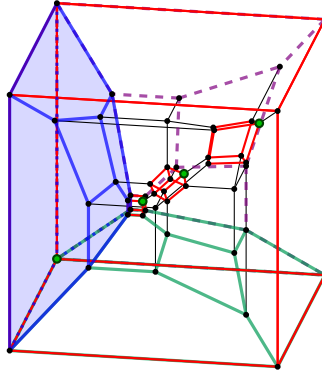
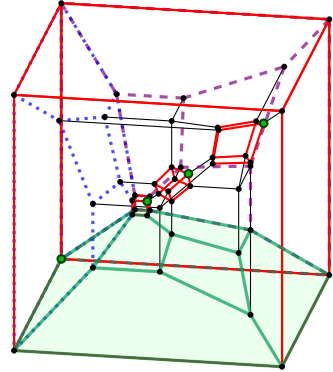
In the remaining part of this section, we recall [28] which considers the combinatorics on mutations in a more general setting. Let \mathcal{Q} be a bipartite quiver and I_+ and I_- be the bipartite decomposition of the vertex set of \mathcal{Q} . Consider the composition $\mu_{\mathcal{Q}} = \mu_+ \mu_-$ of a sequence of mutations where

$$\mu_{\varepsilon} = \prod_{i \in I_{\varepsilon}} \mu_i \quad \text{for } \varepsilon \in \{+, -\}.$$

We call $\mu_{\mathcal{Q}}$ a *Coxeter mutation* as before. We enclose this section by recalling the result [28, Theorem 8.8] on the order of Coxeter mutation on the cluster pattern. Recall from Proposition 2.25 that for an exchange matrix \tilde{B}_{t_0} , if \mathcal{B}_{t_0} is skew-symmetric, then the exchange graph of a seed pattern $\{(\mathbf{x}_t, \tilde{\mathcal{B}}_t)\}_{t \in \mathbb{T}_n}$ and that of a Y -pattern $\{(\mathbf{y}_t, \mathcal{B}_t)\}_{t \in \mathbb{T}_n}$ having algebraically independent variables $y_{1;t_0}, \dots, y_{n;t_0}$ are the same. Accordingly, we obtain the following from [28, Theorem 8.8].

Lemma 2.32 (cf. [28, Theorem 8.8]). *Let $(\mathbf{y}_{t_0}, \mathcal{B}_{t_0})$ be an initial Y -seed. Suppose that $\mathcal{B}_{t_0} = \mathcal{B}(\mathcal{Q})$ for a bipartite quiver \mathcal{Q} and $y_{1;t_0}, \dots, y_{n;t_0}$ are algebraically independent. Then the set $\{\mu_{\mathcal{Q}}^r(\mathbf{y}_{t_0}, \mathcal{B}_{t_0})\}_{r \in \mathbb{Z}_{\geq 0}}$ of Y -seeds is finite if and only if \mathcal{B}_{t_0} is of finite type.*

Moreover, for such a quiver \mathcal{Q} , the order the $\mu_{\mathcal{Q}}$ -action is given by $(h+2)/2$ if h is even, or $h+2$ otherwise, where h is the corresponding Coxeter number.

(a) The generalized associahedron of type D_4 .(b) $F_{-\alpha_1}$.(c) $F_{-\alpha_3}$.(d) $F_{-\alpha_4}$.FIGURE 12. The generalized associahedron of type D_4 and facets corresponding to some negative simple roots $-\alpha_1$, $-\alpha_3$, and $-\alpha_4$.

3. LEGENDRIANS AND N -GRAPHS

We recall from [15] the notion of N -graphs and their combinatorial moves which encode the Legendrian isotopy data of corresponding Legendrian surfaces. As an application, we review how N -graphs can be used to find and to distinguish Lagrangian fillings for Legendrian links.

3.1. N -graphs and Legendrian weaves.

Definition 3.1. [15, Definition 2.2] An N -graph \mathcal{G} on a smooth surface S is an $(N-1)$ -tuple of graphs $(\mathcal{G}_1, \dots, \mathcal{G}_{N-1})$ satisfying the following conditions:

- (1) Each graph \mathcal{G}_i is embedded, trivalent, possibly empty and non necessarily connected.
- (2) Any consecutive pair of graphs $(\mathcal{G}_i, \mathcal{G}_{i+1})$, $1 \leq i \leq N-2$, intersects only at hexagonal points depicted as in Figure 13.
- (3) Any pair of graphs $(\mathcal{G}_i, \mathcal{G}_j)$ with $1 \leq i, j \leq N-1$ and $|i-j| > 1$ intersects transversely at edges.

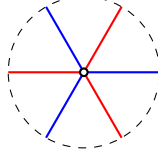


FIGURE 13. A hexagonal point

Let $\pi_F : J^1S \cong T^*S \times \mathbb{R} \rightarrow S \times \mathbb{R}$ be the front projection, and we call the image $\pi_F(\Lambda)$ of a Legendrian $\Lambda \subset J^1S$ a *wavefront*. Since J^1S is equipped with the contact form $dz - p_x dx - p_y dy$, the coordinates (p_x, p_y) of the Legendrian Λ are recovered from (x, y) -slope of the tangent plane $T_{(x,y,z)}\pi_F(\Lambda)$:

$$p_x = \partial_x z(x, y), \quad p_y = \partial_y z(x, y).$$

For any N -graph \mathcal{G} on a surface S , we associate a Legendrian surface $\Lambda(\mathcal{G}) \subset J^1S$. Basically, we construct the Legendrian surface by weaving the wavefronts in $S \times \mathbb{R}$ constructed from a local chart of S .

Let $\mathcal{G} \subset S$ be an N -graph. A finite cover $\{U_i\}_{i \in I}$ of S is called \mathcal{G} -compatible if

- (1) each U_i is diffeomorphic to the open disk $\mathring{\mathbb{D}}^2$,
- (2) $U_i \cap \mathcal{G}$ is connected, and
- (3) $U_i \cap \mathcal{G}$ contains at most one vertex.

For each U_i , we associate a wavefront $\Gamma(U_i) \subset U_i \times \mathbb{R} \subset S \times \mathbb{R}$. Note that there are only five types of nondegenerate local charts for any N -graph \mathcal{G} as follows:

Type 1 A chart without any graph component whose corresponding wavefront becomes

$$\bigcup_{i=1, \dots, N} \mathring{\mathbb{D}}^2 \times \{i\} \subset \mathring{\mathbb{D}}^2 \times \mathbb{R}.$$

Type 2 A chart with single edge. The corresponding wavefront is the union of the A_1^2 -germ along the two sheets $\mathring{\mathbb{D}}^2 \times \{i\}$ and $\mathring{\mathbb{D}}^2 \times \{i+1\}$, and trivial disks $\mathbb{D}^2 \times \{j\}$, $j \in \{1, \dots, N\} \setminus \{i, i+1\}$. The local model of A_1^2 comes from the origin of the singular surface

$$\Gamma(A_1^2) = \{(x, y, z) \in \mathbb{R}^3 \mid x^2 - z^2 = 0\}$$

See Figure 14(a).

Type 3 A chart with transversely intersecting two edges. The wavefront consists of two A_1^2 -germs of $\mathring{\mathbb{D}}^2 \times \{i, i+1\}$ and $\mathring{\mathbb{D}}^2 \times \{j, j+1\}$, and trivial disks $\mathbb{D}^2 \times \{k\}$, $k \in \{1, \dots, N\} \setminus \{i, i+1, j, j+1\}$.

Type 4 A chart with a monochromatic trivalent vertex whose wavefront is the union of the D_4^- -germ, see [3, §2.4], and trivial disks $\mathbb{D}^2 \times \{j\}$, $j \in \{1, \dots, N\} \setminus \{i, i+1\}$. The local model for Legendrian singularity of type D_4^- is given by the image at the origin of

$$\delta_4^- : \mathbb{R}^2 \rightarrow \mathbb{R}^3 : (x, y) \mapsto \left(x^2 - y^2, 2xy, \frac{2}{3}(x^3 - 3xy^2) \right).$$

See Figure 14(c).

Type 5 A chart with a bichromatic hexagonal point. The induced wavefront is the union of the A_1^3 -germ along the three sheets $\mathbb{D}^2 \times \{*\}$, $* = i, i+1, i+2$, and the trivial disks $\mathbb{D}^2 \times \{j\}$, $j \in \{1, \dots, N\} \setminus \{i, i+1, i+2\}$. The local model of A_1^3 is given by the origin of the singular surface

$$\{(x, y, z) \in \mathbb{R}^3 \mid (x^2 - z^2)(y - z) = 0\}.$$

See Figure 14(b).

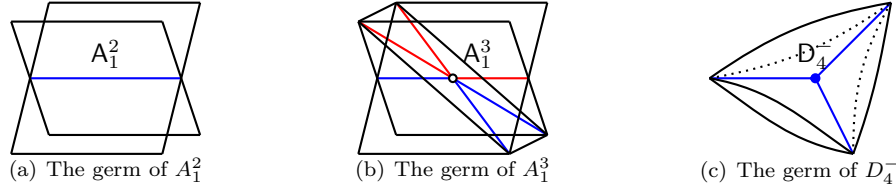


FIGURE 14. Three-types of wavefronts of Legendrian singularities.

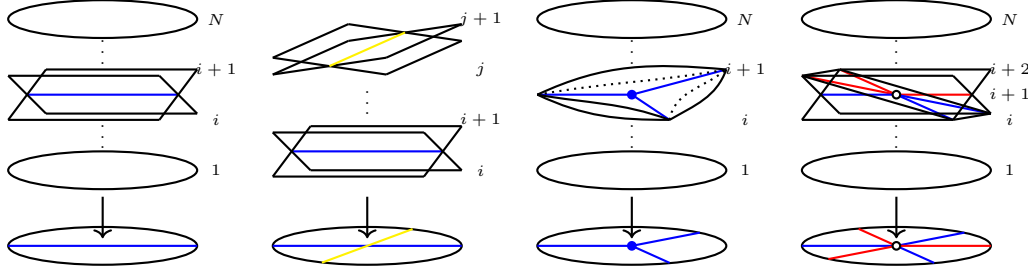


FIGURE 15. Local charts for N -graphs of Type 2, 3, 4, and 5.

Definition 3.2. [15, Definition 2.7] Let \mathcal{G} be an N -graph on a surface S . The *Legendrian weave* $\Lambda(\mathcal{G}) \subset J^1S$ is an embedded Legendrian surface whose wavefront $\Gamma(\mathcal{G}) \subset S \times \mathbb{R}$ is constructed by weaving the wavefronts $\{\Gamma(U_i)\}_{i \in I}$ from a \mathcal{G} -compatible cover $\{U_i\}_{i \in I}$ with respect to the gluing data given by \mathcal{G} .

Remark 3.3. Note that $\Lambda(\mathcal{G})$ is well-defined up to the choice of cover and up to planar isotopies. Let $\{\varphi_t\}_{t \in [0,1]}$ be a compactly supported isotopy of S . Then this induces a Legendrian isotopy of Legendrian surface $\Lambda(\varphi_t(\mathcal{G})) \subset J^1S$ relative to the boundary.

We also list certain degenerate local models of N -graph as follows:

Type D1 A chart with double edges whose wavefront consists of two A_1^2 -germs of $\mathbb{D}^2 \times \{i, i+1\}$ and $\mathbb{D}^2 \times \{j, j+1\}$ for $|i-j| > 1$, and trivial disks $\mathbb{D}^2 \times \{k\}$, $k \in \{1, \dots, N\} \setminus \{i, i+1, j, j+1\}$. See Figure 16(a).

Type D2 A chart with trichromatic graph of $(\mathcal{G}_{i-1}, \mathcal{G}_i, \mathcal{G}_{i+1})$ satisfying

- each has a unique vertex of four valent,
- \mathcal{G}_{i-1} and \mathcal{G}_{i+1} are identical, and
- \mathcal{G}_i and \mathcal{G}_{i+1} are intersecting at the vertex of eight valent in an alternating way, see the middle one in Figure 16(b).

For $i = 2$, the wavefront corresponding to a chart of Type D2 inside $\mathbb{D}^2 \times \mathbb{R}$ consists of four disks $(\mathbb{D}_1, \dots, \mathbb{D}_4)$, which is the cone $C(\lambda) = \lambda \times [0, 1] / \lambda \times \{0\}$ of the following Legendrian front λ in $\mathbb{S}^1 \times \mathbb{R}$

$$(\sigma_{1,3}\sigma_2)^4 = \begin{array}{c} \text{Diagram of a Legendrian front } \lambda \text{ in } \mathbb{S}^1 \times \mathbb{R} \end{array},$$

where $\sigma_{1,3}$ is a 4-braid isotopic to $\sigma_1\sigma_3$ (or equivalently, $\sigma_3\sigma_1$) such that two crossings σ_1 and σ_3 occur simultaneously.

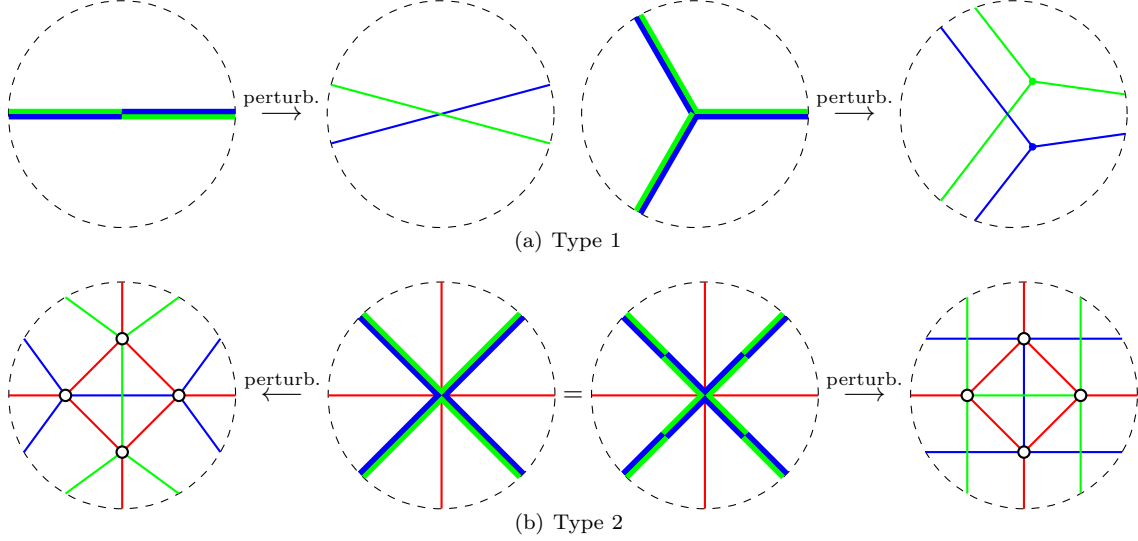


FIGURE 16. Local models for degenerate N -graphs and their perturbations

Remark 3.4. The cone point neighborhood of the wavefront for the degenerate N -graph of **Type D2**, is diffeomorphic to the union of four planes, $\{z = x\}$, $\{z = -x\}$, $\{z = y\}$, and $\{z = -y\}$ in \mathbb{R}^3 , see Figure 17. Moreover, if we regard each of \mathcal{G}_i as a union of transversely intersecting two edges, then we have six edges for the local chart of N -graph $(\mathcal{G}_1, \mathcal{G}_2, \mathcal{G}_3)$. On the other hand, each pair of four disks in the wave front forms the A_1^2 -germ and this corresponds to the (degenerated) six edges.

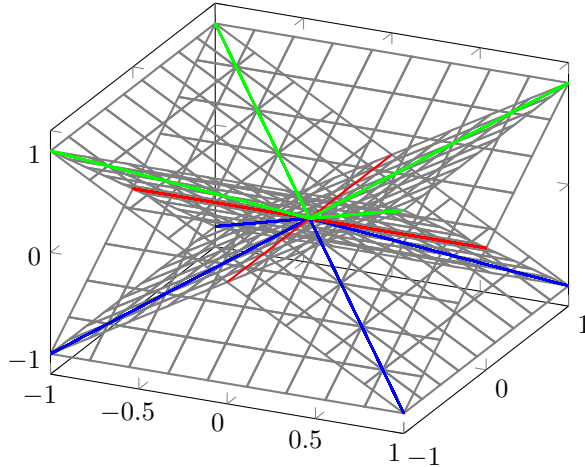


FIGURE 17. A wavefront for the degenerate N -graph.

We obtain (regular) N -graphs from degenerate N -graphs via (generic) perturbation of the wavefront as depicted in Figure 16.

The idea of N -graph is useful in the study of Legendrian surface, because the Legendrian isotopy of the Legendrian weave $\Lambda(\mathcal{G})$ can be encoded in combinatorial moves of N -graphs.

Theorem 3.5. [15, Theorem 1.1] *Let \mathcal{G} be a non-degenerate local N -graph. The combinatorial moves (I) \sim (IV') in Figure 18 are Legendrian isotopies for $\Lambda(\mathcal{G})$.*

We denote the equivalence class of an N -graph \mathcal{G} up to the moves (I) \sim (IV') in Figure 18 by [9]. Let us also list the combinatorial moves (DI) and (DII) for Legendrian isotopies involving degenerate N -graphs as depicted in Figure 18.

Corollary 3.6. *Let \mathcal{G} be a local degenerate N -graph. The combinatorial moves (DI) and (DII) in Figure 18 are Legendrian isotopies for $\Lambda(\mathcal{G})$.*

Proof. It is direct to check that the moves (DI) and (DII) for degenerate N -graphs can be obtained by composing the perturbations in Figure 16 and moves in Figure 18. See Appendix B.1. \square

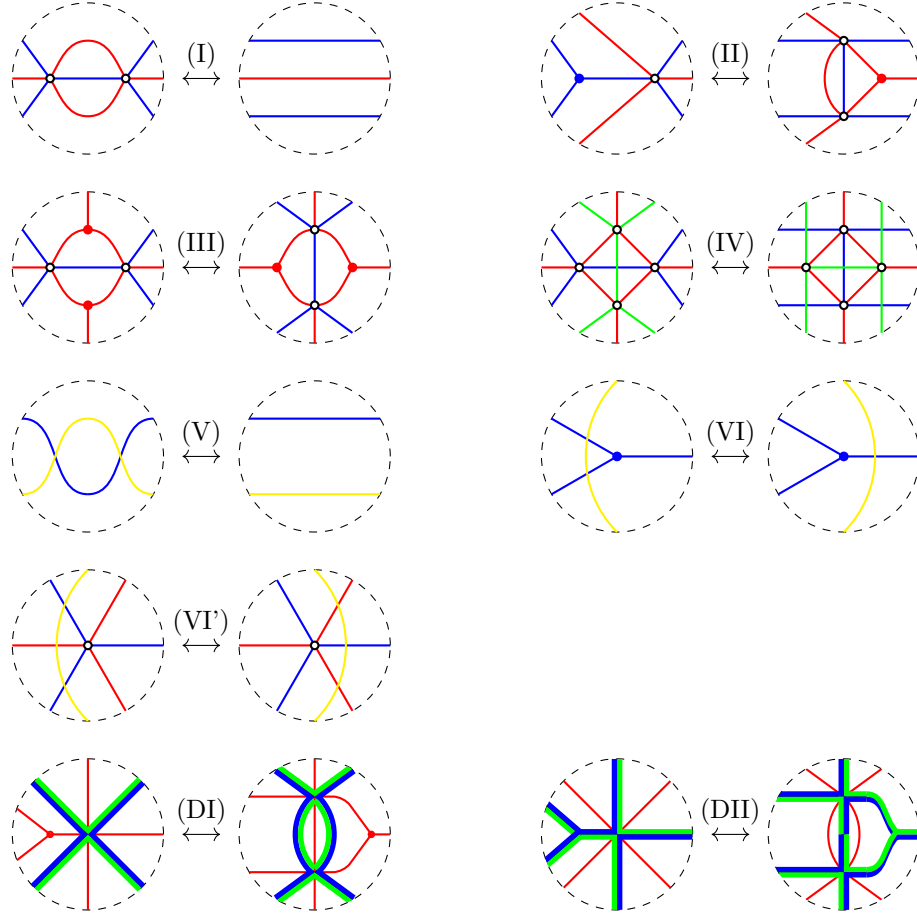


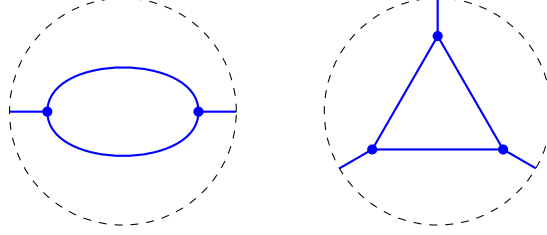
FIGURE 18. Combinatorial moves for Legendrian isotopies of surface $\Lambda(\mathcal{G})$. Here the pairs (blue, red) and (red, green) are consecutive. Other pairs are not.

Definition 3.7. An N -graph \mathcal{G} on S is called *free* if the induced Legendrian weave $\Lambda(\mathcal{G}) \subset J^1 S$ can be woven without interior Reeb chord.

Example 3.8. [15, Example 7.3] Let $\mathcal{G} \subset \mathbb{D}^2$ be a 2-graph such that $\mathbb{D}^2 \setminus \mathcal{G}$ is simply connected relative to the boundary $\partial\mathbb{D}^2 \cap (\mathbb{D}^2 \setminus \mathcal{G})$. Then \mathcal{G} is free if and only if \mathcal{G} has no faces contained in $\mathring{\mathbb{D}}^2$. Note that each of such faces admits at least one Reeb chord, see Figure 19.

In particular, we have the following lemma whose proof is omitted.

Lemma 3.9. *Let $\mathcal{G} = (\mathcal{G}_1, \dots, \mathcal{G}_{N-1})$ be an N -graph on \mathbb{D}^2 . Suppose that each \mathcal{G}_i is a tree or empty. Then \mathcal{G} is free.*

FIGURE 19. N -graphs with Reeb chords

Let us consider the Lagrangian projection $\pi_L : J^1 S \cong T^*S \times \mathbb{R} \rightarrow T^*S$. Then the image

$$L(\mathcal{G}) := \pi_L(\Lambda(\mathcal{G}))$$

of the Legendrian weave gives us an exact, possibly immersed Lagrangian surface in T^*S . The following lemma is a direct consequence of Theorem 3.5 and Definition 3.7.

Lemma 3.10. *Let \mathcal{G} and \mathcal{G}' be two N -graphs on S . Then the following statements hold:*

- (1) *If \mathcal{G} is free, then the Lagrangian surface $L(\mathcal{G}) = \pi_L(\Lambda(\mathcal{G}))$ is exact and embedded.*
- (2) *If $[\mathcal{G}] = [\mathcal{G}']$, then two Lagrangian surfaces*

$$L(\mathcal{G}) = \pi_L(\Lambda(\mathcal{G})) \quad \text{and} \quad L(\mathcal{G}') = \pi_L(\Lambda(\mathcal{G}'))$$

*in T^*S are exact Lagrangian isotopic relative to boundary.*

3.2. N -graphs on \mathbb{D}^2 and \mathbb{A} . In this section, we consider Legendrian links in \mathbb{R}^3 or \mathbb{S}^3 , Lagrangian fillings in \mathbb{R}^4 and how to describe them in terms of N -graphs.

3.2.1. Geometric setup. Let us recall and collect basic facts about contact submanifolds of \mathbb{R}^3 and \mathbb{R}^5 , and their coordinate changes. Let (θ, p_θ, z) be the coordinates of $J^1\mathbb{S}$ with the contact form $\alpha_{J^1\mathbb{S}^1} = dz - p_\theta d\theta$. The Legendrian unknot λ_{unknot} in $J^1\mathbb{S}^1$ is given by

$$\lambda_{\text{unknot}} = \{(\theta, 0, 0) \mid \theta \in \mathbb{S}^1\} \subset J^1\mathbb{S}^1.$$

The symplectization of $J^1\mathbb{S}^1$ is

$$(J^1\mathbb{S}^1 \times \mathbb{R}_s, d(e^s(dz - p_\theta d\theta))),$$

and its contactization becomes

$$(J^1\mathbb{S}^1 \times \mathbb{R}_s \times \mathbb{R}_t, dt + e^s(dz - p_\theta d\theta))$$

which is contactomorphic to $(J^1(\mathbb{S}^1 \times \mathbb{R}_{r>0}), dw - p_\vartheta d\vartheta - p_r dr)$ under the strict contactomorphism ϕ given by

$$(\theta, p_\theta, z, s, t) \mapsto (\vartheta, r, p_\vartheta, p_r, w) = (\theta, e^s, e^s p_\theta, z, t + e^s z).$$

For each symplectization level $s = s_0$, the map ϕ induces a contact embedding $J^1\mathbb{S}^1 \hookrightarrow J^1(\mathbb{S} \times \mathbb{R}_{r>0})$ especially into $J^1(\mathbb{S}^1 \times \mathbb{R}_{r>0}) \cap \{r = e^{s_0}\}$.

Furthermore, there is a strict contactomorphism

$$\psi : (J^1(\mathbb{S}^1 \times \mathbb{R}_{r>0}), dw - p_\vartheta d\vartheta - p_r dr) \rightarrow (J^1(\mathbb{R}^2 \setminus \{\mathbf{0}\}), dw - y_1 dx_1 - y_2 dx_2)$$

defined by

$$(x_1, x_2, y_1, y_2, w) = \left(r \cos \vartheta, r \sin \vartheta, p_r \cos \vartheta - \frac{\sin \vartheta}{r} p_\vartheta, p_r \sin \vartheta + \frac{\cos \vartheta}{r} p_\vartheta, w \right).$$

By compactifying the origin $\mathbf{0} \in \mathbb{R}^2$, we have the following diagram:

$$\begin{array}{ccccc} J^1\mathbb{S}^1 \times \mathbb{R}_s \times \mathbb{R}_t & \xrightarrow[\phi]{\cong} & J^1(\mathbb{S}^1 \times \mathbb{R}_{r>0}) & \xrightarrow[\psi]{\cong} & J^1(\mathbb{R}^2 \setminus \{\mathbf{0}\}) \hookrightarrow J^1\mathbb{R}^2 = T^*\mathbb{R}^2 \times \mathbb{R}_w \\ \downarrow \pi_t & & & & \downarrow \pi_L \\ J^1\mathbb{S}^1 \times \mathbb{R}_s & \xleftarrow{\hspace{10em} \Phi \hspace{10em}} & & & T^*\mathbb{R}^2 \end{array}$$

Here, the symplectic embedding $\Phi: J^1\mathbb{S}^1 \times \mathbb{R}_s \hookrightarrow T^*\mathbb{R}^2$ is defined by

$$(\theta, p_\theta, z, s) \mapsto (x_1, x_2, y_1, y_2) = (e^s \cos \theta, e^s \sin \theta, z \cos \theta - p_\theta \sin \theta, z \sin \theta + p_\theta \cos \theta).$$

On the other hand, we have another symplectomorphism

$$\begin{aligned} \varphi: (\mathbb{S}^3 \times \mathbb{R}_u, d(e^u \alpha_{\mathbb{S}^3})) &\rightarrow (T^*\mathbb{R}^2 \setminus \{(\mathbf{0}, \mathbf{0})\}, dx_1 \wedge dy_1 + dx_2 \wedge dy_2); \\ (z_1, z_2, u) &\mapsto e^{u/2}(r_1 \cos \theta_1, r_2 \cos \theta_2, r_1 \sin \theta_1, r_2 \sin \theta_2) \end{aligned}$$

where \mathbb{S}^3 is the unit sphere in \mathbb{C}_{z_1, z_2}^2 , $z_1 = r_1 e^{i\theta_1}$, $z_2 = r_2 e^{i\theta_2}$, and with the contact form

$$\alpha_{\mathbb{S}^3} = \frac{1}{2}r_1^2 d\theta_1 + \frac{1}{2}r_2^2 d\theta_2, \quad r_1^2 + r_2^2 = 1.$$

So far, we have the following diagram of symplectic embeddings

$$\begin{array}{ccc} J^1\mathbb{S}^1 \times \mathbb{R}_s & \xrightarrow{\quad \Phi \quad} & T^*\mathbb{R}^2 \setminus \{(\mathbf{0}, \mathbf{0})\} \\ & \searrow \Psi \quad \nearrow \cong & \\ & \mathbb{S}^3 \times \mathbb{R}_u & \end{array}$$

where the map $\Psi(\theta, p_\theta, z, s) = (z_1, z_2, u)$ is defined by

$$\begin{aligned} z_1 &= \frac{e^s \cos \theta + i(z \cos \theta - p_\theta \sin \theta)}{\sqrt{e^{2s} + z^2 + p_\theta^2}}, \\ z_2 &= \frac{e^s \sin \theta + i(z \sin \theta + p_\theta \cos \theta)}{\sqrt{e^{2s} + z^2 + p_\theta^2}}, \\ e^u &= e^{2s} + z^2 + p_\theta^2. \end{aligned}$$

Let us define $\iota: J^1\mathbb{S}^1 \rightarrow \mathbb{S}^3$ as the composition of the inclusions $J^1\mathbb{S}^1 \cong J^1\mathbb{S}^1 \times \{s = 0\} \rightarrow J^1\mathbb{S}^1 \times \mathbb{R}_s$, $\Psi: J^1\mathbb{S}^1 \times \mathbb{R}_s \rightarrow \mathbb{S}^3 \times \mathbb{R}_u$ and the projection $\mathbb{S}^3 \times \mathbb{R}_u \rightarrow \mathbb{S}^3$ so that

$$\iota(\theta, p_\theta, z) := \left(\frac{\cos \theta + i(z \cos \theta - p_\theta \sin \theta)}{\sqrt{1 + z^2 + p_\theta^2}}, \frac{\sin \theta + i(z \sin \theta + p_\theta \cos \theta)}{\sqrt{1 + z^2 + p_\theta^2}} \right).$$

Then the image of the Legendrian unknot $\lambda_{\text{unknot}} \subset J^1\mathbb{S}^1$ becomes

$$\{(z_1, z_2) \mid z_1 = \cos \theta, z_2 = \sin \theta, \theta \in \mathbb{S}^1\} \subset \mathbb{S}^3 \subset \mathbb{C}^2.$$

Recall the stereographic projection of \mathbb{S}^3 with respect to $(0, -i) \in \mathbb{C}^2$, and see the corresponding image of λ_{unknot} :

$$\begin{aligned} (\mathbb{S}^3 \setminus \{(0, -i)\}, \alpha_{\mathbb{S}^3}) &\rightarrow (\mathbb{R}^3, dz' + x'dy' - y'dx') \cong \mathbb{C} \times \mathbb{R}; \\ (z_1, z_2) &\mapsto \left(\frac{iz_1}{i + z_2}, \frac{-\text{Re}(z_2)}{|i + z_2|^2} \right); \\ (\cos \theta, \sin \theta) &\mapsto \left(\frac{\cos \theta}{1 + \sin^2 \theta}, \frac{\cos \theta \sin \theta}{1 + \sin^2 \theta}, \frac{-\sin \theta}{1 + \sin^2 \theta} \right). \end{aligned}$$

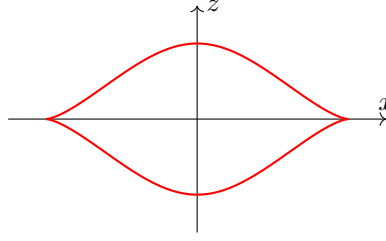
Under the strict contactomorphism

$$\begin{aligned} (\mathbb{R}^3, dz' + x'dy' - y'dx') &\rightarrow (J^1\mathbb{R}, dz - ydx); \\ (x', y', z') &\mapsto (x, y, z) = (x', 2y', z' + x'y'), \end{aligned}$$

the image of λ_{unknot} becomes

$$\left(\frac{\cos \theta}{1 + \sin^2 \theta}, \frac{2 \cos \theta \sin \theta}{1 + \sin^2 \theta}, \frac{-2 \sin^3 \theta}{(1 + \sin^2 \theta)^2} \right)$$

whose front projection looks like as follows:



Let $\lambda \subset J^1\mathbb{S}^1$ be a Legendrian link. Then the image $\iota(\lambda)$ can be isotoped into a neighborhood of the Legendrian unknot in \mathbb{R}^3 . In particular, if λ is a closure of a positive braid β , then $\iota(\lambda)$ looks like a satellite link of the Legendrian unknot in \mathbb{R}^3 .

We consider a Legendrian surface $\widehat{\Lambda} \subset J^1(\mathbb{S}^1 \times \mathbb{R}_{r>0})$ having cylindrical ends so that for some $S_1 > S_2$,

$$\widehat{\Lambda} \cap J^1(\mathbb{S}^1 \times \mathbb{R}_{r \geq e^{S_1}}) \cong \lambda_1 \times \mathbb{R}_{s \geq S_1}, \quad \widehat{\Lambda} \cap J^1(\mathbb{S}^1 \times \mathbb{R}_{r \leq e^{S_2}}) \cong \lambda_2 \times \mathbb{R}_{s \leq S_2}.$$

Then the projection $L_{\widehat{\Lambda}} = \pi_L(\psi(\widehat{\Lambda}))$ of the surface $\widehat{\Lambda}$ inside $\mathbb{S}^3 \times \mathbb{R}_u$ becomes an exact Lagrangian cobordism from $\iota(\lambda_1)$ to $\iota(\lambda_2)$.

Similarly, let $\widehat{\Lambda} \subset J^1\mathbb{R}^2$ be a Legendrian surface having a cylindrical end. That is, for some $S \in \mathbb{R}$,

$$\widehat{\Lambda} \cap J^1\mathbb{R}_{r \geq e^S}^2 \cong \lambda \times \mathbb{R}_{s \geq S}.$$

Then the projection $L_{\widehat{\Lambda}} = \pi_L(\widehat{\Lambda})$ in $T^*\mathbb{R}^2 \cong (\mathbb{C}^2, \omega_{\text{st}})$ becomes an exact Lagrangian filling of $\iota(\lambda)$. Note that the Lagrangian $\pi_L(\widehat{\Lambda})$ is embedded if and only if the Legendrian surface $\widehat{\Lambda}$ has no Reeb chords.

Lemma 3.11. *Let $\widehat{\Lambda}$ and $\widehat{\Lambda}'$ be two Legendrian surfaces in $J^1\mathbb{R}^2$ without Reeb chords having the identical cylindrical ends*

$$\widehat{\Lambda} \cap J^1\mathbb{R}_{r \geq e^S}^2 \cong \lambda \times \mathbb{R}_{s \geq S} \cong \widehat{\Lambda}' \cap J^1\mathbb{R}_{r \geq e^S}^2$$

for some $S \in \mathbb{R}$. If the exact embedded Lagrangian fillings $L_{\widehat{\Lambda}} = \pi_L(\widehat{\Lambda})$ and $L_{\widehat{\Lambda}'} = \pi_L(\widehat{\Lambda}')$ of $\iota(\lambda)$ are exact Lagrangian isotopic, then $\widehat{\Lambda}, \widehat{\Lambda}'$ are Legendrian isotopic.

On the other hand, any compact Legendrian surface $\Lambda \subset J^1\mathbb{D}^2$ can be extended to $\widehat{\Lambda} \subset J^1\mathbb{R}^2$ by attaching the cylindrical end $\partial\Lambda \times [1, \infty)$ in a smooth way. For two compact Legendrian surfaces $\Lambda, \Lambda' \subset J^1\mathbb{D}^2$, if $\widehat{\Lambda}$ and $\widehat{\Lambda}'$ are Legendrian isotopic if and only if Λ and Λ' are Legendrian isotopic relative to boundary.

Corollary 3.12. *Let $\lambda \subset J^1\mathbb{S}^1$ be a Legendrian link and $\Lambda, \Lambda' \subset J^1\mathbb{D}^2$ be two Legendrian surfaces without Reeb chords whose boundaries are λ . Then two exact embedded Lagrangian fillings $\pi_L(\Lambda)$ and $\pi_L(\Lambda')$ are exact Lagrangian isotopic relative to boundary if and only if Λ and Λ' are Legendrian isotopic relative to boundary without making Reeb chords during the isotopy.*

Remark 3.13. We are interested in exact Lagrangian fillings of Legendrian links up to *exact Lagrangian isotopy* relative to boundary, an isotopy through exact Lagrangian fillings which fixes the Legendrian boundary. This is equivalent to exact Lagrangian fillings up to *Hamiltonian isotopy*, which is an isotopy through Hamiltonian diffeomorphism fixing the boundary. The similar holds for Lagrangian cobordisms.

We end this section by investigating certain actions on the symplectic manifold $\mathbb{S}^3 \times \mathbb{R}_u$ and induced actions on $J^1\mathbb{S}^1$. Especially, we are interested in actions on $\mathbb{S}^3 \times \mathbb{R}_u$ preserving the \mathbb{R}_u -coordinate, the symplectization coordinate. So actions on \mathbb{S}^3 determine the actions on the symplectic manifold $\mathbb{S}^3 \times \mathbb{R}_u$.

Recall that \mathbb{S}^3 is the unit sphere in \mathbb{C}^2 , i.e., coordinates $z_1 = r_1 e^{i\theta_1}$, $z_2 = r_2 e^{i\theta_2}$ with $r_1^2 + r_2^2 = 1$.

Rotation. A symplectomorphism $R_{\theta_0} : \mathbb{S}^3 \times \mathbb{R}_u \rightarrow \mathbb{S}^3 \times \mathbb{R}_u$, called *rotation*, is defined by

$$R_{\theta_0}(z_1, z_2, u) = (z_1 \cos \theta_0 - z_2 \sin \theta_0, z_1 \sin \theta_0 + z_2 \cos \theta_0, u).$$

Note that the restriction $R_{\theta_0}|_{\mathbb{S}^3}$ fixes the contact form $\alpha_{\mathbb{S}^3}$. Under the symplectic embedding $\Psi : J^1\mathbb{S}^1 \times \mathbb{R}_s \hookrightarrow \mathbb{S}^3 \times \mathbb{R}_u$, we have the following induced symplectomorphism

$$J^1\mathbb{S}^1 \times \mathbb{R}_s \rightarrow J^1\mathbb{S}^1 \times \mathbb{R}_s, \quad (\theta, p_\theta, z, s) \mapsto (\theta + \theta_0, p_\theta, z, s).$$

By restricting R_{θ_0} on $J^1\mathbb{S}^1$, we obtain

$$J^1\mathbb{S}^1 \rightarrow J^1\mathbb{S}^1, \quad (\theta, p_\theta, z) \mapsto (\theta + \theta_0, p_\theta, z).$$

We are especially interested in $\theta_0 = \pi, 2\pi/3$. They produce $\mathbb{Z}/2\mathbb{Z}$ - and $\mathbb{Z}/3\mathbb{Z}$ -action on the symplectic manifold $\mathbb{S}^3 \times \mathbb{R}_u$ and Lagrangian fillings of satellite links of the Legendrian unknot, respectively.

Conjugation. An anti-symplectic involution $\tau : \mathbb{S}^3 \times \mathbb{R}_u \rightarrow \mathbb{S}^3 \times \mathbb{R}_u$, which we call *conjugation*, is defined by

$$(z_1, z_2, u) \mapsto (\bar{z}_1, \bar{z}_2, u).$$

It is direct to check that τ reverses the sign of symplectic form $\frac{i}{2}(dz_1 \wedge d\bar{z}_1 + dz_2 \wedge d\bar{z}_2)$, and its restriction on \mathbb{S}^3 also reverse the sign of $\alpha_{\mathbb{S}^3}$. Again by the symplectic embedding Ψ , the conjugation induces an action on $J^1\mathbb{S}^1 \times \mathbb{R}_s$

$$(\theta, p_\theta, z, s) \mapsto (\theta, -p_\theta, -z, s)$$

whose restriction on $J^1\mathbb{S}^1$ becomes

$$(\theta, p_\theta, z) \mapsto (\theta, -p_\theta, -z).$$

This anti-symplectic involution naturally produce $\mathbb{Z}/2\mathbb{Z}$ -action on the symplectic manifold and Lagrangian fillings as in the actions from the rotations.

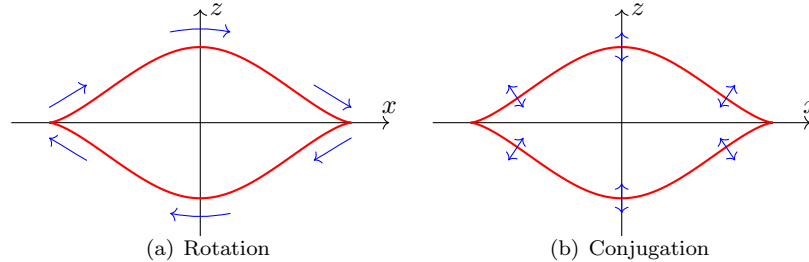


FIGURE 20. Rotations and conjugation near the Legendrian unknot.

Lemma 3.14. Let R_{θ_0} and η be rotation and conjugation defined on $\mathbb{S}^3 \times \mathbb{R}$ as above, respectively. Then the induced maps on the front projection $\pi_F : J^1\mathbb{S}^1 \rightarrow \mathbb{S}^1 \times \mathbb{R}$ becomes as follows:

$$\begin{aligned} R_{\theta_0}|_{\mathbb{S}^1 \times \mathbb{R}} : (\theta, z) &\mapsto (\theta + \theta_0, z); \\ \eta|_{\mathbb{S}^1 \times \mathbb{R}} : (\theta, z) &\mapsto (\theta, -z). \end{aligned}$$

3.2.2. N -graphs on \mathbb{D}^2 and \mathbb{A} . Let $\beta \subset J^1\mathbb{R}^1$ be a positive N -braid given by a word consisting of the generators $\sigma_1, \dots, \sigma_{N-1}$, and let $\lambda = \lambda_\beta \in J^1\mathbb{S}^1$ be a Legendrian link obtained by the closure of β , which can be regarded as a satellite of the Legendrian unknot in \mathbb{R}^3 . The front projection $\pi_F(\lambda) \subset \mathbb{S}^1 \times \mathbb{R}$ of λ consists of N -strands with double points corresponding to the braid word β . Hence, the Legendrian λ gives us an $(N-1)$ -tuple $(\lambda_1, \lambda_2, \dots, \lambda_{N-1})$ of subsets of points in \mathbb{S}^1 , each of which corresponds to the generator σ_i in the braid word β .

Conversely, let $(\lambda_1, \dots, \lambda_{N-1})$ be an $(N-1)$ -tuple of disjoint¹ subsets of \mathbb{S}^1 . Then, from this data $(\lambda_1, \dots, \lambda_{N-1})$, one can build the Legendrian link λ , which is the branched N -fold covering space of \mathbb{S}^1 such that the i -th and $(i+1)$ -st covers are branched along the set λ_i .

¹This condition can be weakened as follows: $\lambda_i \cap \lambda_{i+1} = \emptyset$ for each $1 \leq i < N$.

Let $\mathcal{G} = (\mathcal{G}_1, \dots, \mathcal{G}_{N-1})$ be an N -graph on \mathbb{D}^2 . The *boundary* $\partial\mathcal{G}$ of \mathcal{G} is a Legendrian link defined by an N -graph on $\mathbb{S}^1 = \partial\mathbb{D}^2$ as

$$\partial\mathcal{G} = (\partial\mathcal{G}_1, \dots, \partial\mathcal{G}_{N-1}), \quad \partial\mathcal{G}_i := \mathcal{G}_i \cap \mathbb{S}^1 \subset \mathbb{S}^1.$$

We say that \mathcal{G} is *of type* λ or λ *admits* an N -graph \mathcal{G} if $\partial\mathcal{G} = \lambda$.

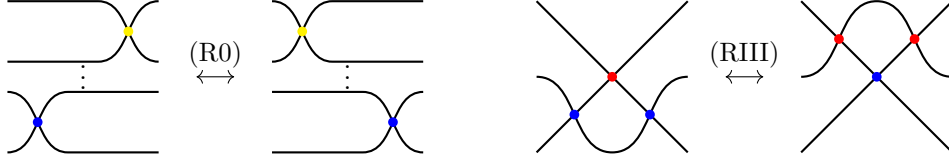
Let \mathbb{A} be the oriented annulus with two boundary components $\partial_+\mathbb{A}$ and $\partial_-\mathbb{A}$. For an N -graph \mathcal{G} on \mathbb{A} , let $\partial_\pm\mathcal{G} := \mathcal{G} \cap \partial_\pm\mathbb{A}$ be Legendrian links at two boundaries $\partial_\pm\mathbb{A}$, respectively. We say that \mathcal{G} is *of type* (λ_+, λ_-) if $\partial_\pm\mathcal{G} = \lambda_\pm$, respectively.

A typical example of annular N -graphs comes from Lagrangian cobordism between Legendrian links, which are closures of positive braids. In particular, for two closures λ_1 and λ_2 of positive braids β_1 and β_2 , any sequence of Legendrian braid moves from λ_2 to λ_1 will give us a special annular N -graph $\mathcal{G}_{\lambda_2\lambda_1}$.² Hence, for an N -graphs \mathcal{G} with $\partial\mathcal{G} = \lambda_1$, we have the N -graph $\mathcal{G}_{\lambda_2\lambda_1}\mathcal{G}$ with boundary

$$\partial(\mathcal{G}_{\lambda_2\lambda_1}\mathcal{G}) = \lambda_2.$$

Remark 3.15. We are dealing with both Legendrian links λ and surfaces Λ . In order to avoid the confusion, we use the terminologies “ ∂ -Legendrian isotopy” and “Legendrian isotopy” for isotopies between Legendrian links and surfaces, respectively.

Since a closure of a Legendrian positive braid in $J^1\mathbb{S}^1$ should not have any cusp, possible ∂ -Legendrian isotopies are either plane isotopies (R0) or the third Reidemeister move (RIII) as follows:



Therefore, any annular N -graph corresponding to a sequence of Reidemeister moves between Legendrian links is a concatenation of *elementary annular N -graphs*, which are $\mathcal{G}_{(R0)}$ and $\mathcal{G}_{(RIII)}$ on the annulus \mathbb{A} as depicted in Figure 21. We call an annular N -graph *tame* if it is a concatenation of elementary annular N -graphs.

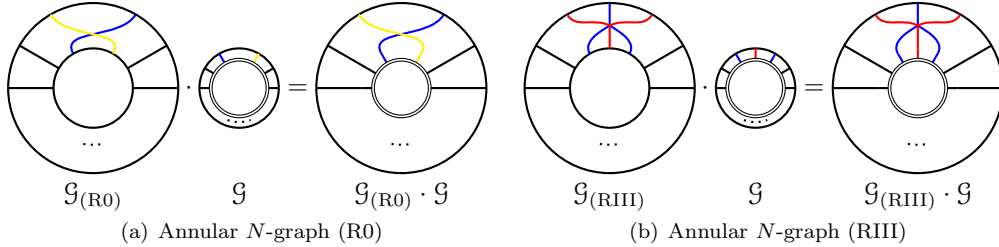
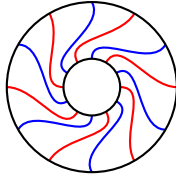


FIGURE 21. ∂ -Legendrian isotopy and elementary annulus N -graphs

Example 3.16. A *rotational annular N -graph*, which has no vertices and rotates a certain angle as depicted below is tame.



It is known that the rotational annular N -graph acts on the set of N -graphs for the Legendrian torus link $\lambda(n, m)$ of maximal Thurston–Bennequin number. This type of annular N -graphs

²One may call the N -graph $\mathcal{G}_{\lambda_2\lambda_1}$ a *strict concordance* since it is a union of cylinders.

play a crucial role in producing a sequence of distinct exact Lagrangian fillings of positive braid Legendrian links, see [36, 13, 30].

Definition 3.17. We say that two N -graphs \mathcal{G} and \mathcal{G}' with $\partial\mathcal{G} = \lambda_1$ and $\partial\mathcal{G}' = \lambda_2$ are ∂ -Legendrian isotopic if there exists a tame annular N -graph $\mathcal{G}_{\lambda_2\lambda_1}$ such that $[\mathcal{G}'] = [\mathcal{G}_{\lambda_2\lambda_1}\mathcal{G}]$.

3.2.3. Stabilizations. For a positive N -braid β in $J^1\mathbb{R}^1$, a *stabilization* $S(\beta)$ is a positive $(N+1)$ -braid which satisfies the following:

- (1) Closures of β and $S(\beta)$ are Legendrian isotopic in \mathbb{S}^3 :

$$\lambda_\beta \cong \lambda_{S(\beta)}.$$

- (2) The braid β can be recovered by forgetting a strand from $S(\beta)$.

More precisely, the second condition is as follows: let $q_{i+}(\beta)$ and $q_{i-}(\beta)$ be braids obtained from β by forgetting the i -th strand from the left and from the right. Then $S(\beta)$ has a decomposition

$$S(\beta) = \beta_1 \sigma_j \beta_2$$

and there exists an index $1 \leq i \leq N+1$ such that the i -th strands from the left and from the right of β meet precisely at the crossing σ_j in the middle of the decomposition $\beta = \beta_1 \sigma_j \beta_2$ and moreover

$$\beta = q_{i+}(\beta_1) q_{i-}(\beta_2).$$

The most typical example of a stabilization is as follows: let β_0 be a positive N -braid and $\beta = \Delta_N \beta_0 \Delta_N$, where Δ_N is the half-twist N -braid. Then it determines a Legendrian link λ_β uniquely up to Legendrian isotopy, but the converse is not true. Indeed, there are infinitely many pairwise distinct positive braids whose rainbow closures are Legendrian isotopic to λ_β in \mathbb{S}^3 . In particular, for a positive N -braid β_0 , a *stabilization* $S(\beta_0)$ is a positive $(N+1)$ -braid defined by $S(\beta_0) = \beta_0 \sigma_N$, where β_0 in $S(\beta_0)$ is regarded as an $(N+1)$ -braid by adding a trivial $(N+1)$ -st strand. Let $S(\beta) = \Delta_{N+1} S(\beta_0) \Delta_{N+1}$. Then

$$S(\beta) = \Delta_{N+1}(\beta_0 \sigma_N) \Delta_{N+1} = (\sigma_1 \dots \sigma_N)(\Delta_N \beta_0 \Delta_N)(\sigma_N \dots \sigma_1) \sigma_1 \doteq \beta(\sigma_N \dots \sigma_2 \sigma_1^3 \sigma_2 \dots \sigma_N),$$

where \doteq means the same up to cyclic permutation of braid words.

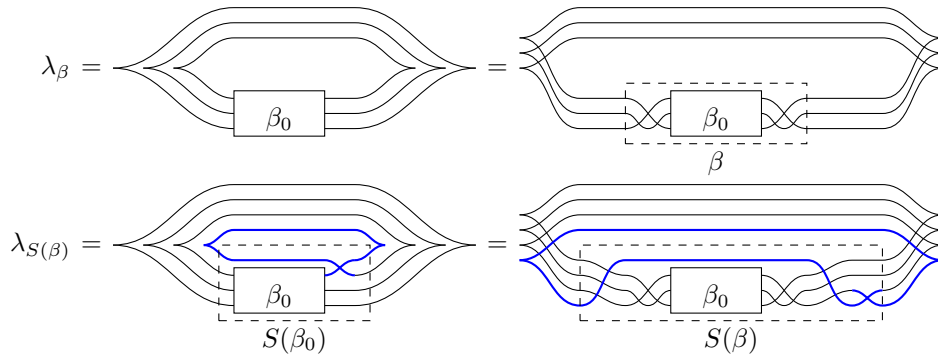


FIGURE 22. A stabilization $\lambda_{S(\beta)}$ of a Legendrian link λ_β

The Legendrian $\lambda_{S(\beta)}$ does depend on the braid word β_0 . For example, for each pair of positive N -braids $\beta_0^{(1)}$ and $\beta_0^{(2)}$ with $\beta_0 = \beta_0^{(1)} \beta_0^{(2)}$, let $\beta'_0 = \beta_0^{(2)} \beta_0^{(1)}$ and $\beta' = \Delta_N \beta'_0 \Delta_N$. Then two Legendrian links λ_β and $\lambda_{\beta'}$ are Legendrian isotopic but $\lambda_{S(\beta)}$ and $\lambda_{S(\beta')}$ are *not* Legendrian isotopic in general. Therefore a stabilization of a Legendrian link λ which is a closure of a positive braid may not be uniquely determined.

Example 3.18. Let $\beta(a, b, c) = \sigma_2 \sigma_1^{a+1} \sigma_2 \sigma_1^{b+1} \sigma_2 \sigma_1^{c+1}$ and $\beta(n) = \sigma_1^{n+3}$. Since $\beta(A_n) = \sigma_1^{n+3} = \sigma_1^c \sigma_1^{b+2}$, we have

$$\begin{aligned} S(\beta(A_n)) &= (\sigma_1 \sigma_2) \sigma_1^c \sigma_1^{b+2} (\sigma_2 \sigma_1) \sigma_1 \doteq \sigma_1^{b+2} (\sigma_2 \sigma_1^3 \sigma_2) \sigma_1^c = \sigma_1^{b+1} \Delta_3 \sigma_1 \Delta_3 \sigma_1^{c-1} \\ &= \sigma_1^{b+1} \sigma_2 \Delta_3^2 \sigma_1^{c-1} = \sigma_1^{b+1} \sigma_2 \sigma_1^{c+1} \sigma_2 \sigma_1^2 \sigma_2 \doteq \beta(1, b, c). \end{aligned}$$

Therefore $\beta(1, b, c)$ is a stabilization of $\beta(n)$ for each $b + c - 1 = n$.

Let us define

$$\tilde{\beta}_0(a, b, c) = (\sigma_2 \sigma_{1,3} \sigma_2) \sigma_2^{a-1} \sigma_1^{b-1} \sigma_3^{c-1} \quad \text{and} \quad \tilde{\beta}(a, b, c) = (\sigma_2 \sigma_{1,3} \sigma_2)^3 \sigma_2^{a-1} \sigma_1^{b+1} \sigma_3^{c+1},$$

where $\sigma_{1,3}$ is a 4-braid isotopic to $\sigma_1 \sigma_3$ (or equivalently, $\sigma_3 \sigma_1$) such that two crossings σ_1 and σ_3 occur simultaneously. Then one can easily show that $\tilde{\beta}(a, b, c)$ is Legendrian isotopic to $\Delta_4 \tilde{\beta}_0(a, b, c) \Delta_4$.

Example 3.19. The Legendrian $\lambda_{\tilde{\beta}_0(a,b,c)}$ is a stabilization of $\lambda_{\beta_0(a,b,c)}$ since

$$S(\beta_0(a, b, c)) = \sigma_1 \sigma_2^a \sigma_1^{b-1} \sigma_2 \sigma_3^c \sigma_2^{-1} = \sigma_1 \sigma_2^a \sigma_1^{b-1} \sigma_3^{c-1} \sigma_2 \sigma_3 \doteq (\sigma_2 \sigma_{1,3} \sigma_2) \sigma_2^{a-1} \sigma_1^{b-1} \sigma_3^{c-1} = \tilde{\beta}(a, b, c).$$

In particular, for $b = c$, we have 4-braids

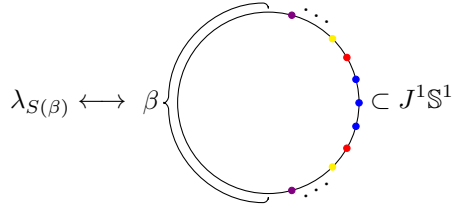
$$\tilde{\beta}_0(a, b, b) = (\sigma_2 \sigma_{1,3} \sigma_2) \sigma_2^{a-1} \sigma_{1,3}^{b-1} \quad \text{and} \quad \tilde{\beta}(a, b, b) = (\sigma_2 \sigma_{1,3} \sigma_2)^3 \sigma_2^{a-1} \sigma_{1,3}^{b-1},$$

and denote $\tilde{\beta}(2, 2, n-1)$ and $\tilde{\beta}(2, 3, 3)$ by $\tilde{\beta}(D_{n+1})$ and $\tilde{\beta}(E_6)$, respectively. Recall the conjugate action on \mathbb{C}^2 , which turns links upside down so that in terms of braid words, it interchanges σ_i and σ_{N-i} for each N -braid. Hence, for 4-braids, it preserves $\sigma_{1,3}$. Therefore $\tilde{\beta}(a, b, b)$ is invariant under conjugation and so is $\lambda_{\tilde{\beta}(a,b,b)}$:

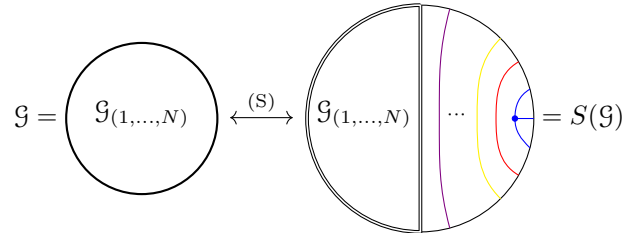
Lemma 3.20. *The Legendrian $\lambda_{\tilde{\beta}(a,b,b)}$ is invariant under conjugation.*

Corollary 3.21. *The Legendrians $\lambda_{\tilde{\beta}(D_{n+1})}$ and $\lambda_{\tilde{\beta}(E_6)}$ are invariant under conjugation.*

On the other hand, a stabilization $\lambda_{S(\beta)}$ of λ_β will be represented by N -colored dots in S^1 while λ_β uses only $(N-1)$ colors. That is,



Then one can transfer an N -graph \mathcal{G} for λ_β into an $(N+1)$ -graph $S(\mathcal{G})$ for $\lambda_{S(\beta)}$ as follows:



3.2.4. Annular N -graphs and Legendrian loops. Let $\beta, \beta_+, \beta_- \subset J^1 \mathbb{R}^1$ be Legendrian positive N -braids. We denote by $\text{Ngraphs}(\beta)$ and $\text{Ngraphs}(\beta_+, \beta_-)$ the sets of equivalence classes of N -graphs on \mathbb{D}^2 and \mathbb{A} satisfying boundary conditions given by the closure λ_β or a pair of closures $(\lambda_{\beta_+}, \lambda_{\beta_-})$.

$$\text{Ngraphs}(\beta) := \{[\mathcal{G}] \mid \mathcal{G} \text{ is an } N\text{-graph on } \mathbb{D}^2 \text{ of type } \lambda_\beta\}$$

$$\text{Ngraphs}(\beta_+, \beta_-) := \{[\mathcal{G}] \mid \mathcal{G} \text{ is an } N\text{-graph on } \mathbb{A} \text{ of type } (\lambda_{\beta_+}, \lambda_{\beta_-})\}.$$

Here, we are assuming that we are aware of where each braid word starts.

Then it is direct to check that these sets are invariant under the cyclic rotation of the braid words up to bijection. More precisely, for N -braids $\beta^{(1)}, \beta^{(2)}$ and $\beta_{\pm}^{(1)}, \beta_{\pm}^{(2)}$, closures of $\beta^{(1)}\beta^{(2)}$ and $\beta^{(2)}\beta^{(1)}$ are identical in $J^1\mathbb{S}^1$ and there are one-to-one correspondences between sets of N -graphs

$$\mathcal{N}\text{graphs}\left(\beta^{(1)}\beta^{(2)}\right) \cong \mathcal{N}\text{graphs}\left(\beta^{(2)}\beta^{(1)}\right), \quad (3.1)$$

$$\begin{aligned} \mathcal{N}\text{graphs}\left(\beta_+, \beta_-^{(1)}\beta_-^{(2)}\right) &\cong \mathcal{N}\text{graphs}\left(\beta_+, \beta_-^{(2)}\beta_-^{(1)}\right), \\ \mathcal{N}\text{graphs}\left(\beta_+^{(1)}\beta_+^{(2)}, \beta_-\right) &\cong \mathcal{N}\text{graphs}\left(\beta_+^{(2)}\beta_+^{(1)}, \beta_-\right) \end{aligned} \quad (3.2)$$

Suppose that $\mathcal{G}_1 \in \mathcal{N}\text{graphs}(\beta_2, \beta_1)$ and $\mathcal{G}_2 \in \mathcal{N}\text{graphs}(\beta_3, \beta_2)$. Then two N -graphs can be merged or piled in a natural way to obtain the annular N -graph, denoted by $\mathcal{G}_2\mathcal{G}_1 \in \mathcal{N}\text{graphs}(\beta_3, \beta_1)$. On the other hand, for $\mathcal{G} \in \mathcal{N}\text{graphs}(\beta)$ and $\mathcal{G}_1 \in \mathcal{N}\text{graphs}(\beta', \beta)$, the concatenation $\mathcal{G}_1\mathcal{G} \in \mathcal{N}\text{graphs}(\beta')$ is well-defined by gluing along the boundary λ_β . Hence, we have two natural maps

$$\begin{aligned} \mathcal{N}\text{graphs}(\beta_3, \beta_2) \times \mathcal{N}\text{graphs}(\beta_2, \beta_1) &\rightarrow \mathcal{N}\text{graphs}(\beta_3, \beta_1), \\ \mathcal{N}\text{graphs}(\beta', \beta) \times \mathcal{N}\text{graphs}(\beta) &\rightarrow \mathcal{N}\text{graphs}(\beta'). \end{aligned}$$

In particular, for each ∂ -Legendrian isotopy from $\lambda' = \lambda_{\beta'}$ and $\lambda = \lambda_\beta$, we have a tame annular N -graph $\mathcal{G}_{\lambda'\lambda} \in \mathcal{N}\text{graphs}(\beta', \beta)$, where λ and λ' are closures of β and β' , respectively. Moreover, we also have a tame annular N -graph $\mathcal{G}_{\lambda'\lambda}^{-1}$ obtained by flipping the annulus inside out corresponding to the inverse isotopy from λ to λ' . Hence, we have two maps inverses to each other

$$\mathcal{N}\text{graphs}(\beta) \rightarrow \mathcal{N}\text{graphs}(\beta'), \quad \text{and} \quad \mathcal{N}\text{graphs}(\beta') \rightarrow \mathcal{N}\text{graphs}(\beta),$$

defined by

$$\mathcal{G} \mapsto \mathcal{G}_{\lambda'\lambda} \cdot \mathcal{G}, \quad \text{and} \quad \mathcal{G}' \mapsto \mathcal{G}_{\lambda'\lambda}^{-1} \cdot \mathcal{G}',$$

respectively.

Let $\mathcal{N}\text{graphs}_0(\beta, \beta)$ be the subset of tame annular N -graphs of type (β, β) .

Lemma 3.22. *Let β be a Legendrian positive N -graph. The set $\mathcal{N}\text{graphs}_0(\beta, \beta)$ becomes a group under the concatenation which acts on the set $\mathcal{N}\text{graphs}(\beta)$.*

Proof. It is easy to see that the set $\mathcal{N}\text{graphs}_0(\beta, \beta)$ is closed under the concatenation, which is associative. The trivial ∂ -Legendrian isotopy gives us the identity annular N -graph.

Finally, for each $\mathcal{G} \in \mathcal{N}\text{graphs}_0(\beta, \beta)$, the N -graph \mathcal{G}^{-1} plays the role of the inverse of \mathcal{G} due to the Move (I) and (V) of N -graphs in Figure 18. Hence $\mathcal{N}\text{graphs}_0(\beta, \beta)$ becomes a group acting on the set $\mathcal{N}\text{graphs}(\beta)$ by concatenation, and so we are done. \square

Definition 3.23 (Legendrian loop). Let $\lambda \subset (\mathbb{R}^3, \xi_{\text{st}})$ be a Legendrian link and $\mathcal{L}(\lambda)$ be the space of Legendrian links isotopic to λ . A *Legendrian loop* ϑ is a continuous map $\vartheta: (\mathbb{S}^1, \text{pt}) \rightarrow (\mathcal{L}(\lambda), \lambda)$ and said to be *tame* if the Legendrian $\vartheta(\theta)$ is a closure of a positive braid for each $\theta \in \mathbb{S}^1$.

Remark 3.24. One can regard each Legendrian loop ϑ for λ as an element of the fundamental group $\pi_1(\mathcal{L}(\lambda), \lambda)$.

Let λ be the closure of a positive braid β . Then each tame Legendrian loop for λ corresponds to a ∂ -Legendrian isotopy from λ to λ and can be regarded as an element \mathcal{G}_ϑ in $\mathcal{N}\text{graphs}_0(\beta, \beta)$. Conversely, any element \mathcal{G} in $\mathcal{N}\text{graphs}_0(\beta, \beta)$ defines a tame Legendrian loop $\vartheta_\mathcal{G}$ obviously.

In summary, we have the following lemma.

Lemma 3.25. *Let β be a Legendrian positive N -braid. Then there is one-to-one correspondence between $\mathcal{N}\text{graphs}_0(\beta, \beta)$ and the subset of homotopy classes of tame Legendrian loops for $\lambda = \lambda_\beta$. In particular, each tame Legendrian loop acts on $\mathcal{N}\text{graphs}(\beta)$.*

3.3. One-cycles in Legendrian weaves. Let us recall from [15] how to construct a seed from an N -graph \mathcal{G} . Each one-cycle in $\Lambda(\mathcal{G})$ corresponds to a vertex of the quiver, and a monodromy along that cycle gives a coordinate function at that vertex. The quiver is obtained from the intersection data among one-cycles. Moreover, there is an operation in N -graph, called *Legendrian mutation*, which is a counterpart of the mutation in the cluster structure. The Legendrian mutation is crucial in constructing and distinguishing N -graphs. In turn, these will give as many Lagrangian fillings as seeds of Legendrian links.

Let $\mathcal{G} \subset \mathbb{D}^2$ be a free N -graph and $\Lambda(\mathcal{G})$ be the induced Legendrian weave. We express one-cycles of $\Lambda(\mathcal{G})$ in terms of subgraphs of \mathcal{G} .

Definition 3.26. A subgraph T of a nondegenerate N -graph \mathcal{G} is said to be *admissible* if at each vertex, it looks locally one of pictures depicted in Figure 23. For a degenerate N -graph \mathcal{G} , a subgraph T is *admissible* if so is its perturbation as a subgraph of the perturbation of \mathcal{G} . See Figure 24.

For an admissible subgraph $T \subset \mathcal{G}$, let $\ell(T) \subset \mathbb{D}^2$ be an oriented, immersed, labelled loop given by gluing paths whose local pictures look as depicted in Figure 23.

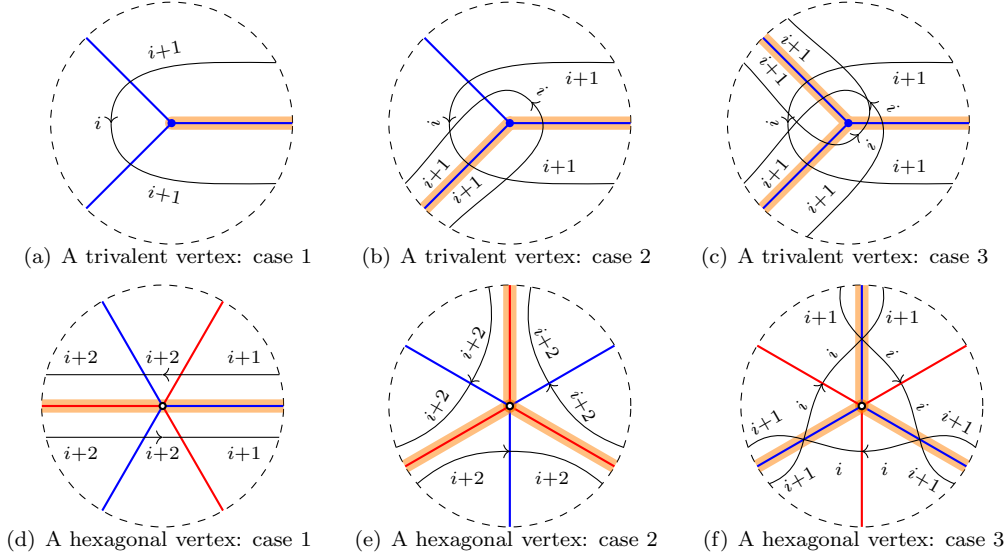


FIGURE 23. Local configurations on cycles and corresponding arcs of $\mathcal{G} \subset \mathbb{D}^2$

The loop $\ell(T)$ defines a unique lift $\tilde{\ell}(T) \subset \Gamma(\mathcal{G})$ via $\pi_{\mathbb{D}^2} : \Gamma(\mathcal{G}) \rightarrow \mathbb{D}^2$ so that each s_j -labelled arc in $\ell(T)$ is contained in the s_j -th sheet of $\Gamma(\mathcal{G})$. Moreover, the immersed loop $\tilde{\ell}(T)$ lifts uniquely to an embedded loop $\gamma(T)$ in $\Lambda(\mathcal{G})$ via the front projection $\pi_F : \Lambda(\mathcal{G}) \rightarrow \Gamma(\mathcal{G})$.

Definition 3.27. [T -cycle] For an admissible subgraph $T \subset \mathcal{G}$, we call the cycle $[\gamma(T)] \in H_1(\Lambda(\mathcal{G}); \mathbb{Z})$ a T -cycle.

Example 3.28 ((Long) l-cycles). For an edge e of \mathcal{G} connecting two trivalent vertices, let $l(e)$ be the subgraph of \mathcal{G} consisting of a single edge e . Then the cycle $[\gamma(l(e))]$ depicted in Figure 25(a) is called an *l-cycle*.

In general, a linear chain of edges (e_1, e_2, \dots, e_n) satisfying

- e_i connects a trivalent vertex and a hexagonal point for $i = 1, n$;
- e_i and e_{i+1} meet at a hexagonal point in the opposite way, see Figure 25(b), for $i = 2, \dots, n-1$

forms an admissible subgraph $l(e_1, \dots, e_n)$, and the cycle $[\gamma(l(e_1, \dots, e_n))]$ is called a *long l-cycle*. See Figure 25(b).

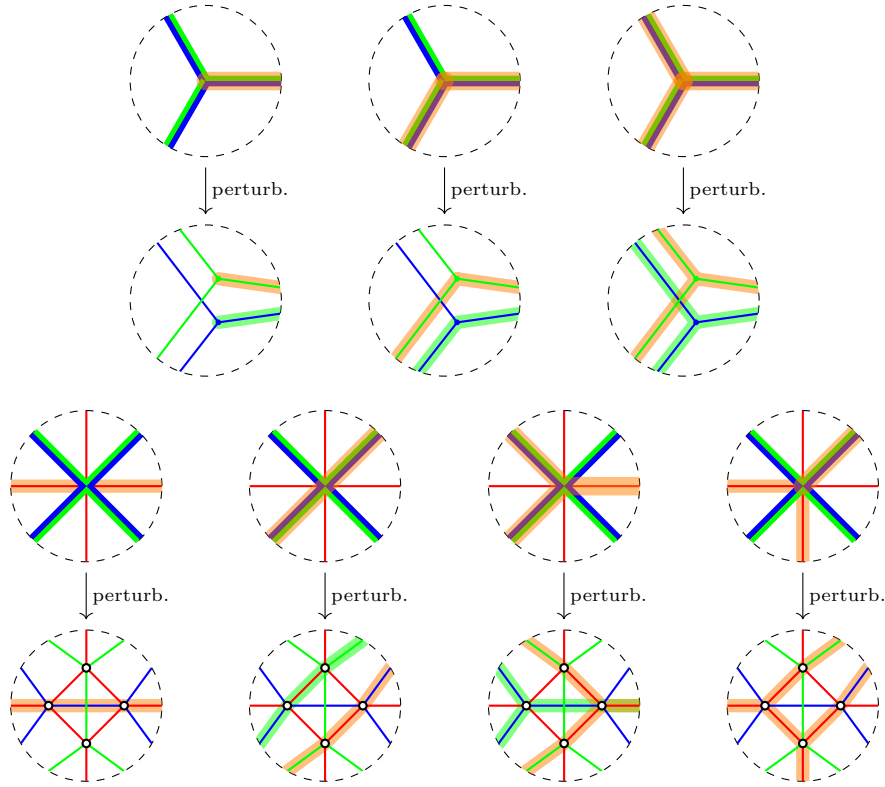
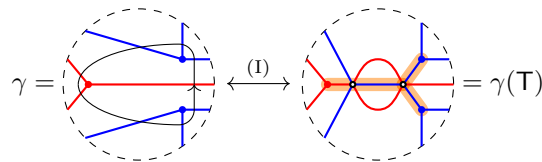


FIGURE 24. Local configurations on degenerate cycles and its perturbation.

Example 3.29 (Y-cycles). Let e_1, e_2, e_3 be monochromatic edges joining a hexagonal point h and trivalent vertices v_i for $i = 1, 2, 3$. Then the subgraph $Y(e_1, e_2, e_3)$ consisting of three edges e_1, e_2 and e_3 is an admissible subgraph of \mathcal{G} and it defines a cycle $[\gamma(Y(e_1, e_2, e_3))]$ called an *upper* or *lower* Y-cycle according to the relative position of sheets that edges represent. See Figures 25(c) and 25(d).

One of the benefit of cycles from admissible subgraphs is that one can keep track how cycles are changed under the N -graph moves described in Figure 18, especially under Move (I) and Move (II). Note that Move (III) can be decomposed into a sequence of Move (I) and Move (II). Some of such changes are given in Figure 26.

Remark 3.30. It is important to note that not every cycle can be represented by a subgraph. For example, the cycle on the left of the following picture can not be expressed by a subtree but it can be after Move (I).



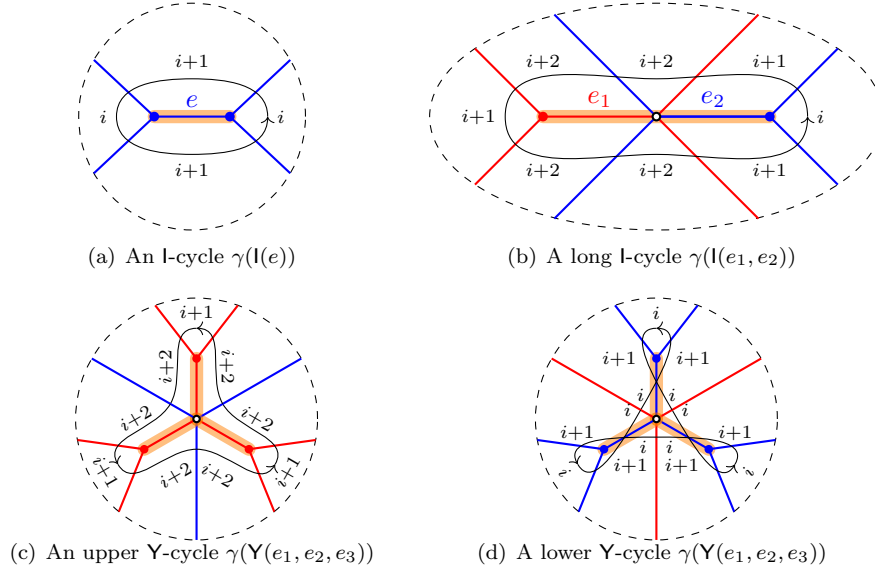
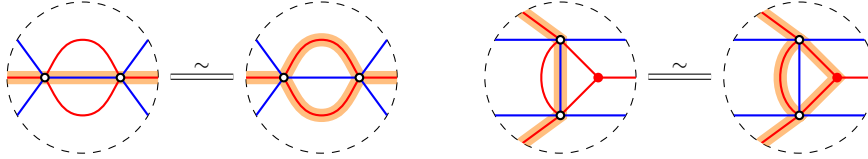


FIGURE 25. (Long) l- and Y-cycles

On the other hand, there might be a one-cycle having two different subgraph presentations as follows:

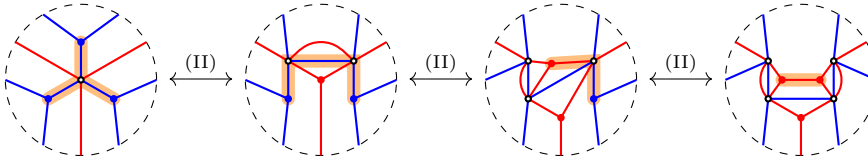


Therefore, there is a bit subtle issue for picking up nice cycles in a consistent way.

Definition 3.31. Let $\mathcal{G} \subset \mathbb{D}^2$ be an N -graph, and let $\Lambda(\mathcal{G})$ be an induced Legendrian surface in $J^1\mathbb{D}^2$. A cycle $[\gamma]$ in $H_1(\Lambda(\mathcal{G}))$ is *good* if $[\gamma]$ can be transformed to an l-cycle in $H_1(\Lambda(\mathcal{G}'))$ for some $[\mathcal{G}'] = [\mathcal{G}]$, respectively.

Example 3.32. The following cycles are good.

- (1) All (long) l- and Y-cycles



- (2) The cycle $\gamma(T)$ for an admissible tree T without local configurations depicted in Figures 23(b) and 23(c)

Definition 3.33. Let $(\mathcal{G}, \mathcal{B})$ and $(\mathcal{G}', \mathcal{B}')$ be pairs of an N -graph and sets of good cycles. We say that $(\mathcal{G}, \mathcal{B})$ and $(\mathcal{G}', \mathcal{B}')$ are *equivalent* if $[\mathcal{G}] = [\mathcal{G}']$ and the induced isomorphism

$$H_1(\Lambda(\mathcal{G})) \cong H_1(\Lambda(\mathcal{G}'))$$

identifies \mathcal{B} with \mathcal{B}' . We denote the equivalent class of $(\mathcal{G}, \mathcal{B})$ by $[\mathcal{G}, \mathcal{B}]$.

Let $(\mathcal{G}, \mathcal{B})$ be a pair of N -graph and a set of (good) cycles. We define the conjugation $\overline{(\mathcal{G}, \mathcal{B})}$ by the pair $(\bar{\mathcal{G}}, \bar{\mathcal{B}})$ such that $\bar{\mathcal{G}}$ is the conjugation of \mathcal{G} and $\bar{\mathcal{B}}$ is the set of (good) cycles in $H_1(\Lambda(\bar{\mathcal{G}}); \mathbb{Z})$ consisting of the images of cycles in \mathcal{B} under the induced isomorphism $H_1(\Lambda(\mathcal{G}); \mathbb{Z}) \rightarrow H_1(\Lambda(\bar{\mathcal{G}}); \mathbb{Z})$.

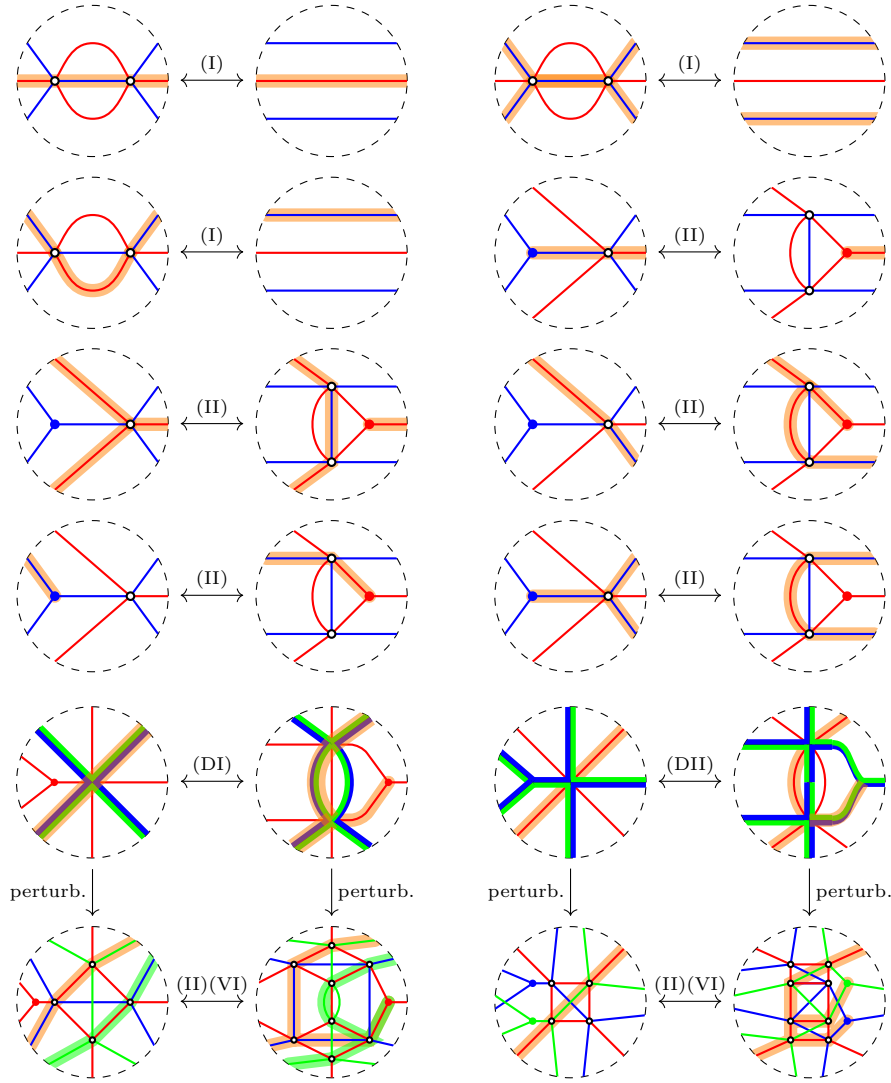


FIGURE 26. Cycles under Moves (I), (II), (DI) and (DII).

3.4. Flag moduli spaces. We recall from [15] a central algebraic invariant $\mathcal{M}(\mathcal{G})$ of the Legendrian weave $\Lambda(\mathcal{G})$. The main idea is to consider moduli spaces of constructible sheaves associated to $\Lambda(\mathcal{G})$. To introduce a legible model for such constructible sheaves, let us consider a full flag, i.e. a nested sequence of subspaces in \mathbb{C}^N ;

$$\mathcal{F}^\bullet \in \{(\mathcal{F}^i)_{i=0}^N \mid \dim \mathcal{F}^i = i, \mathcal{F}^j \subset \mathcal{F}^{j+1}, 1 \leq j \leq N-1, \mathcal{F}^N = \mathbb{C}^N\}.$$

Definition 3.34. [15] Let $\mathcal{G} \subset \mathbb{D}^2$ be an N -graph. Let $\{F_i\}_{i \in I}$ be a set of closures of connected components of $\mathbb{D}^2 \setminus \mathcal{G}$, call each closure a *face*. The *framed flag moduli space* $\widetilde{\mathcal{M}}(\mathcal{G})$ is a collection of flags $\mathcal{F}_{\Lambda(\mathcal{G})} = \{\mathcal{F}^\bullet(F_i)\}_{i \in I}$ in \mathbb{C}^N satisfying the following:

Let F_1, F_2 be a pair of faces sharing an edge in \mathcal{G}_i . Then the corresponding flags $\mathcal{F}^\bullet(F_1), \mathcal{F}^\bullet(F_2)$ satisfy

$$\begin{cases} \mathcal{F}^j(F_1) = \mathcal{F}^j(F_2), & 0 \leq j \leq N, \quad j \neq i; \\ \mathcal{F}^i(F_1) \neq \mathcal{F}^i(F_2). \end{cases} \quad (3.3)$$

The general linear group GL_N acts on $\mathcal{M}(\mathcal{G})$ by transforming all flags at once. The *flag moduli space* of the N -graph \mathcal{G} is defined by the quotient space (a stack, in general)

$$\mathcal{M}(\mathcal{G}) := \widetilde{\mathcal{M}}(\mathcal{G}) / \mathrm{GL}_N.$$

From now on, we will regard flags $\mathcal{F}_{\Lambda(\mathcal{G})}$ as a formal parameter for the flag moduli space $\Lambda(\mathcal{G})$.

Let $\mathbf{Sh}(\mathbb{D}^2 \times \mathbb{R})$ be the category of *constructible sheaves* on $\mathbb{D}^2 \times \mathbb{R}$. Under the identification $J^1\mathbb{D}^2 \cong T^{\infty,-}(\mathbb{D}^2 \times \mathbb{R})$, an N -graph $\mathcal{G} \subset \mathbb{D}^2$ gives a Legendrian

$$\Lambda(\mathcal{G}) \subset J^1\mathbb{D}^2 \cong T^{\infty,-}(\mathbb{D}^2 \times \mathbb{R}) \subset T^{\infty}(\mathbb{D}^2 \times \mathbb{R}).$$

This can be used to define a Legendrian isotopy invariant $\mathbf{Sh}_{\Lambda(\mathcal{G})}^1(\mathbb{D}^2 \times \mathbb{R})_0$ of $\mathbf{Sh}(\mathbb{D}^2 \times \mathbb{R})$ consisting of constructible sheaves

- whose singular support at infinity lies in $\Lambda(\mathcal{G}) \subset T^{\infty}(\mathbb{D}^2 \times \mathbb{R})$,
- whose microlocal rank is one, and
- which are zero near $\mathbb{D}^2 \times \{-\infty\}$.

See [15, 32, 43] for more details.

Theorem 3.35 ([15, Theorem 5.3]). *The flag moduli space $\mathcal{M}(\mathcal{G})$ is isomorphic to $\mathbf{Sh}_{\Lambda(\mathcal{G})}^1(\mathbb{D}^2 \times \mathbb{R})_0$. Hence $\mathcal{M}(\mathcal{G})$ is a Legendrian isotopy invariant of $\Lambda(\mathcal{G})$.*

Remark 3.36. Indeed, the actual theorem is about a connected surface, not only for \mathbb{D}^2 .

3.5. Y -seeds and Legendrian mutations. Let $\mathcal{G} \subset \mathbb{D}^2$ be an N -graph, and let $\mathcal{B} = \{[\gamma_1], \dots, [\gamma_n]\}$ be a set of good cycles. For two cycles $[\gamma_i]$ and $[\gamma_j]$, let $i([\gamma_i], [\gamma_j])$ be the algebraic intersection number in $H_1(\Lambda(\mathcal{G}))$.

In particular, if γ_i is an l-cycle $\gamma(l(e))$ and γ_j is a T-cycle for some admissible subgraph \mathbf{T} , then

$$i([\gamma_i], [\gamma_j]) = \sum_{e' \in \mathbf{T}} i(e, e'),$$

where $i(e, e') \in \{0, 1, -1\}$ is defined as follows:

$$i(e, e') := \begin{cases} 0 & \text{if } e = e' \text{ or } e \cap e' = \emptyset; \\ 1 & \text{if } e' \text{ is lying on the left side of } e; \\ -1 & \text{if } e' \text{ is lying on the right side of } e. \end{cases}$$

Geometrically, two representatives of γ_i and γ_j look locally as depicted in Figure 27. Their intersection $i([\gamma_i], [\gamma_j])$ is defined to be +1 by using the counterclockwise rotation convention of two tangent directions of cycles γ_i and γ_j at the intersection point as depicted in the third picture in Figure 27. Note that our convention is opposite to the one in [15].

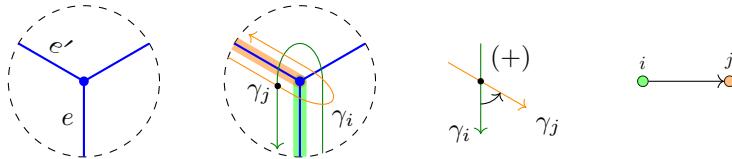


FIGURE 27. l-cycles with intersections.

Definition 3.37. For each a pair $(\mathcal{G}, \mathcal{B})$ of an N -graph and a set of good cycles, we define a quiver $\mathcal{Q} = \mathcal{Q}(\mathcal{G}, \mathcal{B})$ as follows: let $n = \#(\mathcal{B})$.

- (1) the set of vertices is $[n]$,
- (2) the (i, j) -entry $b_{i,j}$ for $\tilde{\mathcal{B}}(\mathcal{Q}) = (b_{i,j})$ is the algebraic intersection number between $[\gamma_i]$ and $[\gamma_j]$

$$b_{i,j} = i([\gamma_i], [\gamma_j]) \quad \text{for } 1 \leq i, j \leq n.$$

In order to assign a coefficient to each one-cycle, let us review the microlocal monodromy functor from [43]

$$\mu\text{mon}_\Lambda : \text{Sh}_\Lambda^\bullet \rightarrow \mathcal{L}\text{oc}^\bullet(\Lambda).$$

In our case, this functor sends microlocal rank-one sheaves $\mathcal{F} \in \mathcal{M}(\mathcal{G}) \cong \text{Sh}_{\Lambda(\mathcal{G})}^1(\mathbb{D}^2 \times \mathbb{R})_0$, or equivalently, flags $\{\mathcal{F}^\bullet(F_i)\}_{i \in I} \in \mathcal{M}(\mathcal{G})$ to rank-one local systems $\mu\text{mon}_{\Lambda(\mathcal{G})}(\mathcal{F})$ on the Legendrian surface $\Lambda(\mathcal{G})$. Then the coefficients in the coefficient tuple \mathbf{y} for the pair $(\mathcal{G}, \mathcal{B})$ are defined by

$$\mathbf{y}(\mathcal{G}, \mathcal{B}) = \left(\mu\text{mon}_{\Lambda(\mathcal{G})}(-)([\gamma_1]), \dots, \mu\text{mon}_{\Lambda(\mathcal{G})}(-)([\gamma_n]) \right),$$

where $\mu\text{mon}_{\Lambda(\mathcal{G})}(-)([\gamma_j]) : \mathcal{M}(\mathcal{G}) \rightarrow \mathbb{C}$. Let us denote the above assignment by

$$\Psi(\mathcal{G}, \mathcal{B}) = (\mathbf{y}(\mathcal{G}, \mathcal{B}), \mathcal{Q}(\mathcal{G}, \mathcal{B})).$$

By the Legendrian isotopy invariance of $\text{Sh}_{\Lambda(\mathcal{G})}^1(\mathbb{D}^2 \times \mathbb{R})_0$ in [32], and the functorial property of the microlocal monodromy functor μmon [43], the assignment Ψ is well-defined up to isotopy of $\Lambda(\mathcal{G})$. That is, if two pairs $(\Lambda(\mathcal{G}), \mathcal{B})$ and $(\Lambda(\mathcal{G}'), \mathcal{B}')$ are Legendrian isotopic, or $[\mathcal{G}, \mathcal{B}] = [\mathcal{G}', \mathcal{B}']$ in particular, then they give us the same seed via Ψ .

Theorem 3.38. [15, §7.2.1] *Let $\mathcal{G} \subset \mathbb{D}^2$ be a N -graph with a tuple \mathcal{B} of cycles in $H_1(\Lambda(\mathcal{G}))$. Then the assignment Ψ to a Y -seed in a cluster structure*

$$\Psi([\mathcal{G}, \mathcal{B}]) = (\mathbf{y}(\mathcal{G}, \mathcal{B}), \mathcal{Q}(\mathcal{G}, \mathcal{B}))$$

is well-defined.

As a corollary, the seed $\Psi(\mathcal{G}, \mathcal{B})$ can be used to distinguish a pair of Legendrian surfaces and hence, by Lemma 3.11, a pair of Lagrangian fillings.

Corollary 3.39. *For two pairs $(\mathcal{G}, \mathcal{B})$, $(\mathcal{G}', \mathcal{B}')$ with the same boundary condition defining different seeds, two induced Lagrangian fillings $(\pi \circ \iota)(\Lambda(\mathcal{G}))$, $(\pi \circ \iota)(\Lambda(\mathcal{G}'))$ bounding $\iota(\lambda)$ are not exact Lagrangian isotopic to each other.*

The monodromy $\mu\text{mon}_{\Lambda(\mathcal{G})}(\mathcal{F})$ along a loop $[\gamma] \in H_1(\Lambda(\mathcal{G}))$ can be obtained by restricting the constructible sheaf \mathcal{F} to a tubular neighborhood of γ . Let us investigate how the monodromy can be computed explicitly in terms of flags $\{\mathcal{F}^\bullet(F_i)\}_{i \in I}$.

Let us consider an l-cycle $[\gamma]$ represented by a loop $\gamma(e)$ for some monochromatic edge e as in Figure 28(a). Let us denote four flags corresponding to each region by F_1, F_2, F_3, F_4 , respectively. Suppose that $e \subset \mathcal{G}_i$, then by the construction of flag moduli space $\mathcal{M}(\mathcal{G})$, a two-dimensional vector space $V := \mathcal{F}^{i+1}(F_*)/\mathcal{F}^{i-1}(F_*)$ is independent of $*$ = 1, 2, 3, 4. Moreover, $\mathcal{F}^i(F_*)/\mathcal{F}^{i-1}(F_*)$ defines a one-dimensional subspace $v_* \subset V$ for $*$ = 1, 2, 3, 4, satisfying

$$v_1 \neq v_2 \neq v_3 \neq v_4 \neq v_1.$$

Then $\mu\text{mon}_{\Lambda(\mathcal{G})}(\mathcal{F})$ along the one-cycle $[\gamma(e)]$ is defined by the cross ratio

$$\mu\text{mon}_{\Lambda(\mathcal{G})}(\mathcal{F})([\gamma]) := \langle v_1, v_2, v_3, v_4 \rangle = \frac{v_1 \wedge v_2}{v_2 \wedge v_3} \cdot \frac{v_3 \wedge v_4}{v_4 \wedge v_1}.$$

Suppose that local flags $\{F_j\}_{j \in J}$ near the upper Y-cycle $[\gamma_U]$ look like in Figure 28(b). Let \mathcal{G}_i and \mathcal{G}_{i+1} be the N -subgraphs in red and blue, respectively. Then the 3-dimensional vector space $V = \mathcal{F}^{i+2}(F_*)/\mathcal{F}^{i-1}(F_*)$ is independent of $*$ = 1, 2, 3, 4. Now regard a, b, c and A, B, C are subspaces of V of dimension one and two, respectively. Then the microlocal monodromy along the Y-cycle $[\gamma_U]$ becomes

$$\mu\text{mon}_{\Lambda(\mathcal{G})}(\mathcal{F})([\gamma_U]) := \frac{A(c)B(a)C(b)}{A(b)B(c)C(a)}.$$

Here, $B(a)$ can be seen as a paring between a vector v_a with $\langle v_a \rangle = a$, and a covector w_B with $\langle w_B \rangle = B^\perp$.

Now consider the lower Y-cycle $[\gamma_L]$ whose local flags given as in Figure 28(c). We already have seen that the orientation convention of the loop in Figure 25 for the upper and lower Y-cycle is different. Then microlocal monodromy along $[\gamma_L]$ follows the opposite orientation and becomes

$$\mu\text{mon}_{\Lambda(\mathcal{G})}(\mathcal{F})([\gamma_L]) := \frac{A(b)B(c)C(a)}{A(c)B(a)C(b)}.$$

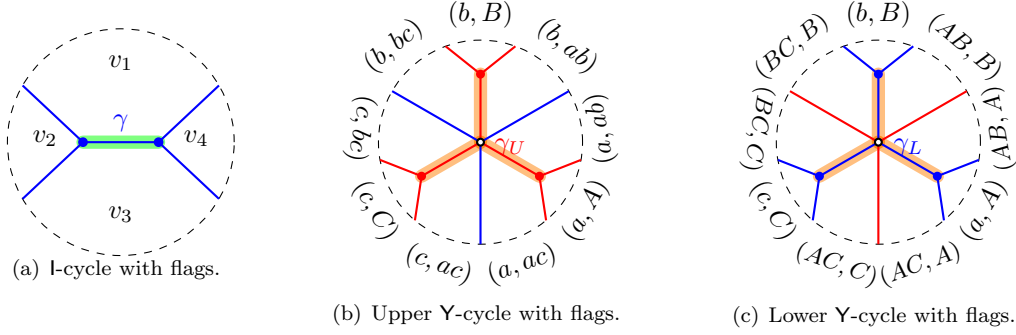


FIGURE 28. l- and Y-cycles with flags. Here ab means the span of a and b , and AB means the intersection of A and B .

Let us define an operation called (*Legendrian*) *mutation* on N -graphs \mathcal{G} which corresponds to a geometric operation on the induced Legendrian surface $\Lambda(\mathcal{G})$ that producing a smoothly isotopic but not necessarily Legendrian isotopic to $\Lambda(\mathcal{G})$, see [15, Definition 4.19]. Note that operation has an intimate relation with the wall-crossing phenomenon [4], Lagrangian surgery [39], and quiver (or Y-seed) mutations [25].

Definition 3.40. [15] Let \mathcal{G} be a (local) N -graph and $e \in \mathcal{G}_i \subset \mathcal{G}$ be an edge between two trivalent vertices corresponding to an l-cycle $[\gamma] = [\gamma(e)]$. The mutation $\mu_\gamma(\mathcal{G})$ of \mathcal{G} along γ is obtained by applying the local change depicted in the left of Figure 29.

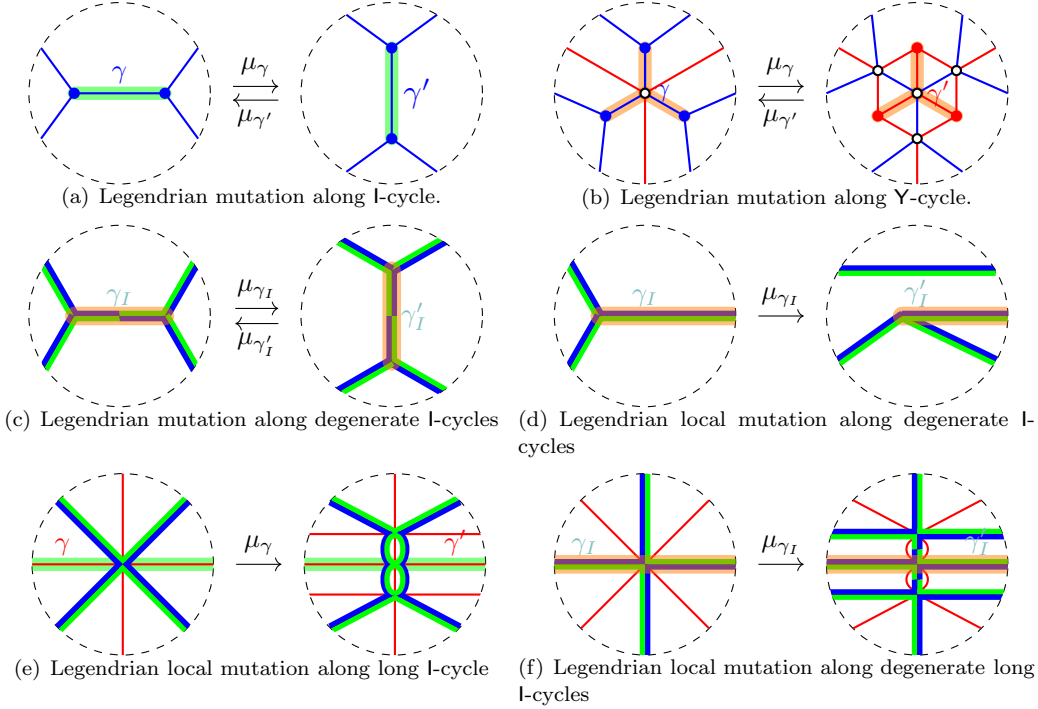


FIGURE 29. Legendrian (local) mutations at (degenerate, long) l- and Y-cycles.

For the Y-cycle, the Legendrian mutation becomes as in the right of Figure 29(b). Note that the mutation at Y-cycle can be decomposed into a sequence of Move (I) and Move (II) together with a mutation at l-cycle.

One can easily verify Legendrian (local) mutations on degenerate N -graph shown in Figures 29(c) and 29(d) via perturbation. For Figures 29(e) and 29(f), see Appendix B.2.

Let us remind our main purpose of finding exact embedded Lagrangian fillings for a Legendrian links. The following lemma guarantees that Legendrian mutation preserves the embedding property of Lagrangian fillings.

Proposition 3.41. [15, Lemma 7.4] *Let $\mathcal{G} \subset \mathbb{D}^2$ be a free N -graph. Then mutation $\mu(\mathcal{G})$ at any l- or Y-cycle is again free N -graph.*

An important observation is the Legendrian mutation on $(\mathcal{G}, \mathcal{B})$ induces a Y -seed mutation on the induced seed $\Psi(\mathcal{G}, \mathcal{B})$.

Proposition 3.42 ([15, §7.2]). *Let $\mathcal{G} \subset \mathbb{D}^2$ be a N -graph and \mathcal{B} be a set of good cycles in $H_1(\Lambda(\mathcal{G}))$. Let $\mu_{\gamma_i}(\mathcal{G}, \mathcal{B})$ be a Legendrian mutation of $(\mathcal{G}, \mathcal{B})$ along a one-cycle γ_i . Then*

$$\Psi(\mu_{\gamma_i}(\mathcal{G}, \mathcal{B})) = \mu_i(\Psi(\mathcal{G}, \mathcal{B})).$$

Here, μ_i is the Y -seed mutation at the vertex i (cf. Remark 2.7).

Remark 3.43. Let λ and λ' be two isotopic closures of positive N -braids. By fixing an isotopy between them, we have an annular N -graph $\mathcal{G}_{\lambda\lambda'}$ which induces a bijection between sets of N -graphs for λ and λ' by attaching $\mathcal{G}_{\lambda\lambda'}$. Then, indeed, this bijection is equivariant under the Legendrian mutation if it is defined, that is, for $[\gamma] \in H_1(\Lambda(\mathcal{G}))$,

$$\mu_\gamma(\mathcal{G}_{\lambda\lambda'} \cdot \mathcal{G}) = \mathcal{G}_{\lambda\lambda'} \cdot \mu_\gamma(\mathcal{G}).$$

In other words, two ∂ -Legendrian isotopic N -graphs will generate equivariantly bijective sets of N -graphs under Legendrian mutations.

Remark 3.44. Similarly, a stabilization $S(\mathcal{G})$ of \mathcal{G} will generate equivariantly bijective sets of N -graphs under Legendrian mutations as well since the stabilization part in $S(\mathcal{G})$ is away from chosen cycles and does not affect the Legendrian mutability.

3.5.1. Flags on λ . Let $\lambda = \lambda_\beta$ be a Legendrian in $J^1\mathbb{S}^1$, which gives us an $(N-1)$ -tuple of points $X = (X_1, \dots, X_{N-1})$ in \mathbb{S}^1 which given by the alphabet $\sigma_1, \dots, \sigma_{N-1}$ of the braid word β . Let $\{f_j\}_{j \in J}$ be the set of closures of connected components of $\mathbb{S}^1 \setminus X$. The flags $\mathcal{F}_\lambda = \{\mathcal{F}_\lambda^\bullet(f_j)\}_{j \in J}$ in \mathbb{C}^N satisfying the conditions in (3.3) and having the trivial monodromy of $\{\mathcal{F}_\lambda^N(f_j)\}_{j \in J}$ along \mathbb{S}^1 will be called simply by *flags on λ* .

It is well known that the moduli space $\mathcal{M}(\lambda)$ of such flags \mathcal{F}_λ up to GL_N is isomorphic to $\mathrm{Sh}_\lambda^1(\mathbb{R}^2)_0$ which is a Legendrian isotopy invariant, see [43, Theorem 1.1]. As before, we will regard \mathcal{F}_λ as a formal parameter for $\mathcal{M}(\lambda)$.

Definition 3.45. Let $\mathcal{G} \subset \mathbb{D}^2$ be an N -graph, and let \mathcal{F}_λ be flags adapted to $\lambda \subset J^1\partial\mathbb{D}^2$ given by $\partial\mathcal{G}$. An N -graph \mathcal{G} is called *deterministic*, if there exist unique flags $\mathcal{F} \in \widetilde{\mathcal{M}}(\mathcal{G})$ in Definition 3.34, for each \mathcal{F}_λ , satisfying $\mathcal{F}|_{\partial\mathbb{D}^2} = \mathcal{F}_\lambda$.

Note that $\mathcal{G}(a, b, c)$ in the introduction is deterministic in an obvious way. If an N -graph $\mathcal{G} \subset \mathbb{D}^2$ is deterministic and $[\mathcal{G}] = [\mathcal{G}']$, then so is \mathcal{G}' .

Proposition 3.46. *Let $\mathcal{G} \subset \mathbb{D}^2$ be a deterministic N -graph. Then, for any l- or Y-cycle γ , the mutation $\mu_\gamma(\mathcal{G})$ is again a deterministic N -graph.*

Proof. The proof is straightforward from the notion of the deterministic N -graph in Definition 3.45 and of the Legendrian mutation depicted in Figure 29(a). Note that the Legendrian mutation $\mu_\gamma(\mathcal{G})$ at Y-cycle γ is also deterministic, since $\mu_\gamma(\mathcal{G})$ is a composition of Moves (I) and (II), and a mutation at l-cycle. \square

Remark 3.47. Especially when an N -graph \mathcal{G} is deterministic, the coefficient tuple \mathbf{y} originally defined on $\mathbb{C}[\mathcal{M}(\mathcal{G})]$ can be restricted to the coordinate ring $\mathbb{C}[\mathcal{M}(\lambda)]$ of the moduli spaces $\mathcal{M}(\lambda)$ of flags on λ . It is important to note that the moduli space $\mathcal{M}(\lambda)$ is actually a cluster Poisson variety (also called a \mathcal{X} -cluster variety or a cluster \mathcal{X} -variety) due to the result of Shen–Weng [41, Theorem 1.7].

4. LAGRANGIAN FILLINGS FOR LEGENDRIAN LINKS OF FINITE OR AFFINE TYPE

Let $\lambda \subset J^1\mathbb{S}^1$ be a Legendrian knot or link which is a closure of a positive braid and bounds a Legendrian surface $\Lambda(\mathcal{G})$ in $J^1\mathbb{D}^2$ for some N -graph \mathcal{G} . We fix a set \mathcal{B} of good cycles in the sense of Definition 3.31. Then, by Theorem 3.38, we obtain a Y -seed $\Psi(\mathcal{G}, \mathcal{B})$ which is a pair of a coefficient tuple $\mathbf{y}(\Lambda(\mathcal{G}), \mathcal{B})$ and a quiver $\mathcal{Q}(\Lambda(\mathcal{G}), \mathcal{B})$.

We say that the pair $(\mathcal{G}, \mathcal{B})$ is of *finite type* or of *infinite type* if so is the cluster algebra defined by $\mathcal{Q}(\Lambda(\mathcal{G}), \mathcal{B})$. Similarly, it is said to be of *type Z* for some Dynkin diagram Z if so is the associated cluster algebra.

In particular, it is said to be of *type ADE* or of *affine type* if the quiver is of type ADE or of affine type. See Definition 2.9.

4.1. N -graphs of finite or affine types.

4.1.1. *Linear N -graphs.* For $n \geq 1$, let us define positive 2-braids

$$\beta_0(\mathbf{A}_n) := \sigma_1^{n+1}, \quad \beta(\mathbf{A}_n) := \sigma_1^{n+3} = \Delta_2 \beta_0(n) \Delta_2,$$

where Δ_N is the half-twist braid of N -strands. Then we define $\lambda(\mathbf{A}_n)$ be the rainbow closure of $\beta_0(\mathbf{A}_n)$.



One can easily check the quiver $\mathcal{Q}^{\text{brick}}(\mathbf{A}_n)$ from the *brick diagram* of $\beta_0(\mathbf{A}_n)$ described in [30] look as shown in Figure 30(a), and there is a canonical N -graph with cycles $(\mathcal{G}^{\text{brick}}(\mathbf{A}_n), \mathcal{B}^{\text{brick}}(\mathbf{A}_n))$ on \mathbb{D}^2 as shown in Figure 30(b) such that

$$\mathcal{Q}^{\text{brick}}(\mathbf{A}_n) = \mathcal{Q}(\mathcal{G}^{\text{brick}}(\mathbf{A}_n), \mathcal{B}^{\text{brick}}(\mathbf{A}_n)).$$

The colors on cycles in Figure 30(b) are nothing to do with the bipartite coloring.

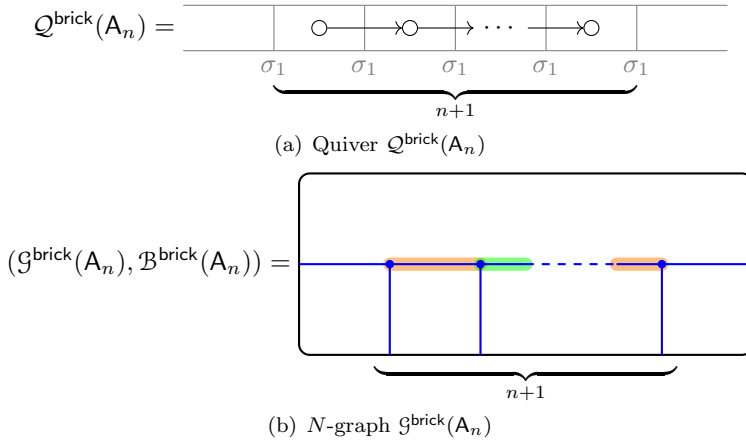


FIGURE 30. Linear quiver $\mathcal{Q}^{\text{brick}}(\mathbf{A}_n)$ and N -graph $\mathcal{G}^{\text{brick}}(\mathbf{A}_n)$

Then the quiver $\mathcal{Q}^{\text{brick}}(\mathbf{A}_n)$ is mutation equivalent to the bipartite quiver $\mathcal{Q}(\mathbf{A}_n)$ as depicted in Figure 31(a).

Definition 4.1 (Linear N -graphs). For $n \geq 1$, the *linear N -graph* $(\mathcal{G}(\mathbf{A}_n), \mathcal{B}(\mathbf{A}_n))$ is the 2-graph on \mathbb{D}^2 depicted in Figure 31(b), which satisfies that

$$\mathcal{Q}(\mathcal{G}(\mathbf{A}_n), \mathcal{B}(\mathbf{A}_n)) = \mathcal{Q}(\mathbf{A}_n).$$

It is easy but important to note that the N -graph $(\mathcal{G}(\mathbf{A}_n), \mathcal{B}(\mathbf{A}_n))$ has symmetries as follows:

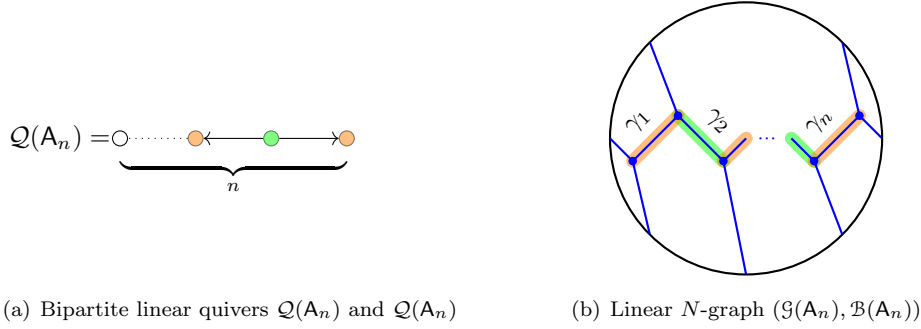


FIGURE 31. Bipartite linear quiver $\mathcal{Q}(A_n)$ and N -graph $(\mathcal{G}(A_n), \mathcal{B}(A_n))$ with chosen cycles

Lemma 4.2. *The N -graph $(\mathcal{G}(A_n), \mathcal{B}(A_n))$ with cycles is invariant under the conjugation. Moreover, when n is odd, it is invariant under π -rotation and the interchanges*

$$\gamma_i \leftrightarrow \gamma_{n+1-i}$$

for cycles $\gamma_i \in \mathcal{B}(A_n)$.

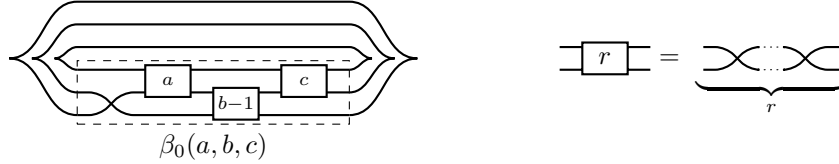
4.1.2. *Tripod N -graphs.* For $a, b, c \geq 1$, we define a Legendrian link $\lambda(a, b, c)$, which is the closure of a braid $\beta(a, b, c)$

$$\lambda(a, b, c) = \lambda_{\beta(a, b, c)}, \quad \beta(a, b, c) = \sigma_2 \sigma_1^{a+1} \sigma_2 \sigma_1^{b+1} \sigma_2 \sigma_1^{c+1},$$

where $\beta(a, b, c)$ is equivalent to the following:

$$\beta(a, b, c) = \sigma_2 \sigma_1^{a+1} \sigma_2 \sigma_1^{b+1} \sigma_2 \sigma_1^{c+1} = \sigma_2 \sigma_1 (\sigma_2 \sigma_1) \sigma_2^a \sigma_1^{b-1} \sigma_2^c (\sigma_1 \sigma_2) \sigma_1 = \Delta_3 \sigma_1 \sigma_2^a \sigma_1^{b-1} \sigma_2^c \Delta_3.$$

Hence $\lambda(a, b, c)$ in $J^1 \mathbb{S}^1$ corresponds to the rainbow closure of the braid $\beta_0(a, b, c) = \sigma_1 \sigma_2^a \sigma_1^{b-1} \sigma_2^c$.



The quiver $\mathcal{Q}^{\text{brick}}(a, b, c)$ obtained from the brick diagram of $\beta_0(a, b, c)$ and the corresponding N -graph with cycles $(\mathcal{G}^{\text{brick}}(a, b, c), \mathcal{B}^{\text{brick}}(a, b, c))$ on \mathbb{D}^2 are shown in Figure 32(b). That is,

$$\mathcal{Q}^{\text{brick}}(a, b, c) = \mathcal{Q}(\mathcal{G}^{\text{brick}}(a, b, c), \mathcal{B}^{\text{brick}}(a, b, c)).$$

As before, the colors on cycles in Figure 32(b) are nothing to do with the bipartite coloring.

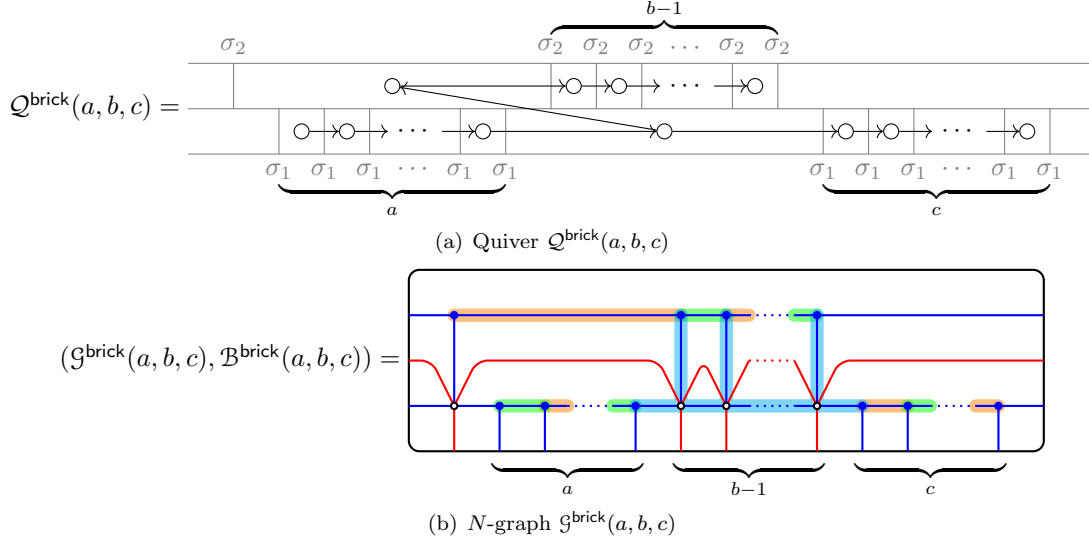
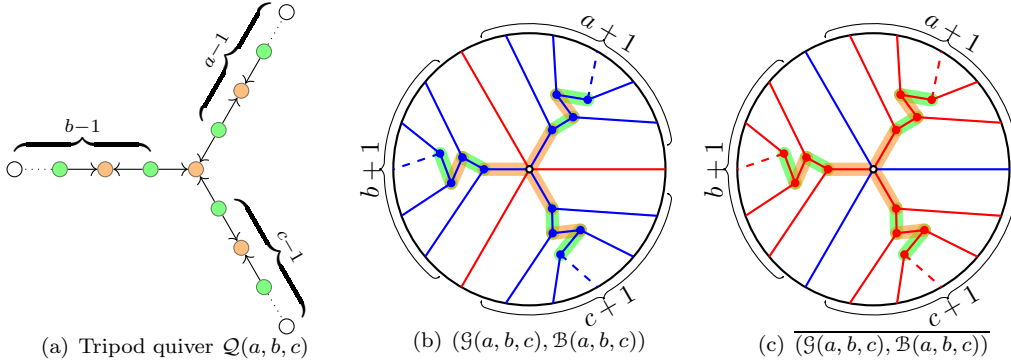
This quiver $\mathcal{Q}^{\text{brick}}(a, b, c)$ is mutation equivalent to the quiver $\mathcal{Q}(a, b, c)$, called the *tripod quiver of type (a, b, c)* , depicted in Figure 33(a).

Definition 4.3 (Tripod N -graphs). For $a, b, c \geq 1$, the *tripod N -graph* $(\mathcal{G}(a, b, c), \mathcal{B}(a, b, c))$ is a free 3-graph on \mathbb{D}^2 depicted in Figure 33(b), which satisfies that

$$\mathcal{Q}(\mathcal{G}(a, b, c), \mathcal{B}(a, b, c)) = \mathcal{Q}(a, b, c).$$

Moreover, the above two N -graphs are essentially equivalent as follows. The proof will be given in Appendix B.4.

Lemma 4.4. *The N -graphs $\mathcal{G}^{\text{brick}}(a, b, c)$ and $\mathcal{G}(a, b, c)$ are equivalent up to ∂ -Legendrian isotopy and Legendrian mutations.*

FIGURE 32. Tripod quiver $\mathcal{Q}^{\text{brick}}(a, b, c)$ and N -graph $\mathcal{G}^{\text{brick}}(a, b, c)$ FIGURE 33. Tripod quiver and N -graphs with chosen cycles

The N -graph $\mathcal{G}(a, b, c)$ is free by Lemma 3.9 and is never invariant under the conjugation, which acts on the Legendrian $\lambda(a, b, c)$ as interchanging σ_1 and σ_2 so that $\overline{\lambda(a, b, c)}$ is the closure of $\overline{\beta(a, b, c)}$

$$\overline{\beta(a, b, c)} = \sigma_1 \sigma_2^{a+1} \sigma_1 \sigma_2^{b+1} \sigma_1 \sigma_2^{c+1}.$$

The conjugation $(\mathcal{B}(a, b, c), \mathcal{B}(a, b, c))$ is depicted in Figure 33(c).

We have the following obvious observation:

Lemma 4.5. *For each $a \geq 1$, the N -graph $\mathcal{G}(a, a, a)$ is invariant under $2\pi/3$ -rotation.*

On the other hand, if one of a, b, c is 1, then the quiver $\mathcal{Q}(a, b, c)$ is of type A_n . Indeed, as seen in Example 3.18, the Legendrian link $\lambda(1, b, c)$ is a stabilization of $\lambda(A_n)$ for $n = b + c - 1$, and the N -graph $\mathcal{G}(a, b, c)$ is a stabilization of $\mathcal{G}(A_n)$. See Appendix B.3 for the proof.

Lemma 4.6. *The N -graph $\mathcal{G}(1, b, c)$ is a stabilization of $\mathcal{G}(A_n)$ for $n = b + c - 1$.*

One consequence of this lemma is that two N -graphs $\mathcal{G}(A_n)$ and $\mathcal{G}(1, b, c)$ with $n = b + c - 1$ will generate bijective sets of N -graphs under mutations as seen in Remarks 3.43 and 3.44, where the bijection preserves the mutation.

Notice that the quivers $\mathcal{Q}(a, b, c)$ together with $\mathcal{Q}(A_n)$ cover all quivers of finite type and some quivers of affine type. Indeed, for $1 \leq a \leq b \leq c$ and $n = a + b + c - 2$, the quivers $\mathcal{Q}(1, b, c)$ and $\mathcal{Q}(A_n)$ are of type A_n , and the quivers $\mathcal{Q}(2, 2, n - 2)$ and $\mathcal{Q}(2, 3, n - 3)$ are of type D_n and E_n . Moreover, $\mathcal{Q}(3, 3, 3)$, $\mathcal{Q}(2, 4, 4)$ and $\mathcal{Q}(2, 3, 6)$ are of type \tilde{E}_6 , \tilde{E}_7 and \tilde{E}_8 , respectively. Hence as seen in Table 8, we denote braids, Legendrians, quivers, and N -graphs with cycles by $\beta(Z)$, $\lambda(Z)$, $\mathcal{Q}(Z)$ and $\mathcal{G}(Z)$ for $Z = D_n, E_n$ or \tilde{E}_n , respectively.

Z	$\beta(Z)$	$\lambda(Z)$	$\mathcal{Q}(Z)$	$(\mathcal{G}(Z), \mathcal{B}(Z))$
$D_n, n \geq 4$	$\beta(n - 2, 2, 2)$	$\lambda(n - 2, 2, 2)$	$\mathcal{Q}(n - 2, 2, 2)$	$(\mathcal{G}(n - 2, 2, 2), \mathcal{B}(n - 2, 2, 2))$
E_6	$\beta(2, 3, 3)$	$\lambda(2, 3, 3)$	$\mathcal{Q}(2, 3, 3)$	$(\mathcal{G}(2, 3, 3), \mathcal{B}(2, 3, 3))$
E_7	$\beta(2, 3, 4)$	$\lambda(2, 3, 4)$	$\mathcal{Q}(2, 3, 4)$	$(\mathcal{G}(2, 3, 4), \mathcal{B}(2, 3, 4))$
E_8	$\beta(2, 3, 5)$	$\lambda(2, 3, 5)$	$\mathcal{Q}(2, 3, 5)$	$(\mathcal{G}(2, 3, 5), \mathcal{B}(2, 3, 5))$
\tilde{E}_6	$\beta(3, 3, 3)$	$\lambda(3, 3, 3)$	$\mathcal{Q}(3, 3, 3)$	$(\mathcal{G}(3, 3, 3), \mathcal{B}(3, 3, 3))$
\tilde{E}_7	$\beta(2, 4, 4)$	$\lambda(2, 4, 4)$	$\mathcal{Q}(2, 4, 4)$	$(\mathcal{G}(2, 4, 4), \mathcal{B}(2, 4, 4))$
\tilde{E}_8	$\beta(2, 3, 6)$	$\lambda(2, 3, 6)$	$\mathcal{Q}(2, 3, 6)$	$(\mathcal{G}(2, 3, 6), \mathcal{B}(2, 3, 6))$

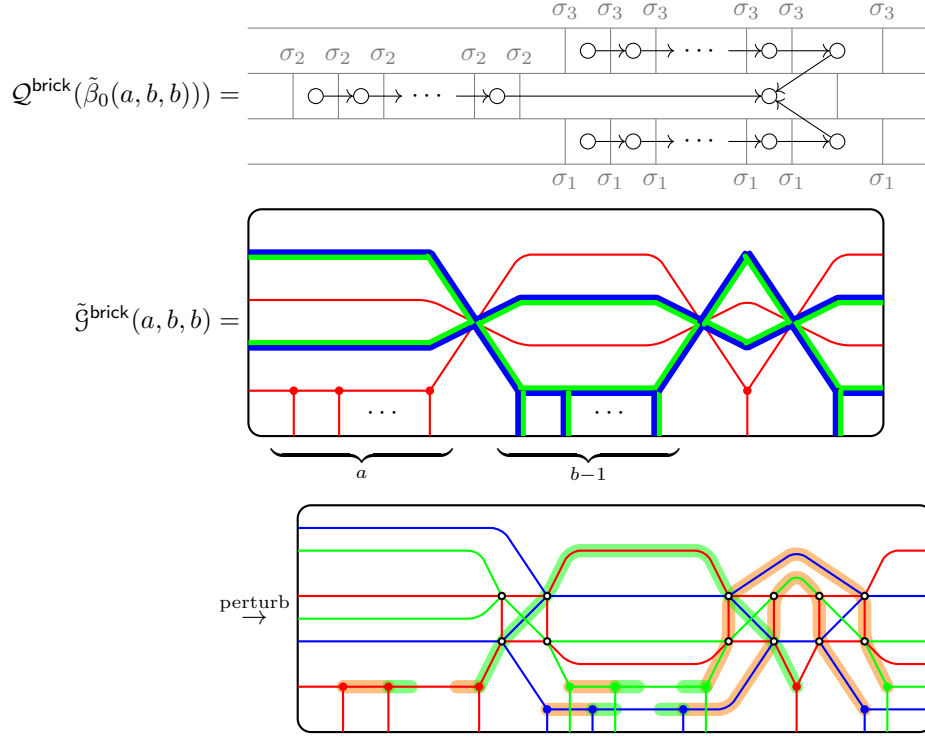
TABLE 8. Braids, Legendrians, quivers, and N -graphs of type DE and \tilde{E}

4.1.3. *Degenerate N -graphs of type $D_{n+1}, E_6, \tilde{E}_6$ and \tilde{E}_7 .* For $a, b \geq 1$, we define positive braids $\tilde{\beta}_0(a, b, b)$ and $\tilde{\beta}(a, b, b)$ as follows:

$$\begin{aligned}
\tilde{\beta}_0(a, b, b) &:= \sigma_2^a \sigma_{1,3}^{b-1} \sigma_2 \sigma_{1,3} \doteq \sigma_1 \sigma_2^a \sigma_1^{b-1} \sigma_3^{b-1} \sigma_2 \sigma_3 = \sigma_1 \sigma_2^a \sigma_1^{b-1} \sigma_2 \sigma_3 \sigma_2^{b-1} = S(\beta_0(a, b, b)) \\
\tilde{\beta}(a, b, b) &:= \sigma_2^{a+1} \sigma_{1,3} \sigma_2 \sigma_{1,3}^b \sigma_2^2 \sigma_{1,3} \sigma_2^2 \sigma_{1,3} \\
&= \sigma_2^a (\sigma_2 \sigma_{1,3} \sigma_2) \sigma_{1,3}^b (\sigma_2 \sigma_{1,3})^3 \\
&= \sigma_2^a \sigma_{1,3}^{b-1} \sigma_2 \sigma_{1,3} (\sigma_2 \sigma_{1,3})^2 (\sigma_2 \sigma_{1,3})^2 \\
&\doteq \Delta_4 \tilde{\beta}_0(a, b, b) \Delta_4.
\end{aligned}$$

Let $\tilde{\lambda}(a, b, b)$ be the closure of $\tilde{\beta}(a, b, b)$. Then since both $\tilde{\beta}_0(a, b, b)$ and $\tilde{\beta}(a, b, b)$ are invariant under the conjugation, so is $\tilde{\lambda}(a, b, b)$.

The quiver $\mathcal{Q}^{\text{brick}}(\tilde{\beta}_0(a, b, b))$ and N -graph $\tilde{\mathcal{G}}^{\text{brick}}(a, b, b)$ look as follows:



Definition 4.7 (Degenerate 4-graphs for $\tilde{\lambda}(a, b, b)$). We define a degenerate 4-graph $\tilde{\mathcal{G}}(a, b, b)$ for $\tilde{\lambda}(a, b, b)$ as depicted in the left of Figure 34.

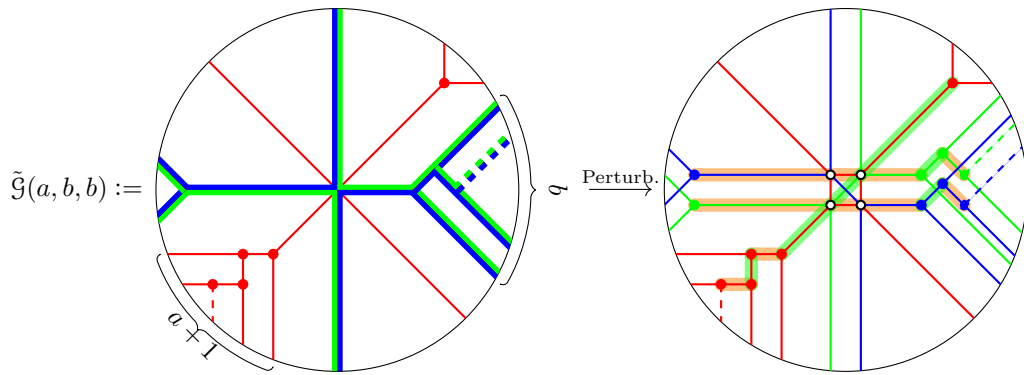
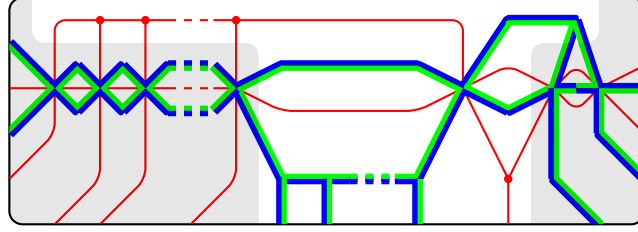


FIGURE 34. Degenerate 4-graphs $\tilde{\mathcal{G}}(a, b, b)$ and cycles in the perturbation

Lemma 4.8. *The N -graph $\tilde{\mathcal{G}}(a, b, b)$ is equivalent to $\tilde{\mathcal{G}}^{\text{brick}}(a, b, b)$ up to ∂ -Legendrian isotopy and Legendrian mutations.*

Proof. It is straightforward to check that we obtain the following degenerate N -graph from $\tilde{\mathcal{G}}^{\text{brick}}(a, b, b)$ by applying a sequence of Move (DI).



Let us ignore the shaded regions whose union is tame under perturbation, see § 3.2.2, then it is obvious that the resulting N -graph becomes $\tilde{\mathcal{G}}(a, b, b)$ in Figure 34 after a sequence of Legendrian mutations. \square

Remark 4.9. Note that the 4-graph $\tilde{\mathcal{G}}(a, b, b)$ is indeed a stablization of the tripod 3-graph $\mathcal{G}(a, b, b)$ up to ∂ -Legendrian isotopy and Legendrian mutations.

In particular, when $(a, b, b) = (n-1, 2, 2), (2, 3, 3), (3, 3, 3)$ and $(2, 4, 4)$, we denote $\tilde{\beta}_0(a, b, b)$ and $\tilde{\beta}(a, b, b)$ by $\tilde{\beta}_0(Z)$ and $\tilde{\beta}(Z)$ for $Z = D_{n+1}, E_6, \tilde{E}_6$ and \tilde{E}_7 , respectively.

$$\begin{aligned} \tilde{\beta}_0(D_{n+1}) &:= \tilde{\beta}_0(n-1, 2, 2), & \tilde{\beta}_0(E_6) &:= \tilde{\beta}_0(2, 3, 3), & \tilde{\beta}_0(\tilde{E}_6) &:= \tilde{\beta}_0(3, 3, 3), & \tilde{\beta}_0(\tilde{E}_7) &:= \tilde{\beta}_0(2, 4, 4) \\ \tilde{\beta}(D_{n+1}) &:= \tilde{\beta}(n-1, 2, 2), & \tilde{\beta}(E_6) &:= \tilde{\beta}(2, 3, 3), & \tilde{\beta}(\tilde{E}_6) &:= \tilde{\beta}(3, 3, 3), & \tilde{\beta}(\tilde{E}_7) &:= \tilde{\beta}(2, 4, 4), \end{aligned}$$

Similarly, we denote their closures and N -graphs by $\tilde{\lambda}(Z)$ and $\tilde{\mathcal{G}}(Z)$. Namely,

$$\begin{aligned} \tilde{\lambda}(D_{n+1}) &:= \tilde{\lambda}(n-1, 2, 2), & \tilde{\lambda}(E_6) &:= \tilde{\lambda}(2, 3, 3), & \tilde{\lambda}(\tilde{E}_6) &:= \tilde{\lambda}(3, 3, 3), & \tilde{\lambda}(\tilde{E}_7) &:= \tilde{\lambda}(2, 4, 4) \\ \tilde{\mathcal{G}}(D_{n+1}) &:= \tilde{\mathcal{G}}(n-1, 2, 2), & \tilde{\mathcal{G}}(E_6) &:= \tilde{\mathcal{G}}(2, 3, 3), & \tilde{\mathcal{G}}(\tilde{E}_6) &:= \tilde{\mathcal{G}}(3, 3, 3), & \tilde{\mathcal{G}}(\tilde{E}_7) &:= \tilde{\mathcal{G}}(2, 4, 4). \end{aligned}$$

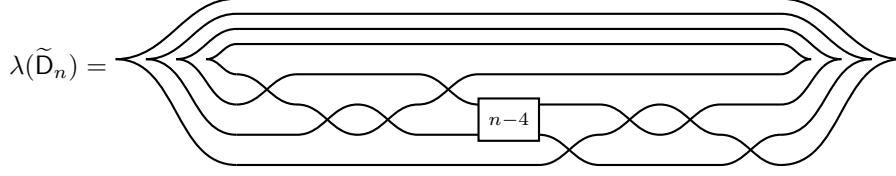
The degenerate N -graphs and the perturbed N -graphs with cycles listed above are depicted in Table 9.

Z	D_{n+1}	E_6	\tilde{E}_6	\tilde{E}_7
$\tilde{\mathcal{G}}(Z)$				
Perturb.				

TABLE 9. Degenerate 4-graphs $\tilde{\mathcal{G}}(D_{n+1}), \tilde{\mathcal{G}}(E_6), \tilde{\mathcal{G}}(\tilde{E}_6)$ and $\tilde{\mathcal{G}}(\tilde{E}_7)$ and cycles in the perturbations

Remark 4.10. As observed in Lemma 4.6, one can think $\mathcal{Q}(1, n, n)$ and $\mathcal{G}(1, n, n)$ for A_{2n-1} instead of $\mathcal{Q}(A_{2n-1})$ and $\mathcal{G}(A_{2n-1})$. Therefore by Lemma 4.8, we may obtain a degenerate N -graph $\tilde{\mathcal{G}}(A_{2n-1})$, which is obviously invariant under the conjugation.

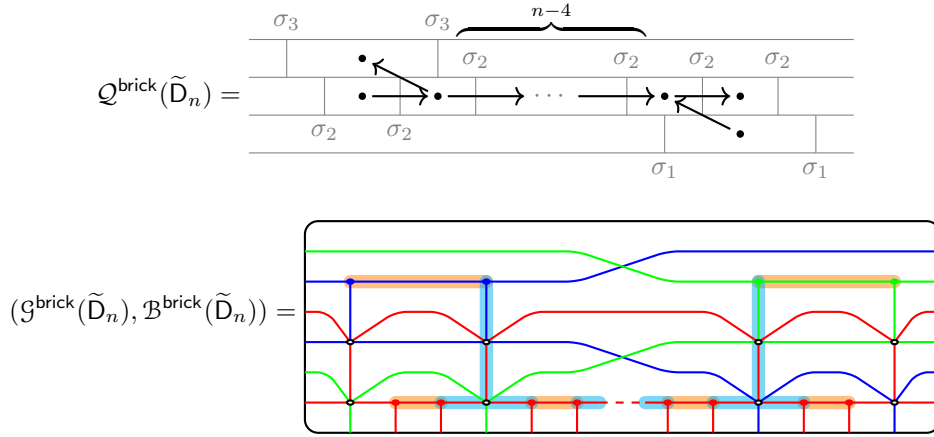
4.1.4. *N-graphs of type \tilde{D}_n .* Let us start by defining the Legendrian link $\lambda(\tilde{D}_n)$ of type \tilde{D}_n



as the rainbow closure of the positive braid $\beta_0(\tilde{D}_n)$

$$\beta_0(\tilde{D}_n) = \sigma_3 \sigma_2 \sigma_2 \sigma_3 \sigma_2^{n-4} \sigma_1 \sigma_2 \sigma_2 \sigma_1.$$

Then the Legendrian link $\lambda(\tilde{D}_n)$ admits the brick quiver diagram $\mathcal{Q}^{\text{brick}}(\tilde{D}_n)$.



In $J^1\mathbb{S}^1$, the Legendrian link $\lambda(\tilde{D}_n)$ is presented by the closure of $\beta(\tilde{D}_n)$

$$\begin{aligned} \tilde{\beta}(\tilde{D}_n) &= (\sigma_2 \sigma_1^3 \sigma_2 \sigma_1^k \sigma_2 \sigma_1^3 \sigma_3) \cdot (\sigma_2 \sigma_1^3 \sigma_2 \sigma_1^\ell \sigma_2 \sigma_1^3 \sigma_3) \\ &\doteq \sigma_1^2 \sigma_2 \sigma_1^3 \sigma_2 \sigma_3 \sigma_1^k \sigma_2 \sigma_1 \cdot \sigma_1^2 \sigma_2 \sigma_1^3 \sigma_2 \sigma_3 \sigma_1^\ell \sigma_2 \sigma_1 \\ &= \sigma_1 \sigma_2 \sigma_1 \sigma_2 \sigma_1^2 \sigma_2 \sigma_3 \sigma_2 \sigma_1 \sigma_2^k \cdot \sigma_1^2 \sigma_2 \sigma_1^3 \sigma_2 \sigma_1^\ell \sigma_3 \sigma_2 \sigma_1 \\ &= \sigma_1 \sigma_2 \sigma_1 \sigma_2 \sigma_1^2 \sigma_3 \sigma_2 \sigma_3 \sigma_1 \sigma_2^k \cdot \sigma_1^2 \sigma_2 \sigma_1^2 \sigma_2^\ell \sigma_1 \sigma_2 \sigma_3 \sigma_2 \sigma_1 \\ &= \sigma_1 \sigma_2 \sigma_1 \sigma_2 \sigma_3 \sigma_1^2 \sigma_2 \sigma_1 \sigma_3 \sigma_2^k \cdot \sigma_1^2 \sigma_2 \sigma_1^2 \sigma_2^\ell \sigma_1 \sigma_2 \sigma_3 \sigma_2 \sigma_1 \\ &= \sigma_1 \sigma_2 \sigma_1 \sigma_2 \sigma_3 \sigma_2 \sigma_1 \sigma_2^2 \sigma_3 \sigma_2^k \cdot \sigma_1 \sigma_2 \sigma_1 \sigma_2 \sigma_1 \sigma_2^\ell \sigma_1 \sigma_2 \sigma_3 \sigma_2 \sigma_1 \\ &= \sigma_1 \sigma_2 \sigma_1 \sigma_3 \sigma_2 \sigma_3 \sigma_1 \sigma_2^2 \sigma_3 \sigma_2^k \cdot \sigma_1 \sigma_2 \sigma_1 \sigma_1^\ell \sigma_2 \sigma_1 \sigma_1 \sigma_2 \sigma_3 \sigma_2 \sigma_1 \\ &= \sigma_1 \sigma_2 \sigma_1 \sigma_3 \sigma_2 \sigma_1 \sigma_3 \sigma_2^2 \sigma_3 \sigma_2^k \cdot \sigma_2^\ell \sigma_1 \sigma_2 \sigma_2 \sigma_1 \sigma_2 \sigma_1 \sigma_2 \sigma_3 \sigma_2 \sigma_1 \\ &= \Delta_4 \beta_0(\tilde{D}_n) \Delta_4, \end{aligned}$$

where $k = \lfloor \frac{n-3}{2} \rfloor$ and $\ell = \lfloor \frac{n-4}{2} \rfloor$.

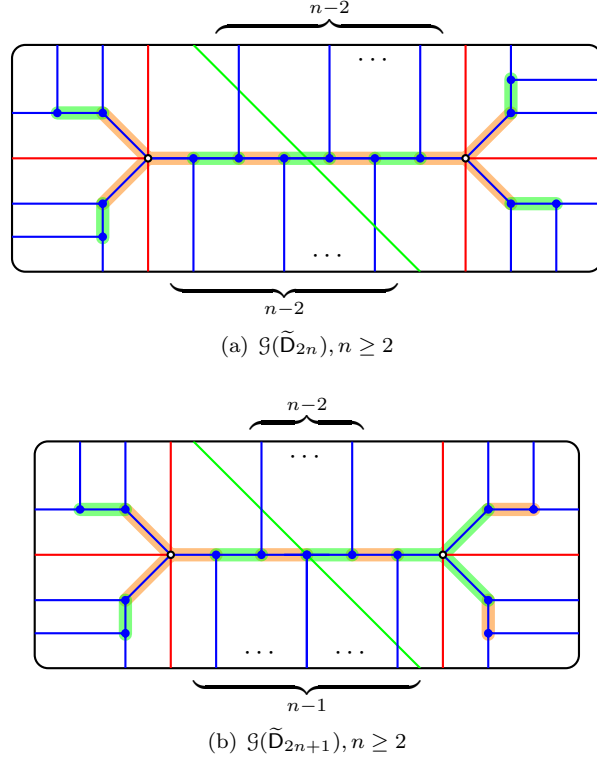
Definition 4.11 (*N-graph of type \tilde{D}_n*). We define a free 4-graph $\mathcal{G}(\tilde{D}_n)$ for $\lambda(\tilde{D}_n)$ as depicted in the left of Figure 35.

Lemma 4.12. *The N-graphs $\mathcal{G}(\tilde{D}_n)$ and $\mathcal{G}^{\text{brick}}(\tilde{D}_n)$ are equivalent up to ∂ -Legendrian isotopy and Legendrian mutations.*

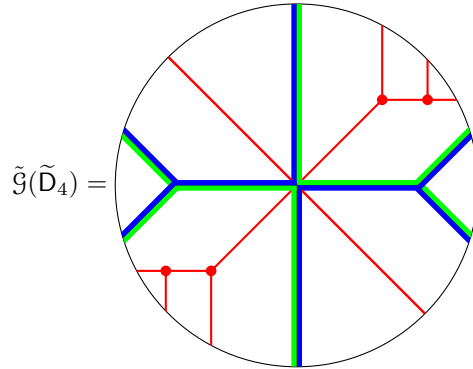
The pictorial proof of the lemma will be given in Appendix B.5.

As before, the freeness is obvious since $\mathcal{G}(\tilde{D}_n)$ consists of trees. Moreover, $\mathcal{G}(\tilde{D}_{2n})$ has a π -rotation symmetry. That is, we obtain the following lemma.

Lemma 4.13. *The pair $\mathcal{G}(\tilde{D}_{2n})$ is invariant under π -rotation.*

FIGURE 35. N -graph of type \tilde{D}_n

4.1.5. *The degenerate 4-graph of type \tilde{D}_4 .* The final N -graph we introduce is a degenerate 4-graph $\tilde{\mathcal{G}}(\tilde{D}_4)$ of type \tilde{D}_4 as follows:



which defines a bipartite quiver of type \tilde{D}_4 .

The boundary Legendrian link $\tilde{\lambda}(\tilde{D}_4)$ is the closure of

$$\begin{aligned}
 \tilde{\beta}(\tilde{D}_4) &= \sigma_2 \sigma_{1,3} \sigma_2 \sigma_{1,3}^2 \sigma_2^3 \sigma_{1,3} \sigma_2 \sigma_{1,3}^2 \sigma_2^2 \\
 &= \Delta_4 \sigma_{1,3} \sigma_2^2 \Delta_4 \sigma_{1,3} \sigma_2^2 \\
 &= \sigma_3 \Delta_4 \sigma_3 \sigma_2^2 \sigma_{1,3} \sigma_2^2 \Delta_4 \\
 &\doteq \Delta_4 \sigma_3 \sigma_2^2 \sigma_3 \sigma_1 \sigma_2^2 \Delta_4 \sigma_3 \\
 &= \Delta_4 \beta_0(\tilde{D}_4) \Delta_4.
 \end{aligned}$$

Lemma 4.14. *The 4-graph $\tilde{\mathcal{G}}(\tilde{\mathcal{D}}_4)$ is equivalent to the 4-graph $\mathcal{G}(\tilde{\mathcal{D}}_4)$ up to ∂ -Legendrian isotopy and Legendrian mutations.*

See Appendix B.6 for the proof.

4.1.6. *Exchange graphs corresponding to linear or tripod N -graphs.* Notice that the N -graphs $\mathcal{G}(\mathbf{Z})$ and $\mathcal{G}^{\text{brick}}(\mathbf{Z})$ are deterministic for $\mathbf{Z} = \mathbf{A}, \mathbf{D}, \mathbf{E}, \tilde{\mathbf{D}}, \tilde{\mathbf{E}}$. Therefore, the coefficients in $\mathbf{y}(\mathcal{G}(\mathbf{Z}), \mathcal{B}(\mathbf{Z}))$ are defined on $\mathbb{C}[\mathcal{M}(\lambda(\mathbf{Z}))]$. Here, $\mathcal{M}(\lambda)$ is the moduli spaces of flags on λ and is turned out to be a cluster Poisson variety as seen in Remark 3.47.

On the other hand, one can show that the variables $\{X_a\}_{a \in I_\lambda}$, Shen–Weng constructed in [41, §3.2], coincide with the coefficients in the coefficient tuple $\mathbf{y}(\mathcal{G}^{\text{brick}}(a, b, c), \mathcal{B}^{\text{brick}}(a, b, c))$ or $\mathbf{y}(\mathcal{G}^{\text{brick}}(n), \mathcal{B}^{\text{brick}}(n))$. Moreover, coefficients are algebraically independent. In summary, we have the following corollary, which is a direct consequence of the above discussion, Proposition 2.25, and (2.3).

Corollary 4.15. *Let $(\mathcal{G}_{t_0}, \mathcal{B}_{t_0})$ be either $(\mathcal{G}(a, b, c), \mathcal{B}(a, b, c))$ or $(\mathcal{G}(n), \mathcal{B}(n))$ of type \mathbf{Z} , and let $(\mathbf{y}_{t_0}, \mathcal{B}_{t_0}) = \Psi(\mathcal{G}_{t_0}, \mathcal{B}_{t_0})$ and $\mathcal{B}_{t_0} = \mathcal{B}(\mathcal{Q}(\mathcal{G}_{t_0}, \mathcal{B}_{t_0}))$. Then the exchange graph of the Y -pattern given by the initial Y -seed $(\mathbf{y}_{t_0}, \mathcal{B}_{t_0})$ is the same as the exchange graph $\text{Ex}(\Phi)$ of the root system Φ of type \mathbf{Z} .*

4.2. **Legendrian Coxeter mutations.** For a bipartite quiver \mathcal{Q} , we have two sets of vertices I_+ and I_- so that all edges are oriented from I_+ to I_- . Let μ_+ and μ_- be sequences of mutations defined by compositions of mutations corresponding to each and every vertex in I_+ and I_- , respectively. A Coxeter mutation $\mu_{\mathcal{Q}}$ and its inverse $\mu_{\mathcal{Q}}^{-1}$ are the compositions

$$\mu_{\mathcal{Q}} = \prod_{i \in I_+} \mu_i \cdot \prod_{i \in I_-} \mu_i, \quad \mu_{\mathcal{Q}}^{-1} = \prod_{i \in I_-} \mu_i \cdot \prod_{i \in I_+} \mu_i.$$

Note that $\prod_{i \in I_+} \mu_i$ does not depend on the order of composition of mutations μ_i among $i \in I_+$, and the same holds for I_- .

Remark 4.16. For any sequence μ of mutations, we will use the right-to-left convention. Namely, the rightmost mutation will be applied first on the quiver \mathcal{Q} .

Similarly, we define the Legendrian Coxeter mutation, which will be denoted by $\mu_{\mathcal{G}}$, on a bipartite N -graph \mathcal{G} as follows:

Definition 4.17 (Legendrian Coxeter mutation). For a bipartite N -graph \mathcal{G} with decomposed sets of cycles $\mathcal{B} = \mathcal{B}_+ \cup \mathcal{B}_-$, we define the *Legendrian Coxeter mutation* $\mu_{\mathcal{G}}$ and its inverse $\mu_{\mathcal{G}}^{-1}$ as the compositions of Legendrian mutations

$$\mu_{\mathcal{G}} = \prod_{\gamma \in \mathcal{B}_+} \mu_{\gamma} \cdot \prod_{\gamma \in \mathcal{B}_-} \mu_{\gamma}, \quad \mu_{\mathcal{G}}^{-1} = \prod_{\gamma \in \mathcal{B}_-} \mu_{\gamma} \cdot \prod_{\gamma \in \mathcal{B}_+} \mu_{\gamma}.$$

It is worth mentioning that each $\mu_{\mathcal{G}}^{\pm 1}$ does not depend on the order of mutations if cycles in each of \mathcal{B}_{\pm} are disjoint. This directly implies that $\mu_{\mathcal{G}}^{-1}$ is indeed the inverse of $\mu_{\mathcal{G}}$. Note that all cycles in each of $\mathcal{B}_{\pm}(\mathbf{Z})$ for $\mathbf{Z} = \mathbf{A}, \mathbf{D}, \mathbf{E}, \tilde{\mathbf{D}}, \tilde{\mathbf{E}}$ are disjoint as seen in Figures 31(b), 33(b), and 35.

4.2.1. *Legendrian Coxeter mutation for linear N -graphs.*

Lemma 4.18. *The effect of the Legendrian Coxeter mutation on $(\mathcal{G}(\mathbf{A}_n), \mathcal{B}(\mathbf{A}_n))$ is the clockwise $\frac{2\pi}{n+3}$ -rotation and therefore*

$$\mu_{\mathcal{G}}(\mathcal{G}(\mathbf{A}_n), \mathcal{B}(\mathbf{A}_n)) = \mathcal{C}(\mathbf{A}_n)(\mathcal{G}(\mathbf{A}_n), \mathcal{B}(\mathbf{A}_n)),$$

where $\mathcal{C}(\mathbf{A}_n)$ is an annular N -graph called the Coxeter padding of type \mathbf{A}_n as follows:

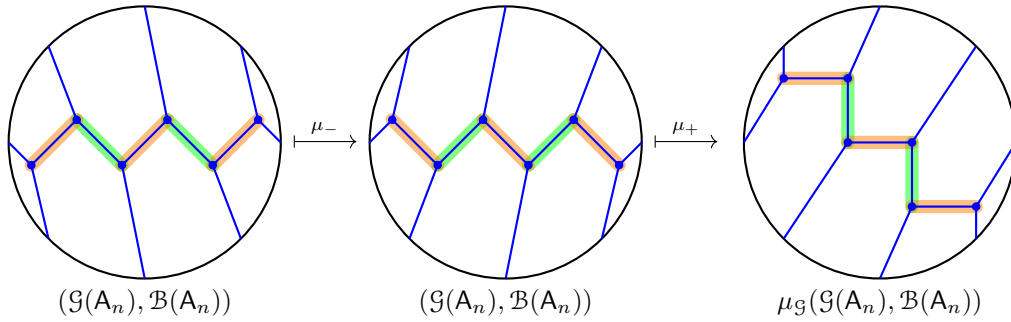
$$\mathcal{C}(\mathbf{A}_n) = \text{[Diagram of an annular N-graph with blue strands]} \quad (4.1)$$

Proof. We may assume that the Coxeter element $\mu_{\mathcal{G}}$ can be represented by the sequence

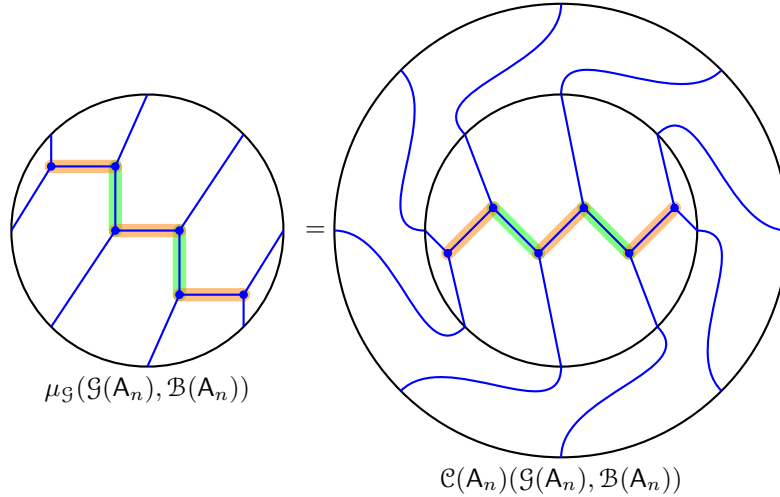
$$\mu_{\mathcal{G}} = \mu_+ \mu_- = (\mu_{\gamma_2} \mu_{\gamma_4} \mu_{\gamma_6} \cdots) (\mu_{\gamma_1} \mu_{\gamma_3} \mu_{\gamma_5} \cdots).$$

Then the action of $\mu_{\mathcal{G}}$ on $\mathcal{G}(\mathbf{A}_n)$ is as depicted in Figure 36(a), which is nothing but the clockwise $\frac{2\pi}{n+3}$ -rotation of the original N -graph $(\mathcal{G}(\mathbf{A}_n), \mathcal{B}(\mathbf{A}_n))$ as claimed.

The last statement is obvious as seen in Figure 36(b). \square



(a) Legendrian Coxeter mutation for $\mathcal{G}(\mathbf{A}_n)$

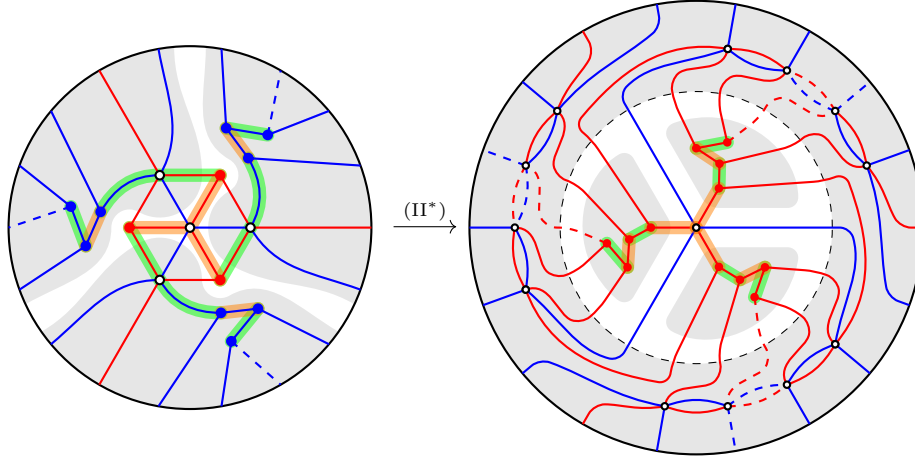


(b) Coxeter padding $\mathcal{C}(\mathbf{A}_n)$ of type \mathbf{A}_n

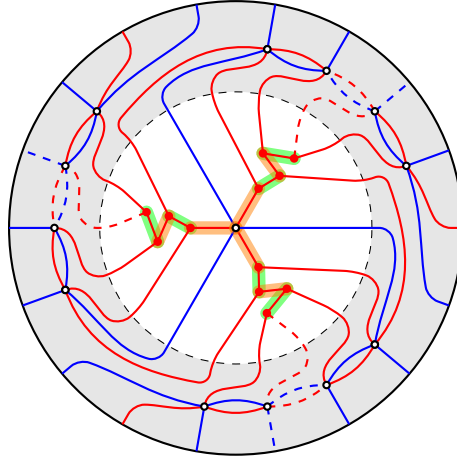
FIGURE 36. Legendrian Coxeter mutation $\mu_{\mathcal{G}}$ on $(\mathcal{G}(\mathbf{A}_n), \mathcal{B}(\mathbf{A}_n))$

Remark 4.19. The order of the Coxeter mutation is either $(n+3)/2$ if n is odd or $n+3$ otherwise. Since the Coxeter number $h = n+1$ for \mathbf{A}_n , this verifies Lemma 2.32 in this case.

4.2.2. Legendrian Coxeter mutation for tripod N -graphs. Let us consider the Legendrian Coxeter mutation for tripod N -graphs. By the mutation convention mentioned in Remark 4.16, for each tripod $\mathcal{G}(a, b, c)$, we always take a mutation at the central Y -cycle γ first. After the Legendrian mutation on $(\mathcal{G}(a, b, c), \mathcal{B}(a, b, c))$ at γ , we have the N -graph on the left in Figure 37(a). Then there are three shaded regions that we can apply the generalized push-through moves so that we obtain the N -graph on the right in Figure 37(a). Notice that in each triangular shaded region,



(a) After the mutation at the central vertex



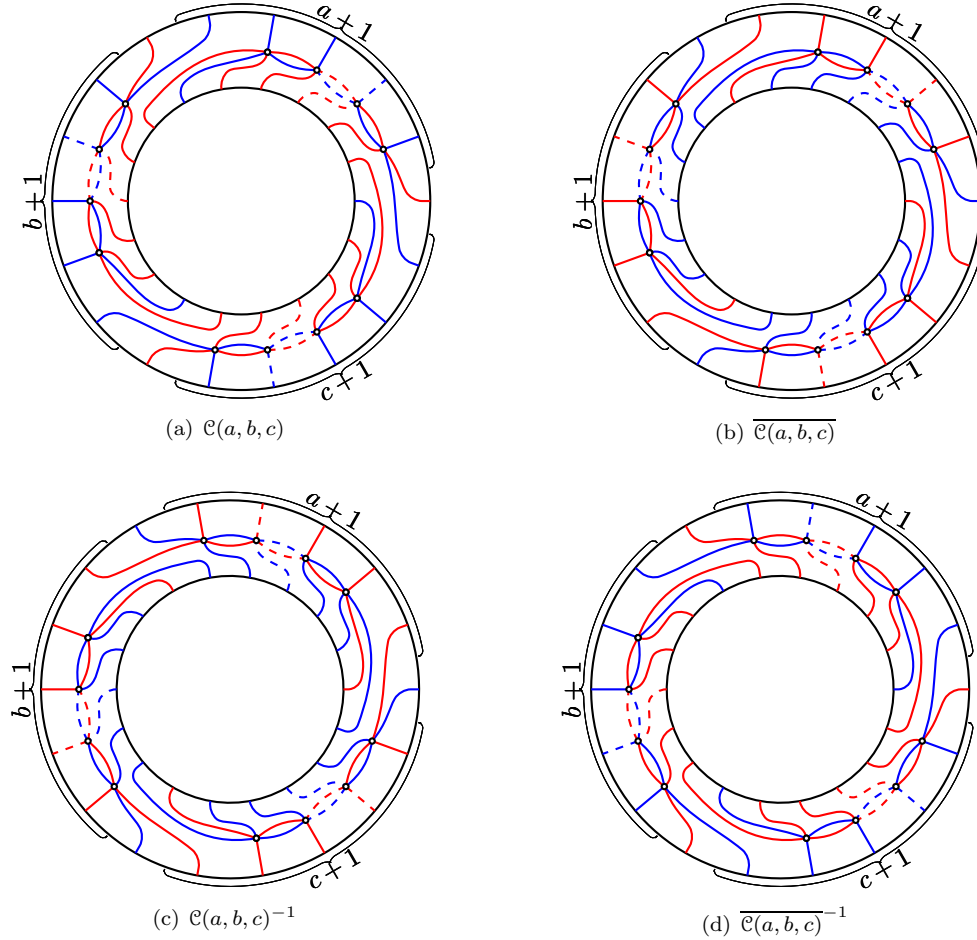
(b) After Legendrian Coxeter mutation

FIGURE 37. Legendrian Coxeter mutation for $(\mathcal{G}(a, b, c), \mathcal{B}(a, b, c))$

the N -subgraph looks like the N -graph of type A_{a-1}, A_{b-1} , or A_{c-1} . Moreover, the mutations corresponding to the rest sequence is just a composition of Legendrian Coxeter mutations of type A_{a-1}, A_{b-1} , and A_{c-1} , which are essentially the same as the clockwise rotations by Lemma 4.18. Therefore, the result of the Legendrian Coxeter mutation will be given as depicted in Figure 37(b).

Then the resulting N -graph becomes very similar to the original N -graph $\mathcal{G}(a, b, c)$. Indeed, the inside is identical to $\mathcal{G}(a, b, c)$ but the colors are switched, which is the conjugation $\overline{\mathcal{G}(a, b, c)}$ by definition. The complement of $\overline{\mathcal{G}(a, b, c)}$ in $\mu_{\mathcal{Q}}(\mathcal{G}(a, b, c), \mathcal{B}(a, b, c))$ is an annular N -graph.

Definition 4.20 (Coxeter padding of type (a, b, c)). For each triple a, b, c , the annular N -graph depicted in Figure 38 is denoted by $\mathcal{C}(a, b, c)$ and called the *Coxeter padding* of type (a, b, c) . We also denote the Coxeter padding with color switched by $\overline{\mathcal{C}(a, b, c)}$, which is the conjugation of $\mathcal{C}(a, b, c)$.

FIGURE 38. Coxeter paddings $\mathcal{C}(a, b, c)$, $\overline{\mathcal{C}(a, b, c)}$ and their inverses.

Notice that two Coxeter paddings $\mathcal{C}(a, b, c)$ and $\overline{\mathcal{C}(a, b, c)}$ can be glued without any ambiguity and so we can also pile up Coxeter paddings $\mathcal{C}(a, b, c)$ and $\overline{\mathcal{C}(a, b, c)}$ alternatively as many times as we want.

We also define the concatenation of the Coxeter padding $\overline{\mathcal{C}(a, b, c)}$ on the pair $(\mathcal{G}(a, b, c), \mathcal{B}(a, b, c))$ as the pair $(\mathcal{G}', \mathcal{B}')$ such that

- (1) the N -graph \mathcal{G}' is obtained by gluing $\overline{\mathcal{C}(a, b, c)}$ on $\mathcal{G}(a, b, c)$, and
- (2) the set \mathcal{B}' of cycles is the set of I- and Y-cycles identified with $\mathcal{B}(a, b, c)$ in a canonical way.

Proposition 4.21. *Let $(\mathcal{G}, \mathcal{B}) = (\mathcal{G}(a, b, c), \mathcal{B}(a, b, c))$. The Legendrian Coxeter mutation on $(\mathcal{G}, \mathcal{B})$ or $(\overline{\mathcal{G}}, \overline{\mathcal{B}})$ is given as the concatenation*

$$\mu_{\mathcal{G}}(\mathcal{G}, \mathcal{B}) = \mathcal{C}(\overline{\mathcal{G}}, \overline{\mathcal{B}}), \quad \mu_{\mathcal{G}}^{-1}(\mathcal{G}, \mathcal{B}) = \overline{\mathcal{C}^{-1}(\mathcal{G}, \mathcal{B})}, \quad \mu_{\overline{\mathcal{G}}}(\overline{\mathcal{G}}, \overline{\mathcal{B}}) = \overline{\mathcal{C}}(\mathcal{G}, \mathcal{B}), \quad \mu_{\overline{\mathcal{G}}}^{-1}(\overline{\mathcal{G}}, \overline{\mathcal{B}}) = \overline{\mathcal{C}^{-1}(\mathcal{G}, \mathcal{B})},$$

where $\mathcal{C} = \mathcal{C}(a, b, c)$, $\overline{\mathcal{C}} = \overline{\mathcal{C}(a, b, c)}$.

In general, for $r \geq 0$, we have

$$\mu_{\mathcal{G}}^r(\mathcal{G}, \mathcal{B}) = \begin{cases} \mathcal{C}\overline{\mathcal{C}} \dots \overline{\mathcal{C}}(\mathcal{G}, \mathcal{B}) & \text{if } r \text{ is even,} \\ \mathcal{C}\overline{\mathcal{C}} \dots \mathcal{C}(\mathcal{G}, \mathcal{B}) & \text{if } r \text{ is odd.} \end{cases}$$

$$\mu_{\mathcal{G}}^{-r}(\mathcal{G}, \mathcal{B}) = \begin{cases} \overline{\mathcal{C}^{-1}\mathcal{C}^{-1} \dots \mathcal{C}^{-1}(\mathcal{G}, \mathcal{B})} & \text{if } r \text{ is even,} \\ \overline{\mathcal{C}^{-1}\mathcal{C}^{-1} \dots \overline{\mathcal{C}^{-1}(\mathcal{G}, \mathcal{B})}} & \text{if } r \text{ is odd.} \end{cases}$$

Proof. This follows directly from the above observation. \square

It is important that this proposition holds only when we take the Legendrian Coxeter mutation on the very standard N -graph $\mathcal{G}(a, b, c)$ with the cycles $\mathcal{B}(a, b, c)$. Otherwise, the Legendrian Coxeter mutation will not be expressed as simple as above.

Let $(\mathcal{G}, \mathcal{B})$ be a pair of a deterministic N -graph, a set of good cycles. Suppose that the quiver $\mathcal{Q}(\mathcal{G}, \mathcal{B})$ is bipartite and the Legendrian Coxeter mutation $\mu_{\mathcal{G}}(\mathcal{G}, \mathcal{B})$ is realizable. Then, by Proposition 3.42, we have

$$\Psi(\mu_{\mathcal{G}}(\mathcal{G}, \mathcal{B})) = \mu_{\mathcal{Q}}(\Psi(\mathcal{G}, \mathcal{B})).$$

In particular, for quivers of type A_n or tripods, we have the following corollary.

Corollary 4.22. *For each $n \geq 1$ and $a, b, c \geq 1$, the Legendrian Coxeter mutation $\mu_{\mathcal{G}}$ on $(\mathcal{G}(A_n), \mathcal{B}(A_n))$ or $(\mathcal{G}(a, b, c), \mathcal{B}(a, b, c))$ corresponds to the Coxeter mutation $\mu_{\mathcal{Q}}$ on $\mathcal{Q}(A_n)$ or $\mathcal{Q}(a, b, c)$, respectively. In other words,*

$$\begin{aligned} \Psi(\mu_{\mathcal{G}}(\mathcal{G}(A_n), \mathcal{B}(A_n))) &= \mu_{\mathcal{Q}}(\Psi(\mathcal{G}(A_n), \mathcal{B}(A_n))); \\ \Psi(\mu_{\mathcal{G}}(\mathcal{G}(a, b, c), \mathcal{B}(a, b, c))) &= \mu_{\mathcal{Q}}(\Psi(\mathcal{G}(a, b, c), \mathcal{B}(a, b, c))). \end{aligned}$$

Theorem 4.23. *For $a, b, c \geq 1$ with $\frac{1}{a} + \frac{1}{b} + \frac{1}{c} \leq 1$, The Legendrian knot or link $\lambda(a, b, c)$ in $J^1\mathbb{S}^1$ admits infinitely many distinct exact embedded Lagrangian fillings.*

Proof. By Proposition 4.21, the effect of the Legendrian Coxeter mutation on $(\mathcal{G}(a, b, c), \mathcal{B}(a, b, c))$ is just to attach the Coxeter padding on $(\bar{\mathcal{G}}(a, b, c), \bar{\mathcal{B}}(a, b, c))$. In particular, as mentioned earlier, the iterated Legendrian Coxeter mutation

$$\mu_{\mathcal{G}}^r(\mathcal{G}(a, b, c), \mathcal{B}(a, b, c))$$

is well-defined for each $r \in \mathbb{Z}$. Each of these N -graphs defines a Legendrian weave $\Lambda(\mu_{\mathcal{G}}^r(\mathcal{G}(a, b, c), \mathcal{B}(a, b, c)))$, whose Lagrangian projection is a Lagrangian filling

$$L_r(a, b, c) := (\pi \circ \iota)(\Lambda(\mu_{\mathcal{G}}^r(\mathcal{G}(a, b, c), \mathcal{B}(a, b, c))))$$

as desired. Therefore it suffices to prove that Lagrangians $L_r(a, b, c)$ for $r \geq 0$ are pairwise distinct up to exact Lagrangian isotopy when $\frac{1}{a} + \frac{1}{b} + \frac{1}{c} \leq 1$.

Now suppose that $\frac{1}{a} + \frac{1}{b} + \frac{1}{c} \leq 1$, or equivalently, $\mathcal{Q}(a, b, c)$ is of infinite type, that is, it is not of finite Dynkin type (cf. Definition 2.9(1)). Then the order of the Coxeter mutation is infinite by Lemma 2.32 and so is the order of the Legendrian Coxeter mutation by Corollary 4.22. In particular, the set

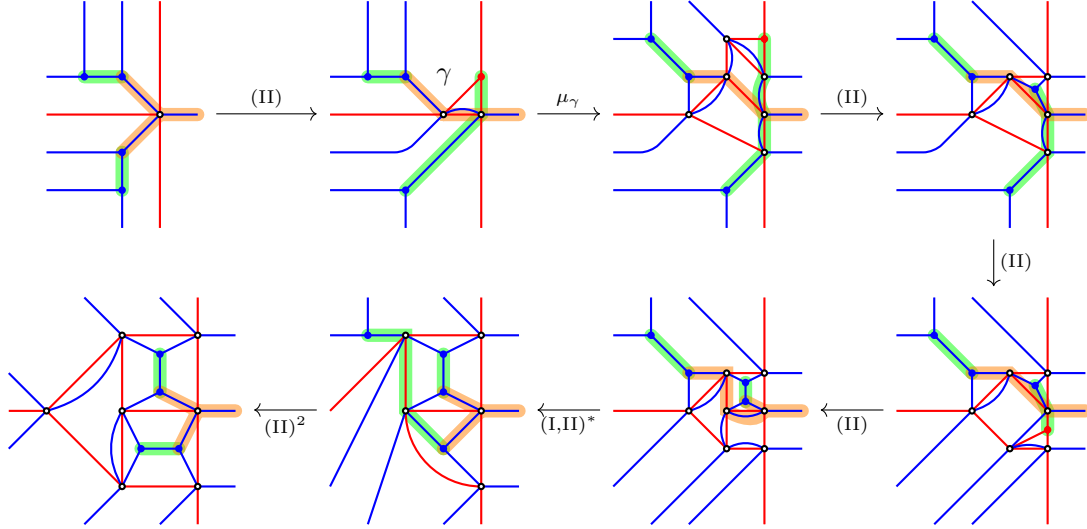
$$\{\Psi(\mu_{\mathcal{G}}^r(\mathcal{G}(a, b, c), \mathcal{B}(a, b, c))) \mid r \in \mathbb{Z}\}$$

is a set of infinitely many pairwise distinct Y -seeds in the Y -pattern for $\mathcal{Q}(a, b, c)$. Hence, by Corollary 3.39, we have pairwise distinct Lagrangian fillings $L_r(a, b, c)$. \square

Remark 4.24. For Legendrian links of non ADE-type, there are lots of examples having infinitely many distinct Lagrangian fillings given by a number of different researchers and groups. A non-exhaustive list includes [13, 14, 15, 30].

4.2.3. Legendrian Coxeter mutations for N -graphs of type \tilde{D}_n . We will perform the Legendrian Coxeter mutation $\mu_{\mathcal{G}}$ on $(\mathcal{G}(\tilde{D}_n), \mathcal{B}(\tilde{D}_n))$ in order to provide the pictorial proof of Proposition 4.26.

Before we take mutations, we first introduce a useful operation on N -graphs described below, called the *move* (Z).



Remark 4.25. The reader should not confuse that even though we call this operation the *move*, it does not induce any equivalence on N -graphs since it involves a mutation μ_γ .

One important observation is that one can take the move (Z) instead of the Legendrian mutation μ_γ on the Y-like cycle³ γ , and after the move, the Y-like cycle becomes the Y-like cycle and l-cycles become l-cycles again.

For example, let us consider $(\mathcal{G}(\tilde{D}_4), \mathcal{B}(\tilde{D}_4))$. Then the Legendrian Coxeter mutation $\mu_{\mathcal{G}}(\mathcal{G}(\tilde{D}_4), \mathcal{B}(\tilde{D}_4))$ is obtained by the composition $(\mu_{\gamma_2}\mu_{\gamma_3}\mu_{\gamma_4}\mu_{\gamma_5})$ followed by the mutation μ_{γ_1} . See Figure 39.

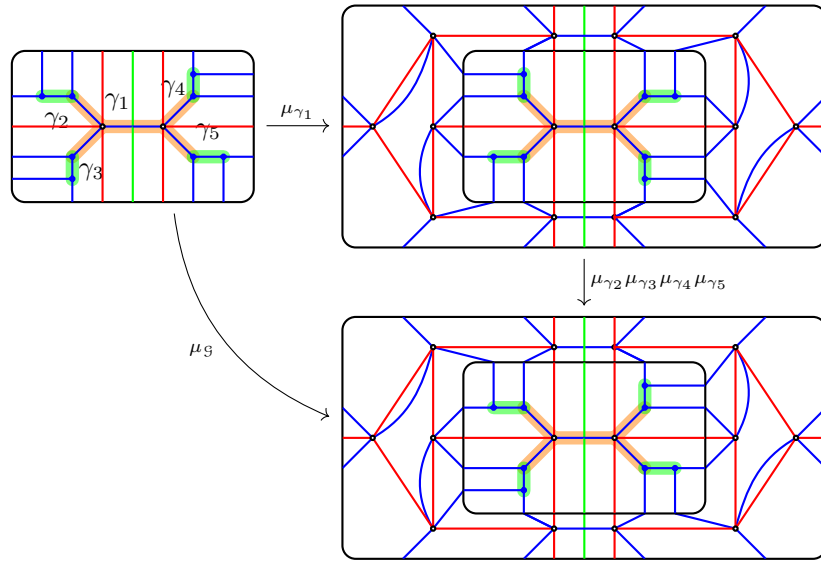


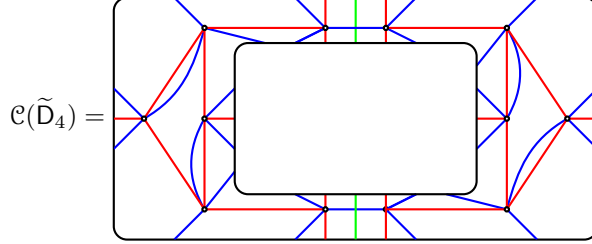
FIGURE 39. Legendrian Coxeter mutation for $\mathcal{G}(\tilde{D}_4)$

³We use an ambiguous terminology ‘Y-like cycle’ since the global shape of γ is unknown. However, the meaning is obvious and we omit the detail.

Therefore, $\mu_{\mathcal{G}}(\mathcal{G}(\tilde{\mathcal{D}}_4), \mathcal{B}(\tilde{\mathcal{D}}_4))$ is the same as the concatenation

$$\mu_{\mathcal{G}}(\mathcal{G}(\tilde{\mathcal{D}}_4), \mathcal{B}(\tilde{\mathcal{D}}_4)) = \mathcal{C}(\tilde{\mathcal{D}}_4)(\mathcal{G}(\tilde{\mathcal{D}}_4), \mathcal{B}(\tilde{\mathcal{D}}_4)),$$

where the annular N -graph $\mathcal{C}(\tilde{\mathcal{D}}_4)$ looks as follows:



In general, for the N -graph $(\mathcal{G}(\tilde{\mathcal{D}}_n), \mathcal{B}(\tilde{\mathcal{D}}_n))$, the Legendrian Coxeter mutation is the same as the concatenation of the Coxeter padding of type $\mathcal{C}^{\pm 1}(\tilde{\mathcal{D}}_n)$, which is an annular N -graph depicted in Figure 40.

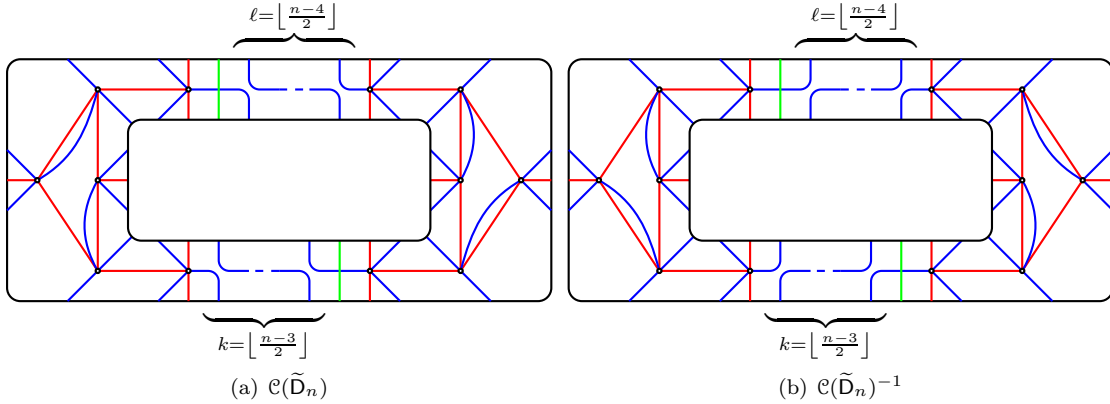


FIGURE 40. Coxeter paddings $\mathcal{C}(\tilde{\mathcal{D}}_n)^{\pm 1}$

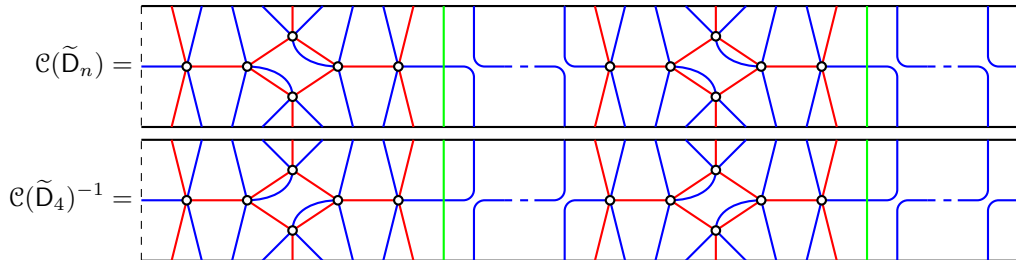
Proposition 4.26. *For any $r \in \mathbb{Z}$, the Legendrian Coxeter mutation $\mu_{\mathcal{G}}^r$ on the pair $(\mathcal{G}(\tilde{\mathcal{D}}_n), \mathcal{B}(\tilde{\mathcal{D}}_n))$ is given by piling the Coxeter paddings $\mathcal{C}(\tilde{\mathcal{D}}_n)^{\pm 1}$. That is,*

$$\mu_{\mathcal{G}}^r(\mathcal{G}(\tilde{\mathcal{D}}_n), \mathcal{B}(\tilde{\mathcal{D}}_n)) = \begin{cases} \mathcal{C}(\tilde{\mathcal{D}}_n)\mathcal{C}(\tilde{\mathcal{D}}_n) \cdots \mathcal{C}(\tilde{\mathcal{D}}_n)(\mathcal{G}(\tilde{\mathcal{D}}_n), \mathcal{B}(\tilde{\mathcal{D}}_n)) & r \geq 0; \\ \mathcal{C}(\tilde{\mathcal{D}}_n)^{-1}\mathcal{C}(\tilde{\mathcal{D}}_n)^{-1} \cdots \mathcal{C}(\tilde{\mathcal{D}}_n)^{-1}(\mathcal{G}(\tilde{\mathcal{D}}_n), \mathcal{B}(\tilde{\mathcal{D}}_n)) & r < 0. \end{cases}$$

Corollary 4.27. *For any $r \in \mathbb{Z}$, the Legendrian Coxeter mutation $\mu_{\mathcal{G}}^r(\mathcal{G}(\tilde{\mathcal{D}}_n), \mathcal{B}(\tilde{\mathcal{D}}_n))$ is realizable by N -graphs and set of good cycles.*

Note that the Coxeter paddings are obtained from the Coxeter mutations $\mu_{\mathcal{G}}^{\pm 1}$ conjugated by a sequence of Move (II). For the notational clarity, it is worth mentioning that $\mathcal{C}(\tilde{\mathcal{D}}_n)$ and $\mathcal{C}(\tilde{\mathcal{D}}_n)^{-1}$ are the inverse to each other with respect to the concatenation introduced in Section 3.2.2.

For example, one can present the Coxeter padding $\mathcal{C}(\tilde{\mathcal{D}}_4)^{\pm 1}$ as follows:



Then it is direct to check that the concatenations $\mathcal{C}(\tilde{D}_4)\mathcal{C}(\tilde{D}_4)^{-1}$ and $\mathcal{C}(\tilde{D}_4)^{-1}\mathcal{C}(\tilde{D}_4)$ become trivial annulus N -graphs after a sequence of Move (I). The same holds for all $n \geq 4$.

4.2.4. *Legendrian Coxeter mutations for degenerate N -graphs.* For degenerate N -graphs $\tilde{\mathcal{G}}(a, b, b)$ and $\tilde{\mathcal{G}}(\tilde{D}_4)$, the Legendrian Coxeter mutations are as depicted in Figure 41.

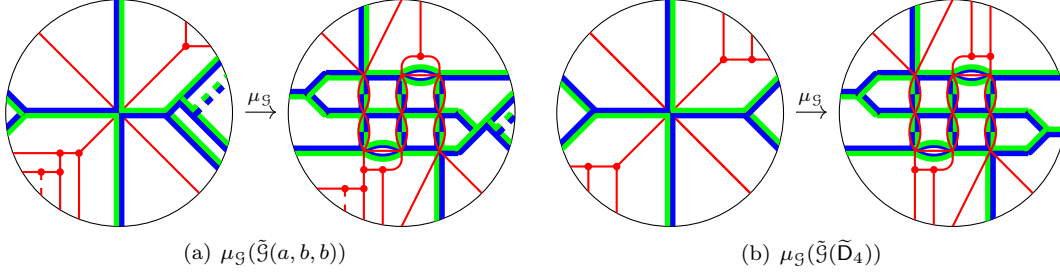
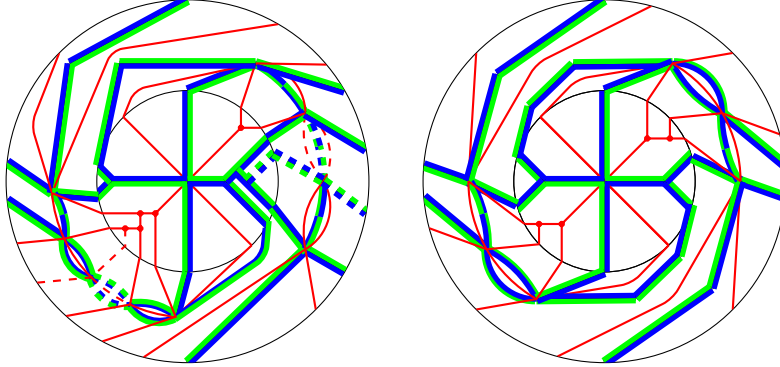


FIGURE 41. Legendrian Coxeter mutations for degenerate N -graphs

Then by using (DI) and (DII) several times, one can show easily that the Legendrian Coxeter mutations are equivalent to N -graphs depicted below:

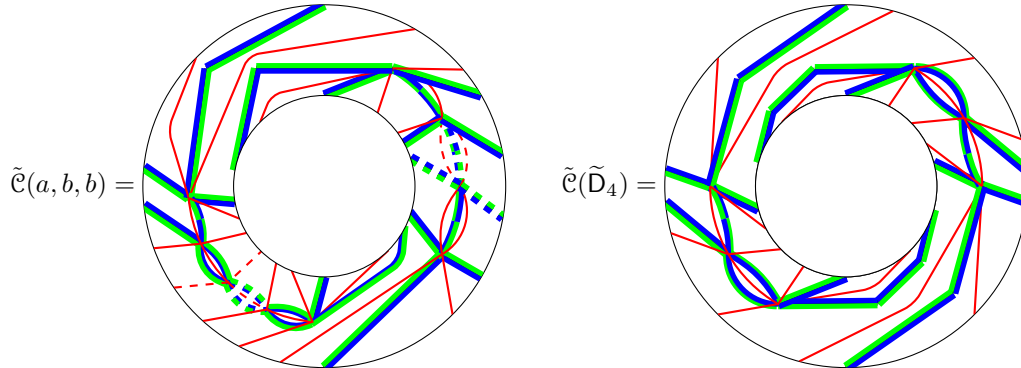


Therefore one can conclude that the effect of the Legendrian Coxeter mutation on each degenerate N -graph $\tilde{\mathcal{G}}(a, b, b)$ or $\tilde{\mathcal{G}}(\tilde{D}_4)$ is equivalent to attaching an annular N -graph which defines the Coxeter padding $\tilde{\mathcal{C}}(a, b, b)$ or $\tilde{\mathcal{C}}(\tilde{D}_4)$.

Proposition 4.28. *Let $(\tilde{\mathcal{G}}, \mathcal{B})$ be either $(\tilde{\mathcal{G}}(a, b, b), \mathcal{B}(a, b, b))$ or $(\tilde{\mathcal{G}}(\tilde{D}_4), \mathcal{B}(\tilde{D}_4))$. Then for each $r \in \mathbb{Z}$, the Legendrian Coxeter mutation $\mu_{\mathcal{G}}^r$ on the pair $(\tilde{\mathcal{G}}, \mathcal{B})$ is given as*

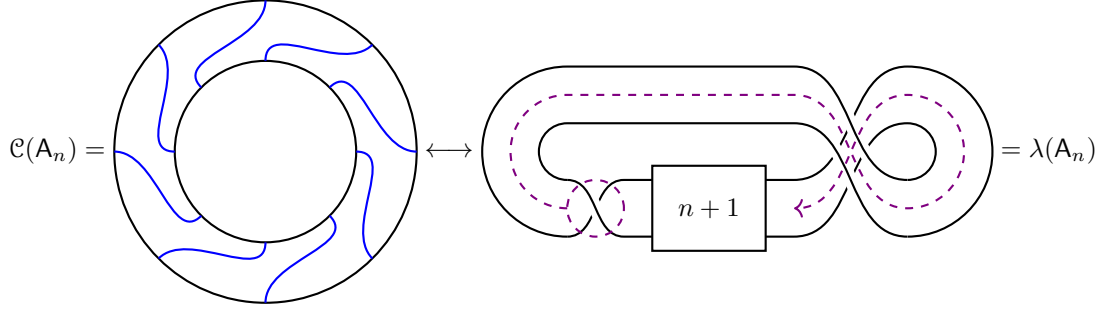
$$\mu_{\mathcal{G}}^r(\tilde{\mathcal{G}}, \mathcal{B}) = \begin{cases} \tilde{\mathcal{C}}\tilde{\mathcal{C}} \dots \tilde{\mathcal{C}}(\mathcal{G}, \mathcal{B}) & r \geq 0; \\ \tilde{\mathcal{C}}^{-1}\tilde{\mathcal{C}}^{-1} \dots \tilde{\mathcal{C}}^{-1}(\mathcal{G}, \mathcal{B}) & r < 0. \end{cases}$$

where $\tilde{\mathcal{C}}$ is either $\tilde{\mathcal{C}}(a, b, b)$ and $\tilde{\mathcal{C}}(\tilde{D}_n)$, which are degenerate annular N -graphs defined as follows:



4.3. Legendrian loops. Recall Legendrian loops defined in Definition 3.23. The goal of this section is to interpret the Legendrian Coxeter paddings with tame Legendrian loops.

Obviously, the Legendrian Coxeter paddings for A_n depicted in (4.1) is tame. Moreover, it corresponds to the tame ∂ -Legendrian isotopy which moves the very first generator σ_1 to the rightmost position along the closure part of $\lambda(A_n)$ as follows:



Lemma 4.29. *Legendrian Coxeter paddings of type (a, b, c) and \tilde{D} are tame.*

Proof. We provide decompositions of the Coxeter paddings $\mathcal{C}(a, b, c)$ and $\mathcal{C}(\tilde{D}_4)$ into sequences of elementary annular N -graphs in Figures 42(a) and 42(b), respectively. We omit other cases. \square

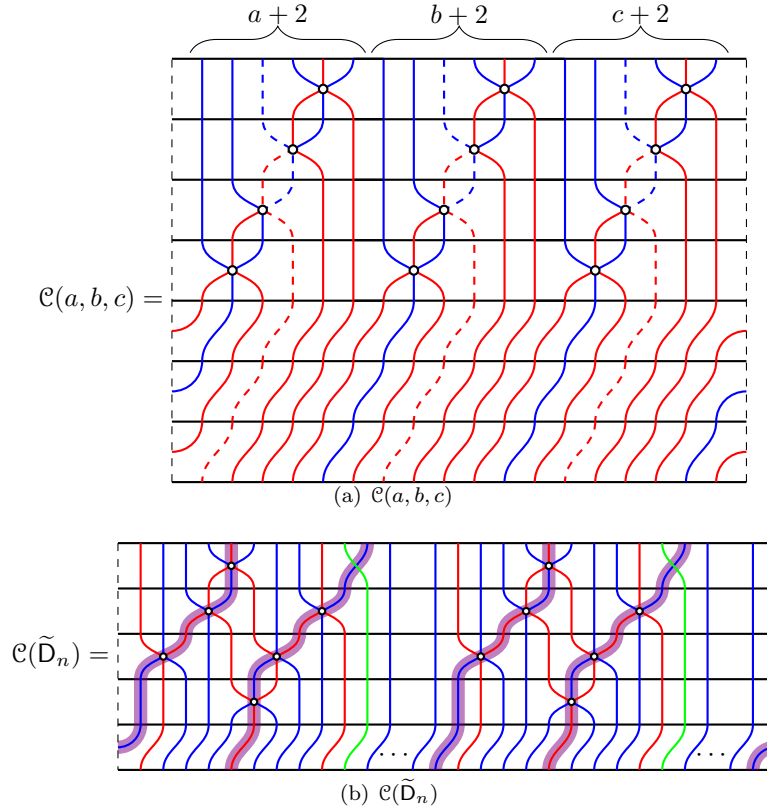


FIGURE 42. A sequence of elementary annulus N -graphs for Legendrian Coxeter paddings

Then we may translate the sequence of Reidemeister moves induced by $\bar{\mathcal{C}}(a, b, c)\mathcal{C}(a, b, c)$ into the Legendrian loop $\vartheta(a, b, c)$ depicted as in Figure 43. Note that the left column of the loop diagram corresponds to $\mathcal{C}(a, b, c)$ while the right column corresponds to $\bar{\mathcal{C}}(a, b, c)$.

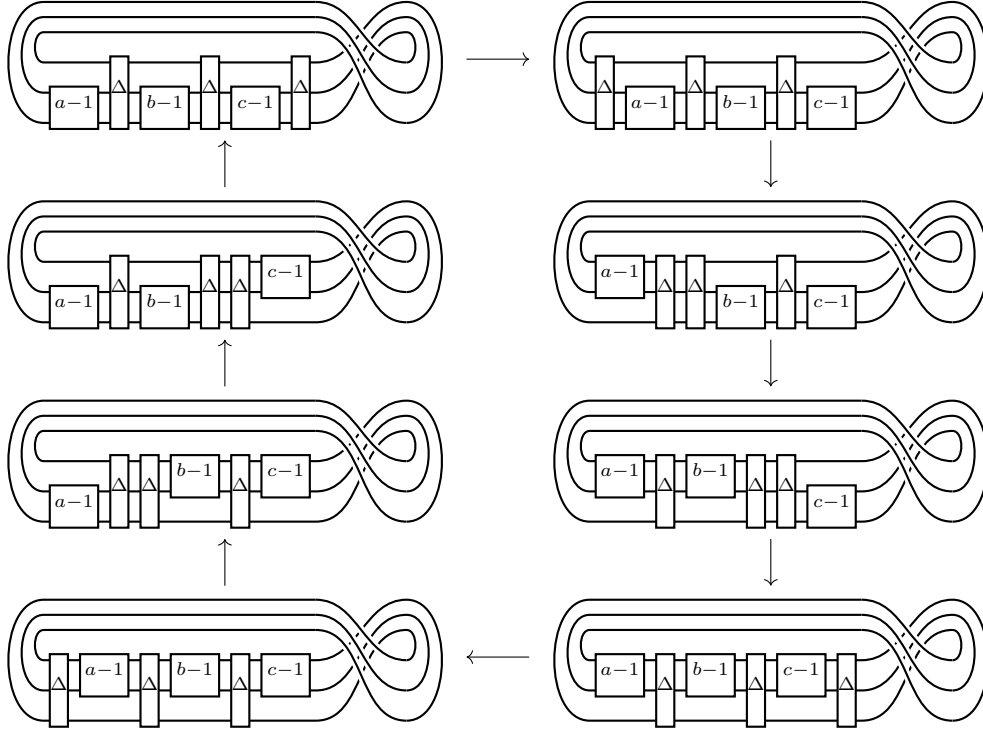


FIGURE 43. A Legendrian loop $\vartheta(a, b, c)$ induced from Legendrian Coxeter mutation $\mu_{\mathcal{G}}^2$ on $(\mathcal{G}(a, b, c), \mathcal{B}(a, b, c))$.

In order to see the effect of Legendrian Coxeter mutation of type \tilde{D}_n efficiently, let us present it by a sequence of braid moves together with keep tracking braid words shaded by violet color as follows:

$$\begin{aligned}
 \beta(\tilde{D}_n) &= \sigma_2 \sigma_1 \sigma_1 \sigma_1 \sigma_2 \sigma_1 \sigma_1 \sigma_1 \sigma_2 \sigma_1 \sigma_1^{k-1} \sigma_3 \sigma_2 \sigma_1 \sigma_1 \sigma_1 \sigma_2 \sigma_1 \sigma_1 \sigma_1 \sigma_2 \sigma_1 \sigma_1^{\ell-1} \sigma_3 \\
 &= \sigma_2 \sigma_1 \sigma_1 \sigma_2 \sigma_1 \sigma_2 \sigma_1 \sigma_1 \sigma_1 \sigma_2 \sigma_1 \sigma_1^{k-1} \sigma_3 \sigma_2 \sigma_1 \sigma_1 \sigma_2 \sigma_1 \sigma_2 \sigma_1 \sigma_1 \sigma_2 \sigma_1 \sigma_1^{\ell-1} \sigma_3 \\
 &= \sigma_2 \sigma_1 \sigma_2 \sigma_1 \sigma_2 \sigma_2 \sigma_1 \sigma_2 \sigma_1 \sigma_2 \sigma_1^{k-1} \sigma_3 \sigma_2 \sigma_1 \sigma_2 \sigma_1 \sigma_2 \sigma_2 \sigma_1 \sigma_2 \sigma_1 \sigma_2 \sigma_1^{\ell-1} \sigma_3 \\
 &= \sigma_1 \sigma_2 \sigma_1 \sigma_1 \sigma_2 \sigma_1 \sigma_2 \sigma_1 \sigma_1 \sigma_2 \sigma_1^{k-1} \sigma_3 \sigma_1 \sigma_2 \sigma_1 \sigma_1 \sigma_2 \sigma_1 \sigma_2 \sigma_1 \sigma_1 \sigma_2 \sigma_1^{\ell-1} \sigma_3 \\
 &\doteq \sigma_2 \sigma_1 \sigma_1 \sigma_2 \sigma_1 \sigma_2 \sigma_1 \sigma_1 \sigma_2 \sigma_1^{k-1} \sigma_3 \sigma_1 \sigma_2 \sigma_1 \sigma_1 \sigma_2 \sigma_1 \sigma_2 \sigma_1 \sigma_1 \sigma_2 \sigma_1^{\ell-1} \sigma_3 \sigma_1 \\
 &= \sigma_2 \sigma_1 \sigma_1 \sigma_2 \sigma_1 \sigma_2 \sigma_1 \sigma_1 \sigma_2 \sigma_1^{k-1} \sigma_1 \sigma_3 \sigma_2 \sigma_1 \sigma_1 \sigma_2 \sigma_1 \sigma_2 \sigma_1 \sigma_1 \sigma_2 \sigma_1^{\ell-1} \sigma_1 \sigma_3 \\
 &= \sigma_2 \sigma_1 \sigma_1 \sigma_1 \sigma_2 \sigma_1 \sigma_1 \sigma_1 \sigma_2 \sigma_1^{k-1} \sigma_1 \sigma_3 \sigma_2 \sigma_1 \sigma_1 \sigma_1 \sigma_2 \sigma_1 \sigma_1 \sigma_2 \sigma_1^{\ell-1} \sigma_1 \sigma_3 = \beta(\tilde{D}_n)
 \end{aligned}$$

The corresponding annular N -graph is depicted in Figure 42(b). Finally, the effect of Coxeter padding $\mathcal{C}(\tilde{D}_n)$ onto $\beta(\tilde{D}_n)$ can be presented as a Legendrian loop $\vartheta(\tilde{D}_n)$, which is a composition

$$\vartheta(\tilde{D}_n) = \varphi \vartheta_0(\tilde{D}_n) \varphi^{-1}$$

as depicted in Figure 44.

Theorem 4.30. *The square $\mu_{\mathcal{G}}^{\pm 2}$ of the Legendrian Coxeter mutation on $(\mathcal{G}(a, b, c), \mathcal{B}(a, b, c))$ and the Legendrian Coxeter mutation $\mu_{\mathcal{G}}^{\pm 1}$ on $(\mathcal{G}(\tilde{D}), \mathcal{B}(\tilde{D}))$ induce tame Legendrian loops $\vartheta(a, b, c)$ and $\vartheta(\tilde{D})$ in Figures 43 and 44, respectively.*

4.4. Lagrangian fillings. In this section, we will prove one of our main theorem on ‘as many exact embedded Lagrangian fillings as seeds’ as follows:

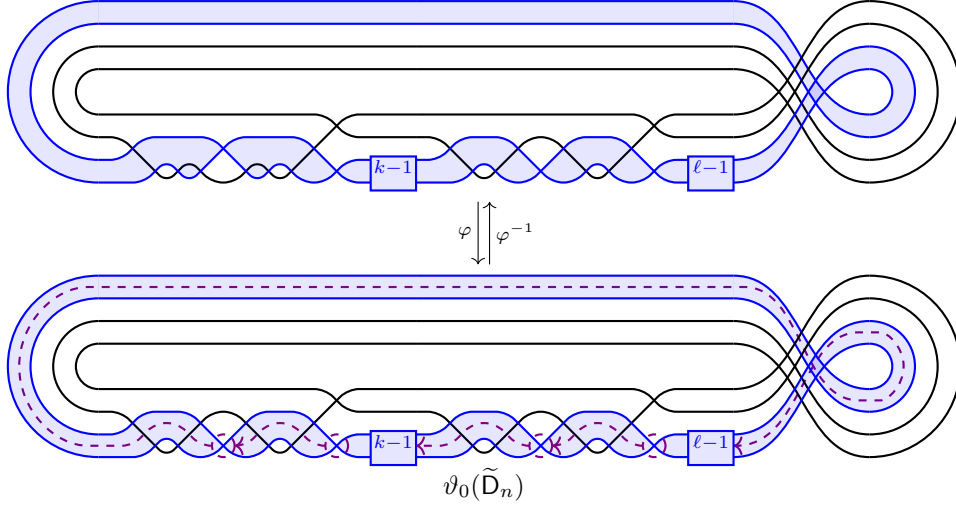


FIGURE 44. A Legendrian loop $\vartheta(\tilde{D}) = \varphi\vartheta_0(\tilde{D}_n)\varphi^{-1}$ induced from Legendrian Coxeter mutation $\mu_{\mathcal{G}}$ on $(\mathcal{G}(\tilde{D}_n), \mathcal{B}(\tilde{D}_n))$.

Theorem 4.31. *Let λ be a Legendrian knot or link of type ADE or type $\tilde{D}\tilde{E}$. Then it admits as many exact embedded Lagrangian fillings as the number of seeds in the seed pattern of the same type.*

Indeed, this theorem follows from considering the following general question.

Question 4.32. For a given N -graph \mathcal{G} with a chosen set \mathcal{B} of cycles, can we take a Legendrian mutation as many times as we want? Or equivalently, after applying a mutation μ_k on $(\mathcal{G}, \mathcal{B})$, is the set $\mu_k(\mathcal{B})$ still good in $\mu_k(\mathcal{G})$?

This question has been raised previously in [15, Remark 7.13]. One of the main reason making the question nontrivial is that the potential difference of geometric and algebraic intersections between two cycles.

Instead of attacking Question 4.32 directly, we will prove the following:

Proposition 4.33. *For $Z = A, D, E, \tilde{D}, \tilde{E}$, let $(\mathcal{G}_{t_0}, \mathcal{B}_{t_0}) = (\mathcal{G}(Z), \mathcal{B}(Z))$. Suppose that $(\mathbf{y}, \mathcal{B})$ is a Y -seed in the Y -pattern given by the initial Y -seed $(\mathbf{y}_{t_0}, \mathcal{B}_{t_0}) = \Psi(\mathcal{G}_{t_0}, \mathcal{B}_{t_0})$. Then $\lambda(Z)$ admits an N -graph $(\mathcal{G}, \mathcal{B})$ on \mathbb{D}^2 with $\partial\mathcal{G} = \lambda(Z)$ such that*

$$\Psi(\mathcal{G}, \mathcal{B}) = (\mathbf{y}, \mathcal{B}).$$

Under the aid of this proposition, one can prove Theorem 4.31.

Proof of Theorem 4.31. Let λ be given as above. Then, by Proposition 4.33, we have the set of pairs of N -graphs and set of good cycles which has a one-to-one correspondence via Ψ with the set of Y -seeds in the Y -pattern of type Z . Hence any pair of the Lagrangian fillings coming from these N -graphs is never exact Lagrangian isotopic by Corollary 3.39. Finally, by Corollary 4.15, there is a one-to-one correspondence between the set of Y -seeds and that of seeds, which completes the proof. \square

4.4.1. *Proof of Proposition 4.33.* We use an induction argument on the rank n of the root system $\Phi(Z)$. The initial step is either

$$(\mathcal{G}_{t_0}, \mathcal{B}_{t_0}) = (\mathcal{G}(1, 1, 1), \mathcal{B}(1, 1, 1)) \quad \text{or} \quad (\mathcal{G}_{t_0}, \mathcal{B}_{t_0}) = (\mathcal{G}(A_1), \mathcal{B}(A_1)).$$

Since there are no obstructions for mutations on these N -graphs, we are done for the initial step of the induction.

Now suppose that $n \geq 2$. By the induction hypothesis, we assume that the assertion holds for each type $Z' = A, D, E, \bar{D}, \bar{E}$ having rank strictly small than n .

Let $(\mathbf{y}, \mathcal{B})$ be an Y -seed of type Z . By Lemma 2.28, there exist $r \in \mathbb{Z}$ and a sequence $\mu_{j_1}, \dots, \mu_{j_L}$ of mutations such that

$$(\mathbf{y}, \mathcal{B}) = \mu'((\mu_{\mathcal{Q}})^r(\mathbf{y}_{t_0}, \mathcal{B}_{t_0})), \quad \mu' = \mu_{j_L} \dots \mu_{j_1},$$

where indices j_1, \dots, j_L miss at least one index i . It suffices to prove that the N -graph

$$(\mathcal{G}, \mathcal{B}) = \mu'((\mu_{\mathcal{G}})^r(\mathcal{G}_{t_0}, \mathcal{B}_{t_0}))$$

is well-defined.

Notice that by Lemma 4.18, Propositions 4.21 and 4.26, the Legendrian Coxeter mutation $\mu_{\mathcal{G}}^r(\mathcal{G}_{t_0}, \mathcal{B}_{t_0})$ is realizable so that

$$\Psi(\mu_{\mathcal{G}}^r(\mathcal{G}_{t_0}, \mathcal{B}_{t_0})) = (\mu_{\mathcal{Q}})^r(\mathbf{y}_{t_0}, \mathcal{B}_{t_0}).$$

Since $\mu_{\mathcal{G}}^r(\mathcal{G}_{t_0}, \mathcal{B}_{t_0})$ is the concatenation of Coxeter paddings on the initial N -graph $(\mathcal{G}_{t_0}, \mathcal{B}_{t_0})$, it suffices to prove that the Legendrian mutation $\mu'(\mu_{\mathcal{G}}^r(\mathcal{G}_{t_0}, \mathcal{B}_{t_0}))$ is realizable, which is equivalent to the realizability of $\mu'(\mathcal{G}_{t_0}, \mathcal{B}_{t_0})$.

By assumption, the indices j_1, \dots, j_L misses the index i and therefore the sequence of mutations $\mu_{j_1}, \dots, \mu_{j_L}$ can be performed inside the subgraph of the exchange graph $\text{Ex}(\Phi(Z))$, which is isomorphic to $\text{Ex}(\Phi(Z \setminus \{i\}))$. Here, with abuse of notation, we denote by Z the Dynkin diagram of type Z . Moreover, we denote by $\Phi(Z \setminus \{i\})$ the root system corresponding to the Dynkin diagram $Z \setminus \{i\}$. Then the root system $\Phi(Z \setminus \{i\})$ is not necessarily irreducible and may be decomposed into $\Phi(Z^{(1)}), \dots, \Phi(Z^{(\ell)})$ for $Z \setminus \{i\} = Z^{(1)} \cup \dots \cup Z^{(\ell)}$ so that

$$\begin{aligned} \Phi(Z \setminus \{i\}) &\cong \Phi(Z^{(1)}) \times \dots \times \Phi(Z^{(\ell)}), \\ \text{Ex}(Z \setminus \{i\}) &\cong \text{Ex}(Z^{(1)}) \times \dots \times \text{Ex}(Z^{(\ell)}), \\ \mathcal{Q}_{t_0} \setminus \{i\} &\cong \mathcal{Q}^{(1)} \amalg \dots \amalg \mathcal{Q}^{(\ell)}, \end{aligned}$$

where the subquiver $\mathcal{Q}^{(k)}$ is of type $Z^{(k)}$. Moreover, the composition μ' of mutations can be decomposed into sequences $\mu^{(1)}, \dots, \mu^{(\ell)}$ of mutations on $\mathcal{Q}^{(1)}, \dots, \mathcal{Q}^{(\ell)}$.

Similarly, we may decompose the N -graph $(\mathcal{G}_{t_0}, \mathcal{B}_{t_0})$ into N -subgraphs

$$(\mathcal{G}^{(1)}, \mathcal{B}^{(1)}), \dots, (\mathcal{G}^{(\ell)}, \mathcal{B}^{(\ell)})$$

along $\gamma_i \in \mathcal{B}_{t_0}$, which are the restrictions of $(\mathcal{G}_{t_0}, \mathcal{B}_{t_0})$ onto $\mathbb{D}^{(i)} \subset \mathbb{D}^2$ as follows:

- (1) For $\lambda = \lambda(A_n)$, we have the following two cases (Figure 45):
 - (a) If γ_i corresponds to a leaf, then we have the 2-subgraph $(\mathcal{G}(A_{n-1}), \mathcal{B}(A_{n-1}))$.
 - (b) If γ_i corresponds to a bivalent vertex, then for some $1 \leq r, s$ with $r + s + 1 = n$, we have two 2-subgraphs $(\mathcal{G}(A_r), \mathcal{B}(A_r))$ and $(\mathcal{G}(A_s), \mathcal{B}(A_s))$.

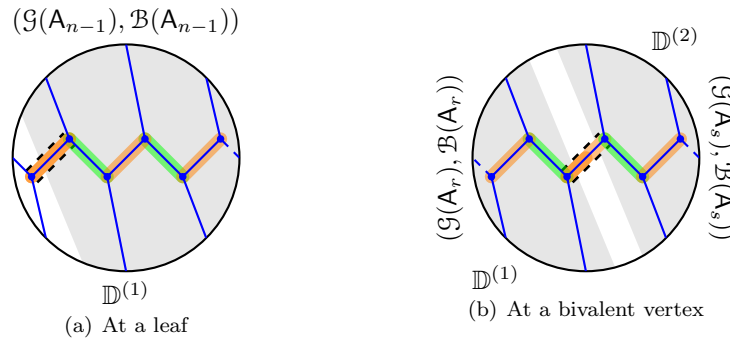
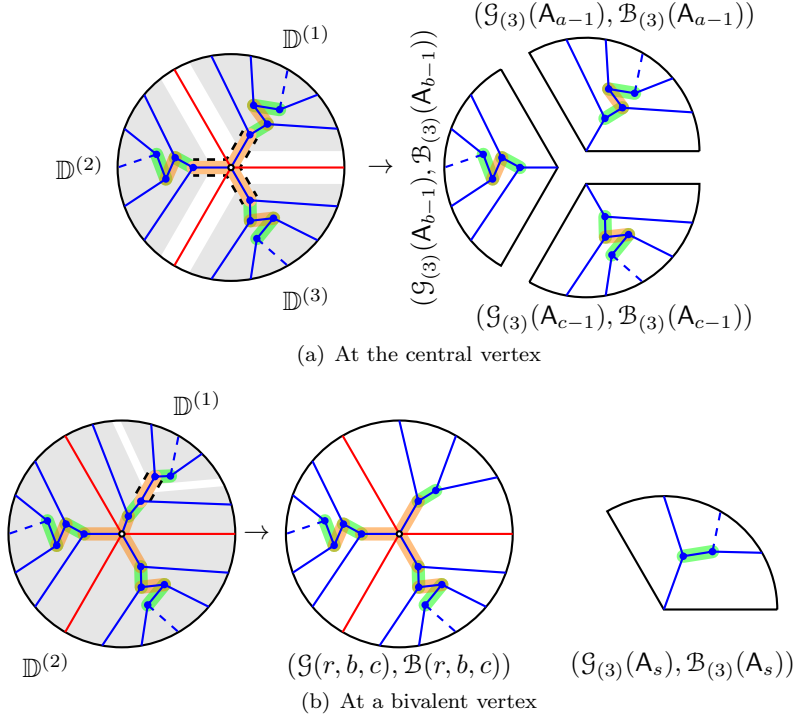


FIGURE 45. Decompositions of $\mathcal{G}(A_n)$

- (2) For $\lambda = \lambda(a, b, c)$, we have the following three cases (Figure 46):

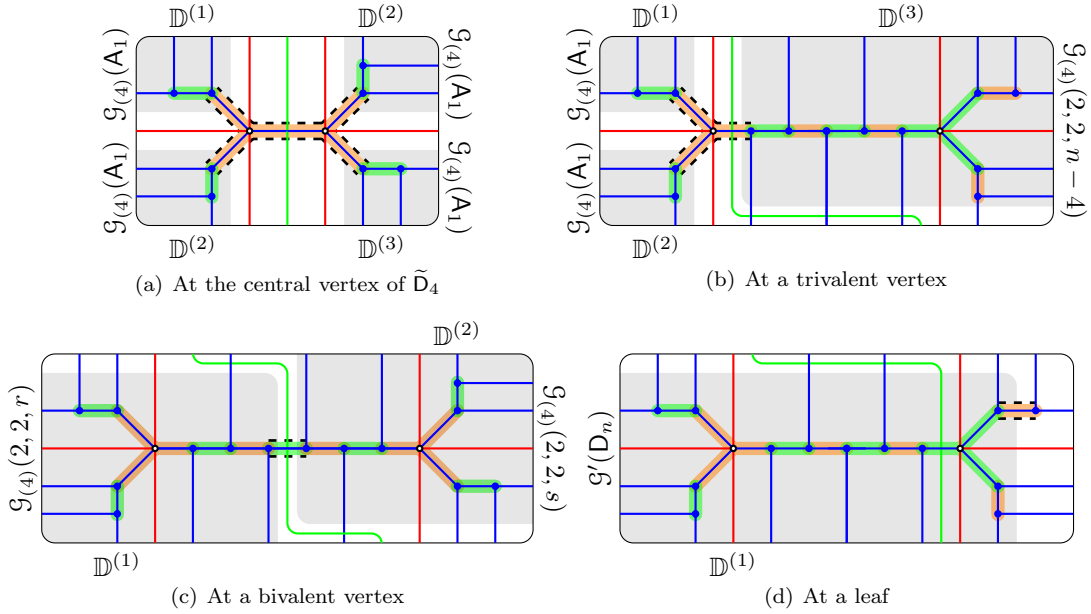
- (a) If γ_i corresponds to the central vertex, then we have three 3-subgraphs $(\mathcal{G}_{(3)}(\mathbf{A}_{a-1}), \mathcal{B}_{(3)}(\mathbf{A}_{a-1}))$, $(\mathcal{G}_{(3)}(\mathbf{A}_{b-1}), \mathcal{B}_{(3)}(\mathbf{A}_{b-1}))$, and $(\mathcal{G}_{(3)}(\mathbf{A}_{c-1}), \mathcal{B}_{(3)}(\mathbf{A}_{c-1}))$.
- (b) If γ_i corresponds to a bivalent vertex, then for some $1 \leq r, s$ with $r + s + 1 = a$, up to permuting indices a, b, c , we have two 3-subgraphs $(\mathcal{G}_{(3)}(\mathbf{A}_s), \mathcal{B}_{(3)}(\mathbf{A}_s))$ and $(\mathcal{G}_{(3)}(r, b, c), \mathcal{B}_{(3)}(r, b, c))$.
- (c) Otherwise, if γ_i corresponds to a leaf, then up to permuting indices a, b, c , we have the 3-subgraph $(\mathcal{G}_{(3)}(a-1, b, c), \mathcal{B}_{(3)}(a-1, b, c))$.

FIGURE 46. Decomposition of $\mathcal{G}(a, b, c)$

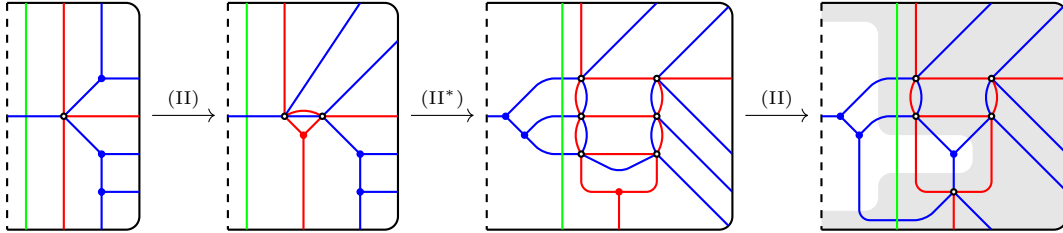
- (3) For $\lambda = \lambda(\tilde{\mathbf{D}}_n)$, we have the following four cases (Figure 47):
 - (a) If $n = 4$ and $\ell = 1$, then we have four 4-graphs of type \mathbf{A}_1 .
 - (b) If $n \geq 5$, $\ell = 1$, $n - 1$, then we have three 4-graphs of type $\mathbf{A}_1, \mathbf{A}_1$ and $(2, 2, n - 4)$.
 - (c) If $n \geq 6$, $\ell = 4, \dots, n - 2$, then for some $r + s = n - 3$, we have two 4-graphs of type $(2, 2, r)$ and $(2, 2, s)$.
 - (d) If $\ell = 2, 3, n, n + 1$, then we have the 4-graph $(\mathcal{G}'(\mathbf{D}_n), \mathcal{B}'(\mathbf{D}_n))$.

Here, $\mathcal{G}_{(3)}(\mathbf{A}_{n'})$, $\mathcal{G}_{(4)}(\mathbf{A}_{n'})$ and $\mathcal{G}_{(4)}(a', b', c')$ are the 3- and 4-graphs obtained from $\mathcal{G}(\mathbf{A}_{n'})$ and $\mathcal{G}(a', b', c')$ by adding trivial planes at the top. Hence, the realizabilities of Legendrian mutations on $\mathcal{G}_{(3)}(\mathbf{A}_{n'})$, $\mathcal{G}_{(4)}(\mathbf{A}_{n'})$ and $\mathcal{G}_{(4)}(a', b', c')$ are the same as those on $\mathcal{G}(\mathbf{A}_{n'})$ and $\mathcal{G}(a', b', c')$.

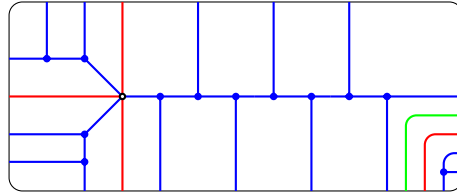
Except for the very last case (3d), all the other cases are reduced to either linear and tripod N -graphs with strictly lower rank. Hence, by the induction hypothesis, any composition $\mu^{(k)}$ of mutations on $\mathcal{Q}^{(k)}$ for $1 \leq k \leq \ell$ can be realized as a composition of Legendrian mutations on $(\mathcal{G}^{(k)}, \mathcal{B}^{(k)})$. This guarantees the realizability of $\mu'(\mathcal{G}_{t_0}, \mathcal{B}_{t_0})$.

FIGURE 47. Decompositions of $\mathcal{G}(\tilde{D}_n)$

For the case (3d), one can apply a sequence of Move (II) on $(\mathcal{G}'(D_n), \mathcal{B}'(D_n))$ as follows:



Then in the last picture, the shaded part corresponds to a tame annular N -graph and so the N -graph $(\mathcal{G}'(D_n), \mathcal{B}'(D_n))$ is ∂ -Legendrian isotopic to the following N -graph



which is a stabilization of $(\mathcal{G}(D_n), \mathcal{B}(D_n)) = (\mathcal{G}(2, 2, n-2), \mathcal{G}(2, 2, n-2))$. Therefore the induction hypothesis completes the proof.

Remark 4.34. It is not claimed above that two mutations μ' and $\mu_{\mathcal{G}}$ commute. Indeed, if we first mutate $(\mathcal{G}_{t_0}, \mathcal{B}_{t_0})$ via μ' , then the result may not look like either $(\mathcal{G}_{t_0}, \mathcal{B}_{t_0})$ or $(\mathcal{G}_{t_0}, \mathcal{B}_{t_0})$ and hence $\mu_{\mathcal{G}}$ will not work as expected. Besides it is not even clear whether $\mu_{\mathcal{G}}\mu'(\mathcal{G}_{t_0}, \mathcal{B}_{t_0})$ is realizable.

5. FOLDINGS

In this section, we will consider cluster structures of type BCFG and all standard affine type on N -graphs with certain symmetry.

Recall that if a quiver of type Z is globally foldable with respect to the G -action, then the folded cluster pattern is of type Z^G . We consider the triples (Z, G, Z^G) shown in Table 10.

rotation	$(A_{2n-1}, \mathbb{Z}/2\mathbb{Z}, B_n)$	$(D_4, \mathbb{Z}/3\mathbb{Z}, G_2)$	$(\tilde{E}_6, \mathbb{Z}/3\mathbb{Z}, \tilde{G}_2)$
	$(\tilde{D}_{2n \geq 6}, \mathbb{Z}/2\mathbb{Z}, \tilde{B}_n)$	$(\tilde{D}_4, \mathbb{Z}/2\mathbb{Z}, \tilde{C}_2)$	
conjugation	$(D_{n+1}, \mathbb{Z}/2\mathbb{Z}, C_n)$	$(E_6, \mathbb{Z}/2\mathbb{Z}, F_4)$	
	$(\tilde{E}_6, \mathbb{Z}/2\mathbb{Z}, E_6^{(2)})$	$(\tilde{E}_7, \mathbb{Z}/2\mathbb{Z}, \tilde{F}_4)$	$(\tilde{D}_4, \mathbb{Z}/2\mathbb{Z}, A_5^{(2)})$

TABLE 10. Folding by rotation and conjugation

5.1. Group actions on N -graphs. For each triple (Z, G, Z^G) , we first consider the G -action on each N -graph of type Z .

5.1.1. Rotation action. Let (Z, G, Z^G) be one of five cases in the first row of Table 10. We will denote the generator of $G = \mathbb{Z}/2\mathbb{Z}$ or $\mathbb{Z}/3\mathbb{Z}$ by τ , which acts on N -graphs \mathcal{G} by π - or $2\pi/3$ -rotation, respectively.

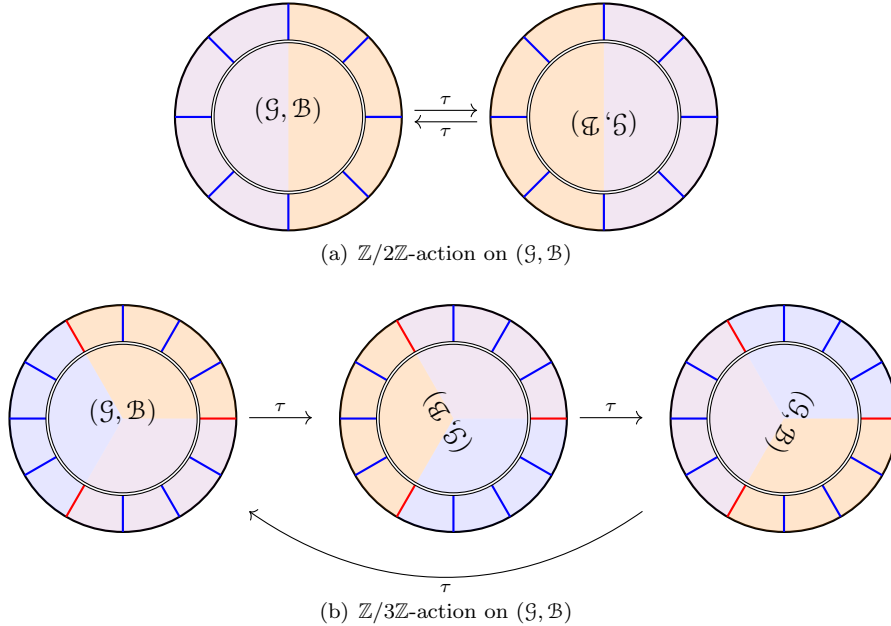
Notice that for each $Z = A_{2n-1}, D_4, \tilde{E}_6, \tilde{D}_{2n \geq 6}$, or \tilde{D}_4 , we may assume that the Legendrian $\lambda(Z)$ in $J^1\mathbb{S}^1$ is invariant under the π -rotation since the braid $\beta(Z)$ representing $\lambda(Z)$ has the rotation symmetry as follows:

$$\begin{aligned} \beta(A_{2n-1}) &= (\sigma_1^{n+1})^2, & \beta(D_4) &= (\sigma_2 \sigma_1^3)^3, & \beta(\tilde{E}_6) &= (\sigma_2 \sigma_1^4)^3, \\ \beta(\tilde{D}_{2n}) &= (\sigma_2 \sigma_1^3 \sigma_2 \sigma_1^3 \sigma_2 \sigma_3 \sigma_1^{n-2})^2, \quad n \geq 3, & \beta(\tilde{D}_4) &= (\sigma_2 \sigma_1^3 \sigma_2 \sigma_1^3 \sigma_2 \sigma_3)^2. \end{aligned}$$

Now the generator τ acts on the set $\text{Ngraphs}(\lambda(Z))$ of equivalent classes of N -graphs with cycles whose boundary is precisely $\lambda(Z)$. Indeed, for each $(\mathcal{G}, \mathcal{B})$ in $\text{Ngraphs}(\lambda(Z))$, we have

$$\tau \cdot (\mathcal{G}, \mathcal{B}) = \begin{cases} R_\pi(\mathcal{G}, \mathcal{B}) & \text{if } \tau \in \mathbb{Z}/2\mathbb{Z}; \\ R_{2\pi/3}(\mathcal{G}, \mathcal{B}) & \text{if } \tau \in \mathbb{Z}/3\mathbb{Z}, \end{cases}$$

where R_θ is the induced action on N -graphs with cycles from the θ -rotation on \mathbb{D}^2 . See Figure 48(a).

FIGURE 48. Rotation actions on N -graphs

5.1.2. *Conjugation action.* Assume that (Z, G, Z^G) is one of five cases in the second row of Table 10. We denote the generator for $G = \mathbb{Z}/2\mathbb{Z}$ by η . Then, as before, the Legendrian $\tilde{\lambda}(Z)$ is represented by the braid $\tilde{\beta}(Z)$ which is invariant under the conjugation as follows:

$$\begin{aligned}\tilde{\beta}(D_{n+1}) &= \sigma_2^n \sigma_{1,3} \sigma_2 \sigma_{1,3}^3 \sigma_2 \sigma_{1,3} \sigma_2^2 \sigma_{1,3}, & \tilde{\beta}(E_6) &= \sigma_2^3 \sigma_{1,3} \sigma_2 \sigma_{1,3}^4 \sigma_2 \sigma_{1,3} \sigma_2^2 \sigma_{1,3}, \\ \tilde{\beta}(\tilde{E}_6) &= \sigma_2^4 \sigma_{1,3} \sigma_2 \sigma_{1,3}^4 \sigma_2 \sigma_{1,3} \sigma_2^2 \sigma_{1,3}, & \tilde{\beta}(\tilde{E}_7) &= \sigma_2^3 \sigma_{1,3} \sigma_2 \sigma_{1,3}^5 \sigma_2 \sigma_{1,3} \sigma_2^2 \sigma_{1,3}, & \tilde{\beta}(\tilde{D}_4) &= (\sigma_2 \sigma_{1,3} \sigma_2 \sigma_{1,3}^2)^2.\end{aligned}$$

Therefore, the generator η acts on the set $\mathcal{N}\text{graphs}(\tilde{\lambda}(Z))$ by conjugation. That is, for each $(\mathcal{G}, \mathcal{B}) \in \mathcal{N}\text{graphs}(\tilde{\lambda}(Z))$, we have

$$\eta \cdot (\mathcal{G}, \mathcal{B}) = \overline{(\mathcal{G}, \mathcal{B})}.$$

Remark 5.1. One may consider the conjugation invariant degenerate N -graph $\tilde{\mathcal{G}}(A_{2n-1})$ instead of the rotation invariant N -graph $\mathcal{G}(A_{2n-1})$ as seen earlier in Remark 4.10. Then it can be checked that these two actions are identical.

Remark 5.2. The denegated N -graph $\tilde{\mathcal{G}}(\tilde{D}_4)$ admits the π -rotation action as well, which is essentially equivalent to the conjugation action on $\tilde{\mathcal{G}}(\tilde{D}_4)$. We omit the detail.

5.2. **Invariant N -graphs and Lagrangian fillings.** Throughout this section, we assume that (Z, G, Z^G) is one of the triples in Table 10. For an N -graph \mathcal{G} in $\mathcal{N}\text{graphs}(\lambda(Z))$ or $\mathcal{N}\text{graphs}(\tilde{\lambda}(Z))$, we say that $(\mathcal{G}, \mathcal{B})$ is G -invariant if for each $g \in G$,

$$g \cdot (\mathcal{G}, \mathcal{B}) = (\mathcal{G}, \mathcal{B}).$$

Namely,

- (1) the N -graph \mathcal{G} is invariant under the action of g ,
- (2) the sets of cycles \mathcal{B} and $g(\mathcal{B})$ are identical up to relabeling $\gamma \leftrightarrow g(\gamma)$ for $\gamma \in \mathcal{B}$.

The following statements are obvious but important observations.

Lemma 5.3. *For a free N -graph \mathcal{G} , let*

$$L(\mathcal{G}) := (\pi \circ \iota)(\Lambda(\mathcal{G}))$$

be the Lagrangian surface defined by \mathcal{G} in \mathbb{C}^2 .

- (1) *If \mathcal{G} is invariant under the θ -rotation, then $L(\mathcal{G})$ is invariant under the θ -rotation in \mathbb{C}^2*

$$(z_1, z_2) \mapsto (z_1 \cos(\theta) + z_2 \sin(\theta), -z_1 \sin(\theta) + z_2 \cos(\theta)).$$

- (2) *If \mathcal{G} is invariant under the conjugation, then $L(\mathcal{G})$ is invariant under the antisymplectic involution in \mathbb{C}^2*

$$(z_1, z_2) \mapsto (\bar{z}_1, \bar{z}_2).$$

Lemma 5.4. *The N -graphs $\mathcal{G}(Z)$ for $Z = A_{2n-1}, D_4, \tilde{E}_6, \tilde{D}_{2n \geq 6}, \tilde{D}_4$ and the degenerate N -graphs $\tilde{\mathcal{G}}(Z)$ for $Z = D_{n+1}, E_6, \tilde{E}_6, \tilde{E}_7, \tilde{D}_4$ are all invariant under the G -action.*

Lemma 5.5. *Suppose that $g \in G$ acts on $(\mathcal{G}, \mathcal{B})$. If the Legendrian mutation $\mu_\gamma(\mathcal{G}, \mathcal{B})$ is realizable, then*

$$\mu_{g(\gamma)}(g \cdot (\mathcal{G}, \mathcal{B})) = g \cdot (\mu_\gamma(\mathcal{G}, \mathcal{B})).$$

In particular, for a G -orbit $I \subset \mathcal{B}$ consists of pairwise disjoint cycles, if $(\mathcal{G}, \mathcal{B})$ is G -invariant and the Legendrian orbit mutation $\mu_I(\mathcal{G}, \mathcal{B})$ is realizable, then $\mu_I(\mathcal{G}, \mathcal{B})$ is G -invariant as well.

On the other hand, if we have a G -invariant N -graph $(\mathcal{G}, \mathcal{B})$ with cycles, it gives us a G -admissible quiver $\mathcal{Q}(\mathcal{G}, \mathcal{B})$.

Lemma 5.6. *Let $(\mathcal{G}, \mathcal{B})$ be a G -invariant N -graph with cycles. Then the quiver $\mathcal{Q}(\mathcal{G}, \mathcal{B})$ is G -admissible.*

Proof. By definition of G -invariance of $(\mathcal{G}, \mathcal{B})$, it is obvious that the quiver $\mathcal{Q} = \mathcal{Q}(\mathcal{G}, \mathcal{B})$ is G -invariant. On the other hand, since Z is either a finite or an affine Dynkin diagram, the G -invariance of the quiver \mathcal{Q} implies the G -admissibility of \mathcal{Q} by Theorem 2.21. \square

Proposition 5.7. *For each Y -seed $(\mathbf{y}', \mathcal{B}')$ of type Z^G , there exists a G -invariant N -graph with cycles $(\mathcal{G}, \mathcal{B})$ of type Z such that*

$$\Psi(\mathcal{G}, \mathcal{B})^G = (\mathbf{y}', \mathcal{B}').$$

Proof. For each Z , let $(\mathcal{G}_{t_0}, \mathcal{B}_{t_0})$ be the N -graph with cycles defined as follows:

$$(\mathcal{G}_{t_0}, \mathcal{B}_{t_0}) := \begin{cases} (\mathcal{G}(Z), \mathcal{B}(Z)) & \text{if } Z = A_{2n-1}, D_4, \tilde{E}_6, \tilde{D}_{2n \geq 6}, \tilde{D}_4, G \text{ acts as rotation;} \\ (\tilde{\mathcal{G}}(Z), \tilde{\mathcal{B}}(Z)) & \text{if } Z = D_{n+1}, E_6, \tilde{E}_6, \tilde{E}_7, \tilde{D}_4, G \text{ acts as conjugation.} \end{cases}$$

We regard the Y -seed defined by $(\mathcal{G}_{t_0}, \mathcal{B}_{t_0})$ as the initial seed $(\mathbf{y}_{t_0}, \mathcal{B}_{t_0})$

$$(\mathbf{y}_{t_0}, \mathcal{B}_{t_0}) = \Psi(\mathcal{G}_{t_0}, \mathcal{B}_{t_0}).$$

As seen in Lemmas 5.4 and 5.6, $(\mathcal{G}_{t_0}, \mathcal{B}_{t_0})$ is G -invariant and so is the quiver $\mathcal{Q}(\mathcal{G}_{t_0}, \mathcal{B}_{t_0})$. Therefore, we have the folded seed $(\mathbf{y}_{t_0}, \mathcal{B}_{t_0})^G$ which plays the role of the initial seed of the Y -pattern of type Z^G .

Let $(\mathbf{y}', \mathcal{B}')$ be an Y -seed of the Y -pattern of type Z^G . By Lemma 2.28, there exist $r \in \mathbb{Z}$ and a sequence of mutations $\mu_{j_1}^{Z^G}, \dots, \mu_{j_L}^{Z^G}$ such that

$$(\mathbf{y}', \mathcal{B}') = (\mu_{j_L}^{Z^G} \cdots \mu_{j_1}^{Z^G})((\mu_{\mathcal{Q}}^{Z^G})^r((\mathbf{y}_{t_0}, \mathcal{B}_{t_0})^G)).$$

Moreover, the indices j_1, \dots, j_L misses at least one index, say i .

Then Theorem 2.21 implies the existence of the G -admissible Y -seed $(\mathbf{y}, \mathcal{B})$ of type Z such that $(\mathbf{y}, \mathcal{B})^G = (\mathbf{y}', \mathcal{B}')$ and

$$(\mathbf{y}, \mathcal{B}) = (\mu_{I_L}^Z \cdots \mu_{I_1}^Z)((\mu_{\mathcal{Q}}^Z)^r(\mathbf{y}_{t_0}, \mathcal{B}_{t_0})),$$

where I_k is G -orbit corresponding to j_k for each $1 \leq k \leq L$. It suffices to prove that the N -graph

$$(\mathcal{G}, \mathcal{B}) = (\mu_{I_L} \cdots \mu_{I_1})((\mu_{\mathcal{G}})^r(\mathcal{G}_{t_0}, \mathcal{B}_{t_0}))$$

is well-defined and G -invariant so that $(\mathbf{y}, \mathcal{B}) = \Psi(\mathcal{G}, \mathcal{B})$ is G -admissible by Proposition 3.42 as desired.

By Lemma 4.18, Propositions 4.21, 4.26 and 4.28, the Legendrian Coxeter mutation $\mu_{\mathcal{G}}^r(\mathcal{G}_{t_0}, \mathcal{B}_{t_0})$ is realizable so that

$$\Psi(\mu_{\mathcal{G}}^r(\mathcal{G}_{t_0}, \mathcal{B}_{t_0})) = (\mu_{\mathcal{Q}})^r(\mathbf{y}_{t_0}, \mathcal{B}_{t_0}).$$

Since $\mu_{\mathcal{G}}^r(\mathcal{G}_{t_0}, \mathcal{B}_{t_0})$ is the concatenation of Coxeter paddings on the initial N -graph $(\mathcal{G}_{t_0}, \mathcal{B}_{t_0})$, it suffices to prove that the Legendrian mutation $(\mu_{I_L} \cdots \mu_{I_1})(\mu_{\mathcal{G}}^r(\mathcal{G}_{t_0}, \mathcal{B}_{t_0}))$ is realizable, which is equivalent to the realizability of $(\mu_{I_L} \cdots \mu_{I_1})(\mathcal{G}_{t_0}, \mathcal{B}_{t_0})$.

On the other hand, since the indices j_1, \dots, j_L misses the index i , the orbits I_1, \dots, I_L misses one orbit I corresponding to i . In other words, the sequence of mutations $\mu_{I_1}, \dots, \mu_{I_L}$ can be performed inside the subgraph of the exchange graph $\text{Ex}(\Phi(Z))$, which is isomorphic to $\text{Ex}(\Phi(Z \setminus I))$. Then the root system $\Phi(Z \setminus I)$ is decomposed into $\Phi(Z^{(1)}), \dots, \Phi(Z^{(\ell)})$, where $Z \setminus I = Z^{(1)} \cup \dots \cup Z^{(\ell)}$. Moreover, the sequence of mutations $\mu_{I_1}, \dots, \mu_{I_L}$ can be decomposed into sequences $\mu^{(1)}, \dots, \mu^{(\ell)}$ of mutations on $Z^{(1)}, \dots, Z^{(\ell)}$.

Similarly, we may decompose the N -graph $(\mathcal{G}_{t_0}, \mathcal{B}_{t_0})$ into N -subgraphs

$$(\mathcal{G}^{(1)}, \mathcal{B}^{(1)}), \dots, (\mathcal{G}^{(\ell)}, \mathcal{B}^{(\ell)})$$

along cycles in $I \subset \mathcal{B}_{t_0}$ as done in the previous section. Then the Legendrian mutation $(\mu_{I_L} \cdots \mu_{I_1})(\mathcal{G}_{t_0}, \mathcal{B}_{t_0})$ is realizable if and only if so is $\mu^{(j)}(\mathcal{G}^{(j)}, \mathcal{B}^{(j)})$ for each $1 \leq j \leq \ell$. This can be done by induction on rank of the root system and so the N -graph $(\mathcal{G}, \mathcal{B})$ with $\Psi(\mathcal{G}, \mathcal{B}) = (\mathbf{y}, \mathcal{B})$ is well-defined.

Finally, the G -invariance of $(\mathcal{G}, \mathcal{B})$ follows from Lemma 5.5. \square

Theorem 5.8 (Folding of N -graphs). *The following holds:*

- (1) *The Legendrian $\lambda(A_{2n-1})$ has $\binom{2n}{n}$ Lagrangian fillings which are invariant under the π -rotation and admit the Y -pattern of type B_n .*
- (2) *The Legendrian $\lambda(D_4)$ has 8 Lagrangian fillings which are invariant under the $2\pi/3$ -rotation and admit the Y -pattern of type G_2 .*
- (3) *The Legendrian $\lambda(\tilde{E}_6)$ has Lagrangian fillings which are invariant under the $2\pi/3$ -rotation and admit the Y -pattern of type \tilde{G}_2 .*

- (4) The Legendrian $\lambda(\tilde{\mathbf{D}}_{2n})$ with $n \geq 3$ has Lagrangian fillings which are invariant under the π -rotation and admit the Y -pattern of type $\tilde{\mathbf{B}}_n$.
- (5) The Legendrian $\lambda(\tilde{\mathbf{D}}_4)$ has Lagrangian fillings which are invariant under the π -rotation and admit the Y -pattern of type $\tilde{\mathbf{C}}_2$.
- (6) The Legendrian $\tilde{\lambda}(\mathbf{E}_6)$ has 105 Lagrangian fillings which are invariant under the antisymplectic involution and admit the Y -pattern of type \mathbf{F}_4 .
- (7) The Legendrian $\tilde{\lambda}(\mathbf{D}_{n+1})$ has $\binom{2n}{n}$ Lagrangian fillings which are invariant under the anti-symplectic involution and admit the Y -pattern of type \mathbf{C}_n .
- (8) The Legendrian $\tilde{\lambda}(\tilde{\mathbf{E}}_6)$ has Lagrangian fillings which are invariant under the antisymplectic involution and admit the Y -pattern of type $\mathbf{E}_6^{(2)}$.
- (9) The Legendrian $\tilde{\lambda}(\tilde{\mathbf{E}}_7)$ has Lagrangian fillings which are invariant under the antisymplectic involution and admit the Y -pattern of type $\tilde{\mathbf{F}}_4$.
- (10) The Legendrian $\tilde{\lambda}(\tilde{\mathbf{D}}_4)$ has Lagrangian fillings which are invariant under the antisymplectic involution and admit the Y -pattern of type $\mathbf{A}_5^{(2)}$.

Proof. Let (Z, G, Z^G) be one of the triples in Table 10. By Proposition 5.7, each Y -seed of the Y -pattern of type Z^G is realizable by a G -invariant N -graph, which gives us a Lagrangian filling with a certain symmetry by Lemma 5.3. This completes the proof. \square

APPENDIX A. G -INVARIANCE AND G -ADMISSIBILITY OF FINITE TYPE

In this section, we will provide a proof of Theorem 2.20.

Lemma A.1. *Let \mathcal{Q} be a quiver of type \mathbf{A}_{2n-1} . Suppose that \mathcal{Q} is invariant under an action of $G = \mathbb{Z}/2\mathbb{Z}$ defined by*

$$\tau(i) = 2n - i$$

for all $i \in [2n - 1]$. Here, we denote by $\tau \in \mathbb{Z}/2\mathbb{Z}$ the generator of G . Then there is no oriented cycle of the form

$$j \rightarrow i \rightarrow \tau(j) \rightarrow \tau(i) \rightarrow j$$

for any $i, j \neq n$.

Proof. It is well known that a quiver \mathcal{Q} of type \mathbf{A} corresponds to a triangulation of a polygon, where diagonals and triangles define mutable vertices and arrows. Therefore, any minimal cycle in \mathcal{Q} if exists is of length 3, which is also proved in [9, §2]. Hence if an oriented cycle $j \rightarrow i \rightarrow \tau(j) \rightarrow \tau(i) \rightarrow j$ of length 4 exists, then there must be an edge $i - \tau(i)$ or $j - \tau(j)$ in \mathcal{Q} . Hence $b_{i,\tau(i)} \neq 0$ or $b_{j,\tau(j)} \neq 0$ for $\mathcal{B} = (b_{k,\ell}) = \mathcal{B}(\mathcal{Q})$.

This is impossible because \mathcal{Q} is $\mathbb{Z}/2\mathbb{Z}$ -invariant and so

$$b_{i,\tau(i)} = b_{\tau(i),\tau(\tau(i))} = b_{\tau(i),i} = -b_{i,\tau(i)} \implies b_{i,\tau(i)} = 0.$$

Therefore we are done. \square

Proposition A.2. *Let \mathcal{Q} be a quiver of type \mathbf{A}_{2n-1} , which is $\mathbb{Z}/2\mathbb{Z}$ -invariant as above. Then \mathcal{Q} is $\mathbb{Z}/2\mathbb{Z}$ -admissible.*

Proof. We will check the conditions (2a), (2b), and (2c) for the admissibility according to Definition 2.14. Let $\mathcal{B} = (b_{i,j}) = \mathcal{B}(\mathcal{Q})$.

(2a) Since all vertices in \mathcal{Q} are mutable, the condition (2a) is obviously satisfied.

(2b) On the other hand, for each $i \in [2n - i]$, we have

$$b_{i,\tau(i)} = (\gamma_i, \gamma_{\tau(i)}) = (\gamma_{\tau(i)}, \gamma_{\tau(\tau(i))}) = (\gamma_{\tau(i)}, \gamma_i) = -b_{i,\tau(i)},$$

which implies

$$b_{i,\tau(i)} = 0.$$

(2c) Finally, we need to prove that for each i, j ,

$$b_{i,j}b_{\tau(i),j} \geq 0.$$

If $j = n$, then since $\tau(n) = n$, we have

$$b_{i,n}b_{\tau(i),n} = b_{i,n}b_{\tau(i),\tau(n)} = b_{i,n}b_{i,n} \geq 0.$$

Similarly, if $i = n$, then

$$b_{n,j}b_{\tau(n),j} = b_{n,j}b_{n,j} \geq 0.$$

Suppose that for some $i, j \neq n$,

$$b_{i,j}b_{\tau(i),j} < 0.$$

By changing the roles of i and $\tau(i)$ if necessary, we may assume that $b_{i,j} < 0 < b_{\tau(i),j}$. Then we also have

$$b_{\tau(i),\tau(j)} < 0 < b_{i,\tau(j)},$$

which implies that there is an oriented cycle in \mathcal{Q}

$$j \rightarrow i \rightarrow \tau(j) \rightarrow \tau(i) \rightarrow j.$$

However, this contradicts to Lemma A.1 and therefore \mathcal{Q} satisfies all conditions in Definition 2.14. \square

Proposition A.3. *Let \mathcal{Q} be a quiver on $[4]$ of type D_4 , which is invariant under the $\mathbb{Z}/3\mathbb{Z}$ -action given by*

$$1 \xleftrightarrow{\tau} 1, \quad 2 \xrightarrow{\tau} 3 \xrightarrow{\tau} 4 \xrightarrow{\tau} 2.$$

Here, we denote by τ the generator of $\mathbb{Z}/3\mathbb{Z}$. Then the quiver \mathcal{Q} is $\mathbb{Z}/3\mathbb{Z}$ -admissible.

Proof. (2a) This is obvious as before.

(2b) Let $\mathcal{B} = (b_{i,j}) = \mathcal{B}(\mathcal{Q})$. Suppose that $b_{2,3} \neq 0$. Since the quiver is $\mathbb{Z}/3\mathbb{Z}$ -invariant,

$$b_{2,3} = b_{3,4} = b_{4,2} \neq 0$$

and so \mathcal{Q} has a directed cycle either

$$2 \rightarrow 3 \rightarrow 4 \rightarrow 2 \quad \text{or} \quad 2 \rightarrow 4 \rightarrow 3 \rightarrow 2.$$

Then according to the value $b_{1,2}$, the underlying graph of the quiver \mathcal{Q} is either the complete graph K_4 or a disconnected graph. However, both are impossible as shown in [8, Figure 1]. Therefore, we obtain

$$b_{2,3} = b_{3,4} = b_{4,2} = 0.$$

(2c) The only entries we need to check are $b_{1,j}$'s, which are all equal by the $\mathbb{Z}/3\mathbb{Z}$ -invariance of \mathcal{Q} . Therefore

$$b_{1,j}b_{1,j'} \geq 0.$$

This completes the proof. \square

Lemma A.4. *Let \mathcal{Q} be a quiver on $[6]$ of type E_6 , which is invariant under the $\mathbb{Z}/2\mathbb{Z}$ -action defined by*

$$i \xleftrightarrow{\eta} i, i \leq 2, \quad 3 \xleftrightarrow{\eta} 5, \quad 4 \xleftrightarrow{\eta} 6.$$

Here, we denote by η the generator of $\mathbb{Z}/2\mathbb{Z}$. Then there is no oriented cycle, which is either

$$3 \rightarrow 4 \rightarrow 5 \rightarrow 6 \rightarrow 3 \quad \text{or} \quad 3 \rightarrow 6 \rightarrow 5 \rightarrow 4 \rightarrow 3. \quad (\text{A.1})$$

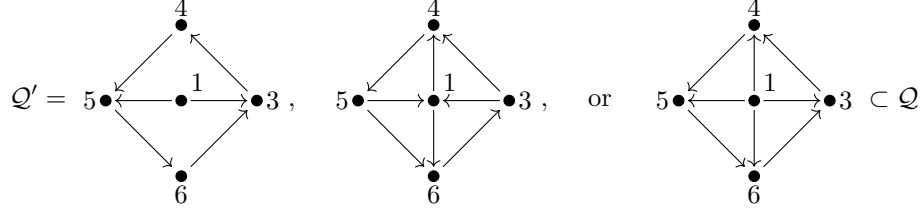
Proof. We first recall from [26, Theorem 1.8] that

$$|b_{i,j}| \leq 1 \quad \text{for all } i, j \in [6]. \quad (\text{A.2})$$

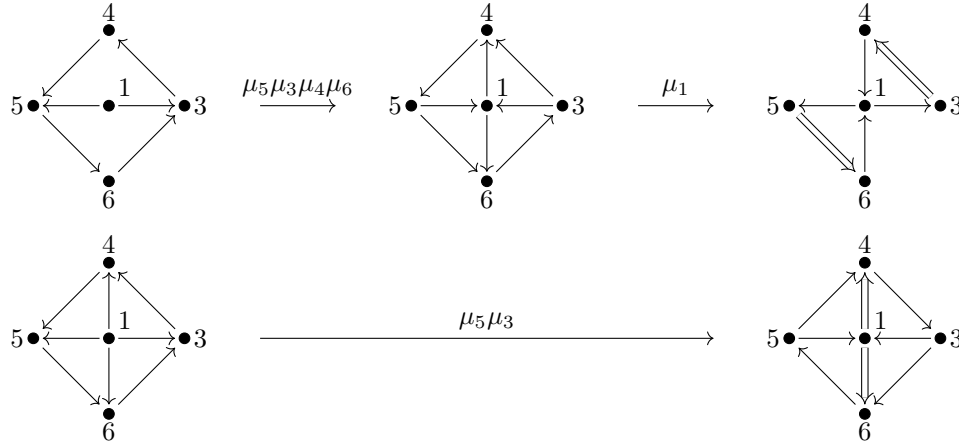
Otherwise, \mathcal{Q} produces a cluster pattern of infinite type. Hence, \mathcal{Q} is a simple directed graph.

Suppose that \mathcal{Q} contains an oriented cycle in (A.1). By relabeling if necessary, we may assume that the \mathcal{Q} contains an oriented cycle $3 \rightarrow 4 \rightarrow 5 \rightarrow 6 \rightarrow 3$. Then, since \mathcal{Q} is connected, at least one of vertices 1 and 2 is joined with one of vertices 3, 4, 5 and 6 by an edge. Without loss of generality, we may assume that such a vertex is 1.

Let \mathcal{Q}' be the quiver on $\{1, 3, 4, 5, 6\}$ obtained by forgetting the vertex 2 in \mathcal{Q} . Then, by the invariance of \mathcal{Q} under $\mathbb{Z}/2\mathbb{Z}$ -action,



up to relabeling and the mutation μ_1 . Then, via further mutations, each of these quivers can be transformed to a quiver producing a cluster pattern of infinite type because of the condition (A.2) as follows:



Since any subquiver of a quiver mutation equivalent to \mathcal{Q} is of finite type, we get a contradiction which completes the proof. \square

Remark A.5. Since there are only finitely many quivers of type E_6 , the above lemma can be verified by a computer but we gave here a combinatorial proof.

Proposition A.6. *Let \mathcal{Q} be a quiver of type $Z = D_{n+1}$ or E_6 , which is invariant under $\mathbb{Z}/2\mathbb{Z}$ -action defined by*

$$i \xleftrightarrow{\eta} i, i < n, \quad n \xleftrightarrow{\eta} n+1$$

for $Z = D_{n+1}$, or

$$i \xleftrightarrow{\eta} i, i \leq 2, \quad 3 \xleftrightarrow{\eta} 5, \quad 4 \xleftrightarrow{\eta} 6,$$

for $Z = E_6$. Here, η is the generator of $\mathbb{Z}/2\mathbb{Z}$. Then the quiver \mathcal{Q} is $\mathbb{Z}/2\mathbb{Z}$ -admissible.

Proof. (2a) This is obvious as before.

(2b) Let $\mathcal{B} = (b_{i,j}) = \mathcal{B}(\mathcal{Q})$. Then, by the $\mathbb{Z}/2\mathbb{Z}$ -invariance of \mathcal{Q} ,

$$b_{i,\eta(i)} = b_{\eta(i),\eta(\eta(i))} = b_{\eta(i),i} = -b_{i,\eta(i)} \implies b_{i,\eta(i)} = 0.$$

(2c) If $Z = D_{n+1}$, then we only need to show

$$b_{i,n} b_{i,n+1} \geq 0$$

for $i < n$. This is obvious since

$$b_{i,n+1} = b_{\eta(i),\eta(n+1)} = b_{i,n}.$$

If $Z = E_6$, then all we need to show inequalities

$$b_{i,j} b_{i,j+2} \geq 0, \quad b_{3,4} b_{3,6} \geq 0$$

hold for $i = 1, 2$ and $j = 3, 4$.

The first inequality is obvious since

$$b_{i,j+2} = b_{\eta(i),\eta(j+2)} = b_{i,j}.$$

Suppose that $b_{3,4}b_{3,6} < 0$. Then, since $b_{3,4} = b_{5,6}$ and $b_{3,6} = b_{5,4}$, the \mathcal{Q} has a loop either

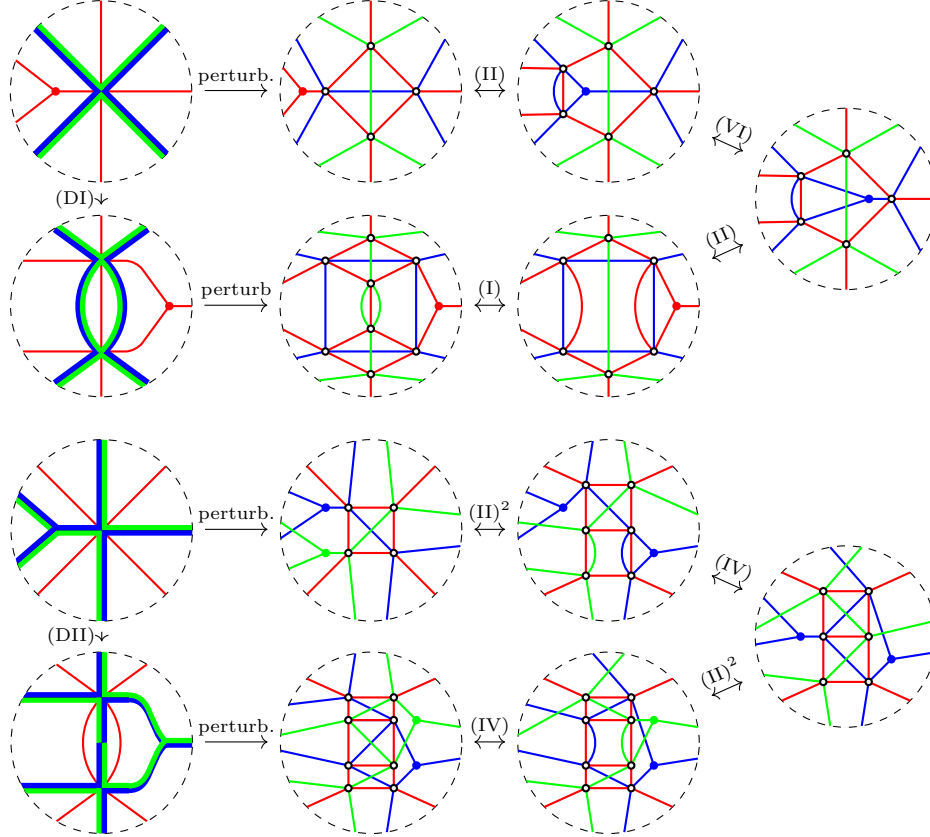
$$3 \rightarrow 4 \rightarrow 5 \rightarrow 6 \rightarrow 3 \quad \text{or} \quad 3 \rightarrow 6 \rightarrow 5 \rightarrow 4 \rightarrow 3$$

which yields a contradiction by Lemma A.4. This completes the proof. \square

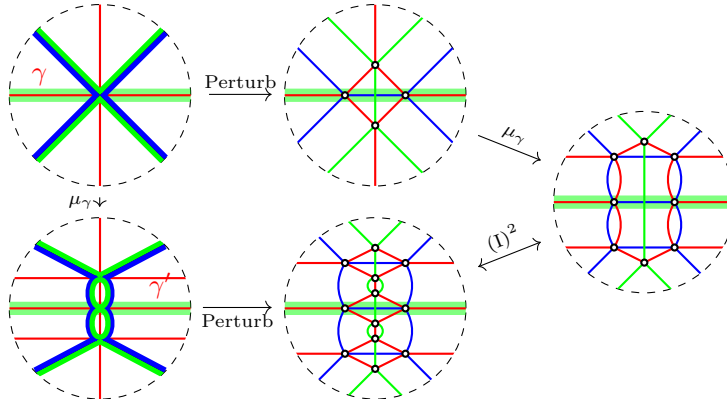
Proof of Theorem 2.20. This follows from Propositions A.2, A.3, and A.6. \square

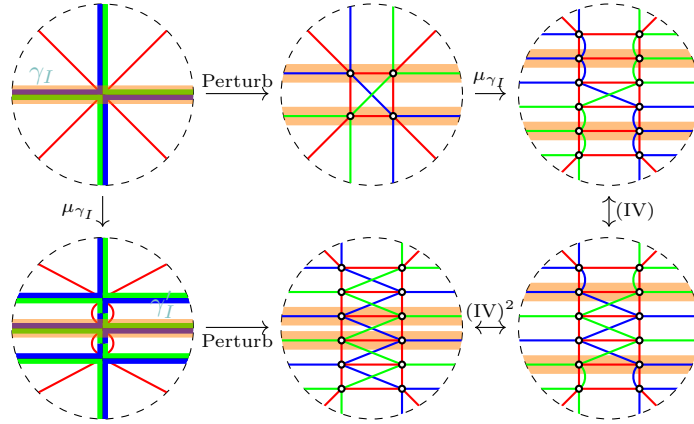
APPENDIX B. SUPPLEMENTARY PICTORIAL PROOFS

B.1. Justifications of moves (DI) and (DII) for denegenerate N -graphs.

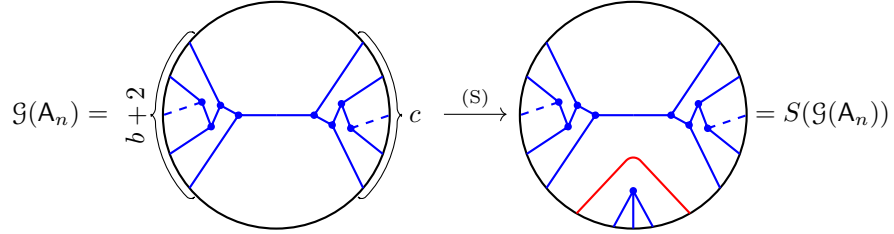


B.2. Justifications of Legendrian local mutations in degenerate N -graphs.

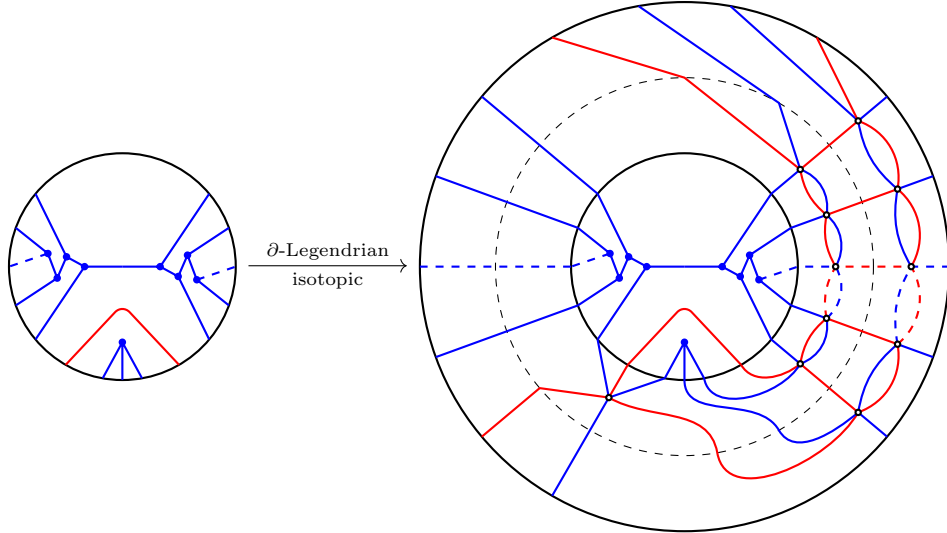




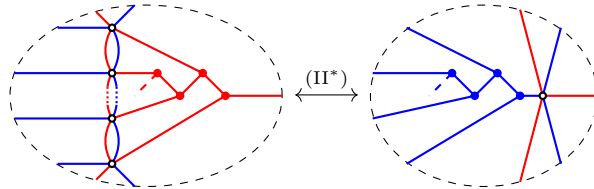
B.3. Equivalence between $\mathcal{G}(1, b, c)$ and a stabilization of $\mathcal{G}(A_n)$. A stabilization of $\mathcal{G}(A_n)$ is a 3-graph which is ∂ -Legendrian isotopic to a 3-graph $S(\mathcal{G}(A_n))$ given as follows:



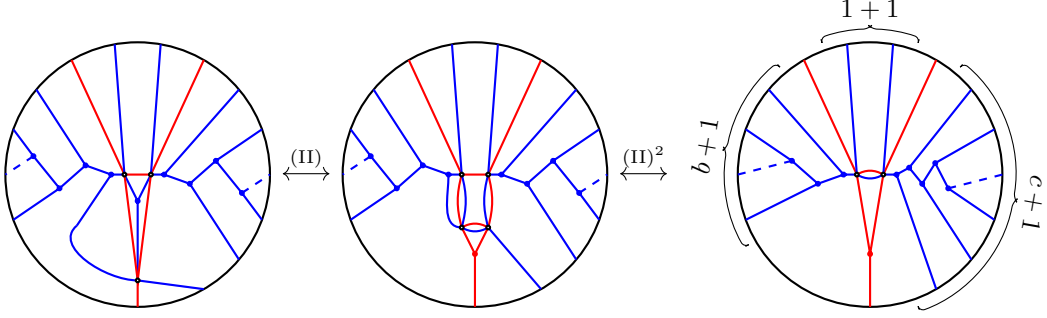
Now we attach the annular 3-graph corresponding to Legendrian isotopy from $S(\beta(A_n))$ to $\beta(1, b, c)$ given above. Then we have the following 3-graph which is ∂ -Legendrian isotopic to $S(\mathcal{G}(A_n))$.



By applying the following generalized push-through move,

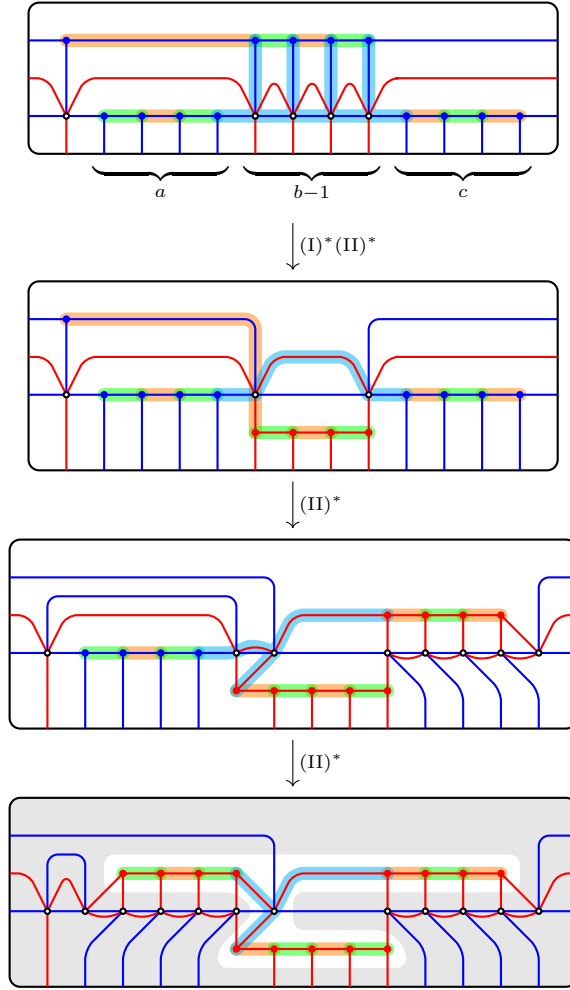


we obtain the 3-graph in the left of the following three equivalent 3-graphs



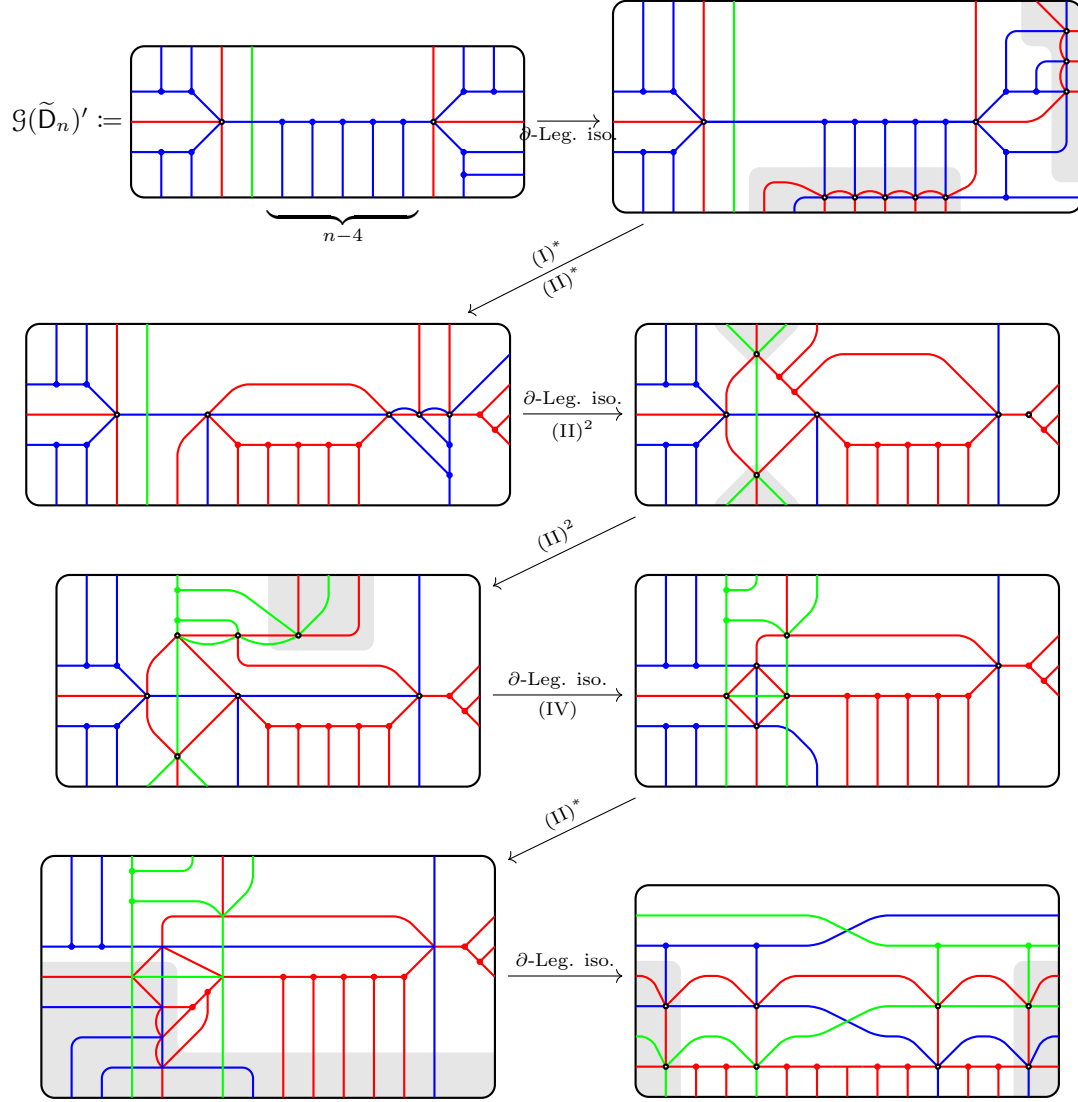
where the right one is equivalent to the 3-graph $\mathcal{G}(1, b, c)$ via the Move (II) as claimed.

B.4. Equivalence between $\mathcal{G}^{\text{brick}}(a, b, c)$ and $\mathcal{G}(a, b, c)$.

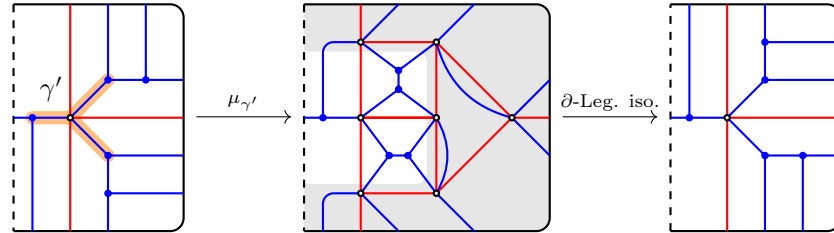


The innermost N -graph is the same as $\overline{\mathcal{G}(a, b, c)}$ up to Legendrian mutations, which is ∂ -Legendrian isotopic to the Legendrian Coxeter mutation of $\mathcal{G}(a, b, c)$ by Proposition 4.21.

B.5. Equivalence between $\mathcal{G}^{\text{brick}}(\tilde{D}_n)$ and $\mathcal{G}(\tilde{D}_n)$. We first show that $\mathcal{G}^{\text{brick}}(\tilde{D}_n)$ is Legendrian mutation equivalent to the following N -graph up to ∂ -Legendrian isotopy:

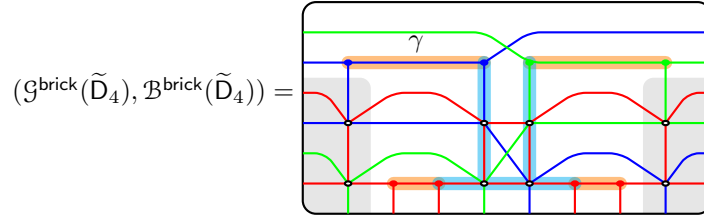


On the other hand, we have the following move

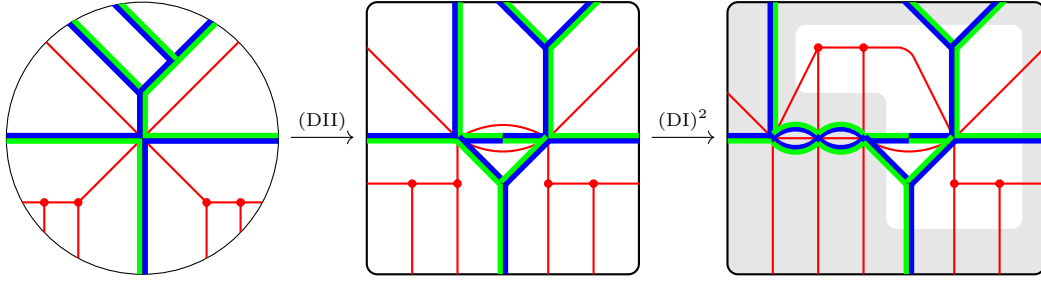


which flips up the downward leg. Finally, the downward and upward legs can be interchanged via Legendrian mutations and therefore the N -graph $\mathcal{G}(\tilde{D}_n)'$ is Legendrian mutation equivalent to $\mathcal{G}(\tilde{D}_n)$ up to ∂ -Legendrian isotopy.

B.6. Equivalence between $\tilde{\mathcal{G}}(\tilde{D}_4)$ and $\mathcal{G}(\tilde{D}_4)$. It is enough to show the equivalence between $\tilde{\mathcal{G}}(\tilde{D}_4)$ and $\mathcal{G}^{\text{brick}}(\tilde{D}_4)$ by Lemma 4.12.



By cutting out the shaded region and taking a Legendrian mutation on γ , we have a degenerate N -graph below, which is $\tilde{\mathcal{G}}(\tilde{\mathcal{D}}_4)$ up to ∂ -Legendrian isotopy and Legendrian mutations.



REFERENCES

- [1] Byung Hee An, Youngjin Bae, and Eunjeong Lee. Lagrangian fillings for Legendrian links of finite type. arXiv:2101.01943v1, 2021.
- [2] Byung Hee An and Eunjeong Lee. On folded cluster patterns of affine type. arXiv:2107.02973v1, 2021.
- [3] Vladimir Igorevich Arnold. *Singularities of caustics and wave fronts*, volume 62 of *Mathematics and its Applications (Soviet Series)*. Kluwer Academic Publishers Group, Dordrecht, 1990.
- [4] Denis Auroux. Mirror symmetry and T -duality in the complement of an anticanonical divisor. *J. Gökova Geom. Topol. GGT*, 1:51–91, 2007.
- [5] Arkady Berenstein, Sergey Fomin, and Andrei Zelevinsky. Cluster algebras. III. Upper bounds and double Bruhat cells. *Duke Math. J.*, 126(1):1–52, 2005.
- [6] Lara Bossinger, Xin Fang, Ghislain Fourier, Milena Hering, and Martina Lanini. Toric degenerations of $\text{Gr}(2, n)$ and $\text{Gr}(3, 6)$ via plabic graphs. *Ann. Comb.*, 22(3):491–512, 2018.
- [7] Nicolas Bourbaki. *Lie groups and Lie algebras. Chapters 4–6*. Elements of Mathematics (Berlin). Springer-Verlag, Berlin, 2002. Translated from the 1968 French original by Andrew Pressley.
- [8] Aslak Bakke Buan and Hermund André Torkildsen. The number of elements in the mutation class of a quiver of type D_n . *Electron. J. Combin.*, 16(1):Research Paper 49, 23, 2009.
- [9] Aslak Bakke Buan and Dagfinn F. Vatne. Derived equivalence classification for cluster-tilted algebras of type A_n . *J. Algebra*, 319(7):2723–2738, 2008.
- [10] Philippe Caldero and Bernhard Keller. From triangulated categories to cluster algebras. II. *Ann. Sci. École Norm. Sup. (4)*, 39(6):983–1009, 2006.
- [11] Peigen Cao, Min Huang, and Fang Li. A conjecture on C -matrices of cluster algebras. *Nagoya Math. J.*, 238:37–46, 2020.
- [12] Roger Casals. Lagrangian skeleta and plane curve singularities. arXiv:2009.06737, 2020.
- [13] Roger Casals and Honghao Gao. Infinitely many Lagrangian fillings. arXiv:2001.01334, 2020.
- [14] Roger Casals and Lenhard Ng. Braid loops with infinite monodromy on the Legendrian contact dga. arXiv:2101.02318, 2021.
- [15] Roger Casals and Eric Zaslow. Legendrian weaves. arXiv:2007.04943, 2020.
- [16] Giovanni Cerulli Irelli, Bernhard Keller, Daniel Labardini-Fragoso, and Pierre-Guy Plamondon. Linear independence of cluster monomials for skew-symmetric cluster algebras. *Compos. Math.*, 149(10):1753–1764, 2013.
- [17] Frédéric Chapoton, Sergey Fomin, and Andrei Zelevinsky. Polytopal realizations of generalized associahedra. *Canad. Math. Bull.*, 45(4):537–566, 2002. Dedicated to Robert V. Moody.
- [18] Yuri Chekanov. Differential algebra of Legendrian links. *Invent. Math.*, 150(3):441–483, 2002.
- [19] Grégoire Dupont. An approach to non-simply laced cluster algebras. *J. Algebra*, 320(4):1626–1661, 2008.
- [20] Tobias Ekholm, Ko Honda, and Tamás Kálmán. Legendrian knots and exact Lagrangian cobordisms. *J. Eur. Math. Soc. (JEMS)*, 18(11):2627–2689, 2016.
- [21] Yakov M. Eliashberg, Alexander B. Givental, and Helmut H. W. Hofer. Introduction to symplectic field theory. *Geom. Funct. Anal.*, (Special Volume, Part II):560–673, 2000. GAFA 2000 (Tel Aviv, 1999).
- [22] Anna Felikson, Michael Shapiro, and Pavel Tumarkin. Cluster algebras of finite mutation type via unfoldings. *Int. Math. Res. Not. IMRN*, 2012(8):1768–1804, 2012.

- [23] Sergey Fomin, Michael Shapiro, and Dylan Thurston. Cluster algebras and triangulated surfaces. I. Cluster complexes. *Acta Math.*, 201(1):83–146, 2008.
- [24] Sergey Fomin, Lauren Williams, and Andrei Zelevinsky. Introduction to cluster algebras. Chapters 4–5. arXiv:1707.07190, 2017.
- [25] Sergey Fomin and Andrei Zelevinsky. Cluster algebras. I. Foundations. *J. Amer. Math. Soc.*, 15(2):497–529, 2002.
- [26] Sergey Fomin and Andrei Zelevinsky. Cluster algebras. II. Finite type classification. *Invent. Math.*, 154(1):63–121, 2003.
- [27] Sergey Fomin and Andrei Zelevinsky. Y-systems and generalized associahedra. *Ann. of Math. (2)*, 158(3):977–1018, 2003.
- [28] Sergey Fomin and Andrei Zelevinsky. Cluster algebras. IV. Coefficients. *Compos. Math.*, 143(1):112–164, 2007.
- [29] Honghao Gao, Linhui Shen, and Daping Weng. Augmentations, fillings, and clusters. arXiv:2008.10793, 2020.
- [30] Honghao Gao, Linhui Shen, and Daping Weng. Positive braid links with infinitely many fillings. arXiv:2009.00499, 2020.
- [31] Hansjörg Geiges. *An introduction to contact topology*, volume 109. Cambridge University Press, 2008.
- [32] Stéphane Guillermou, Masaki Kashiwara, and Pierre Schapira. Sheaf quantization of Hamiltonian isotopies and applications to nondisplaceability problems. *Duke Math. J.*, 161(2):201–245, 2012.
- [33] James Hughes. Weave realizability for D-type. arXiv:2101.10306, 2021.
- [34] James E. Humphreys. *Introduction to Lie algebras and representation theory*, volume 9 of *Graduate Texts in Mathematics*. Springer-Verlag, New York-Berlin, 1978. Second printing, revised.
- [35] Victor G. Kac. *Infinite-dimensional Lie algebras*, volume 44 of *Progress in Mathematics*. Birkhäuser Boston, Inc., Boston, MA, 1983. An introduction.
- [36] Tamás Kálmán. Braid-positive Legendrian links. *Int. Math. Res. Not.*, pages Art ID 14874, 29, 2006.
- [37] Lenhard Ng, Dan Rutherford, Vivek Shende, Steven Sivek, and Eric Zaslow. Augmentations are sheaves. *Geom. Topol.*, 24(5):2149–2286, 2020.
- [38] Yu Pan. Exact Lagrangian fillings of Legendrian $(2, n)$ torus links. *Pacific J. Math.*, 289(2):417–441, 2017.
- [39] Leonid Polterovich. The surgery of Lagrange submanifolds. *Geom. Funct. Anal.*, 1(2):198–210, 1991.
- [40] Nathan Reading and Salvatore Stella. An affine almost positive roots model. *J. Comb. Algebra*, 4(1):1–59, 2020.
- [41] Linhui Shen and Daping Weng. Cluster structures on double Bott–Samelson cells. arXiv:1904.07992, 2019.
- [42] Vivek Shende, David Treumann, Harold Williams, and Eric Zaslow. Cluster varieties from Legendrian knots. *Duke Math. J.*, 168(15):2801–2871, 2019.
- [43] Vivek Shende, David Treumann, and Eric Zaslow. Legendrian knots and constructible sheaves. *Invent. Math.*, 207(3):1031–1133, 2017.
- [44] David Treumann and Eric Zaslow. Cubic planar graphs and Legendrian surface theory. *Adv. Theor. Math. Phys.*, 22(5):1289–1345, 2018.
- [45] Dagfinn F. Vatne. The mutation class of D_n quivers. *Comm. Algebra*, 38(3):1137–1146, 2010.

Email address: anbyhee@knu.ac.kr

DEPARTMENT OF MATHEMATICS EDUCATION, KYUNGPOOK NATIONAL UNIVERSITY, REPUBLIC OF KOREA

Email address: yjbae@inu.ac.kr

DEPARTMENT OF MATHEMATICS, INCHEON NATIONAL UNIVERSITY, REPUBLIC OF KOREA

Email address: eunjeong.lee@ibs.re.kr

CENTER FOR GEOMETRY AND PHYSICS, INSTITUTE FOR BASIC SCIENCE (IBS), POHANG 37673, REPUBLIC OF KOREA